Investigations of the birnessite interlayer for water oxidation chemistry

ECI Talk

Samantha Shumlas

March 31, 2017

RESEARCH FOCUSES ON OVERCOMING CHALLENGES

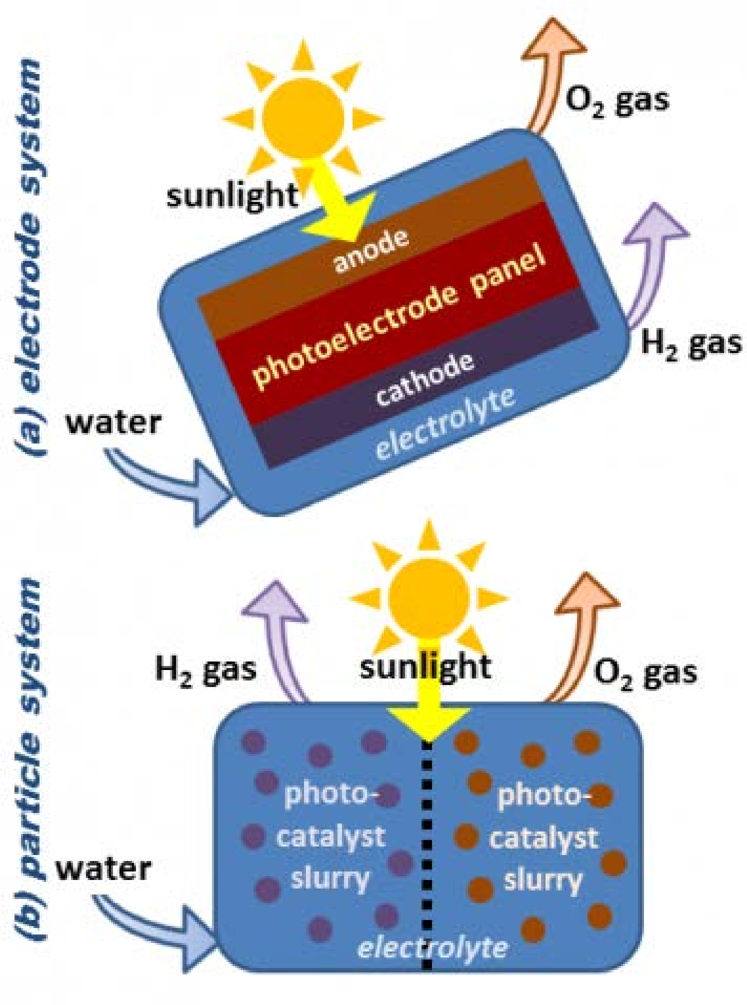

Continued improvements in efficiency, durability, and cost are still needed for market viability. Ongoing research and development of PEC materials, devices, and systems is making important strides, benefiting from strong synergies with contemporary research efforts in photovoltaics, nano-technologies, and computational materials.

https://energy.gov/eere/fuelcells/hydrogen-production-photoelectrochemical-water-splitting

Water Splitting
Water Oxidation

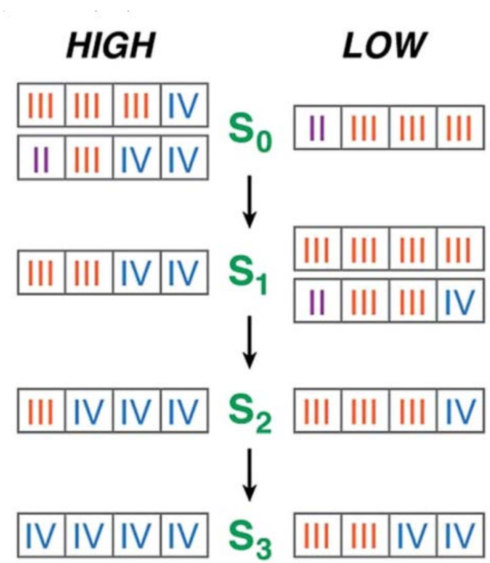

$$2\ H_2O \rightarrow O_2 + 4H^+ + 4e^-$$

$$2\ H^+ + 2\ e^- \rightarrow H_2$$

$$2\ H_2O \rightarrow O_2 + 2H_2$$

1.23 V

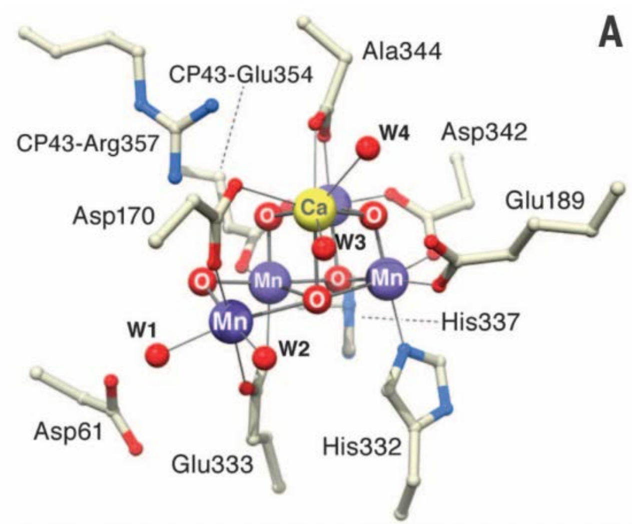

Oxygen Evolving Complex
Photosystem II
Photosynthesis

Mn(IV) and Mn(III)

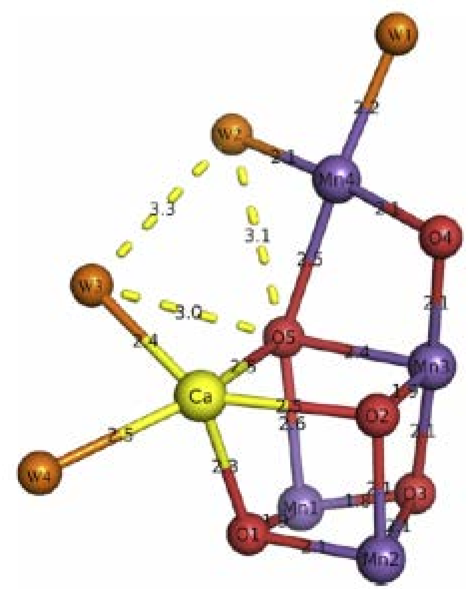

Cox, et.al. *Science*. 2014. 345. 6198. 804-808.
Blakemore JD, et.al. Chemical Reviews. 2015 Jul 7;115(23):12974-3005.
M.M. Najafpour et al. Biochimica et Biophysica Acta, 2017. 1858, 156–174

Birnessite

- Formed by precipitation in lakes, oceans and groundwater
  - Manganese nodules

- Structure
- $K_{0.20\text{-}0.018}Mn(IV_{0.59}III_{0.26}II_{0.13})\ O_{1.66} \bullet nH_2O$
- $Na_{0.58}Mn(IV_{1.42}III_{0.58})\ O_2 \bullet nH_2O$
- Ca, any other cation

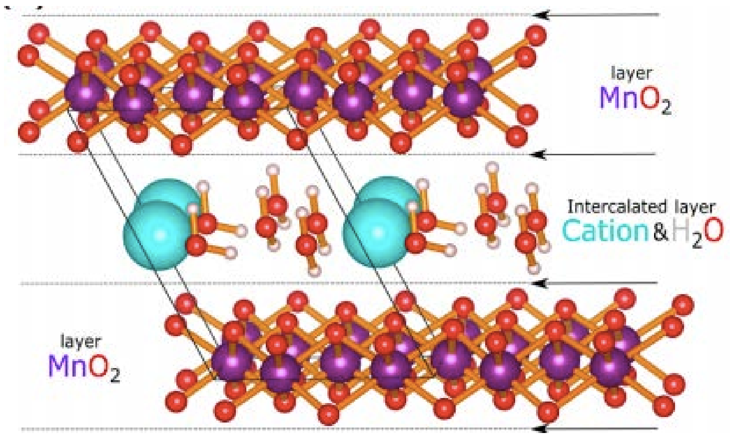

Lucht, et. al, J. Phys. Chem. C 2015, 119, 22838–22846
“Manganese nodule”. J. Wikipedia.org

BULK

Mn^{2+}

OH^-
O_2

Mn^{4+}
Mn^{3+}

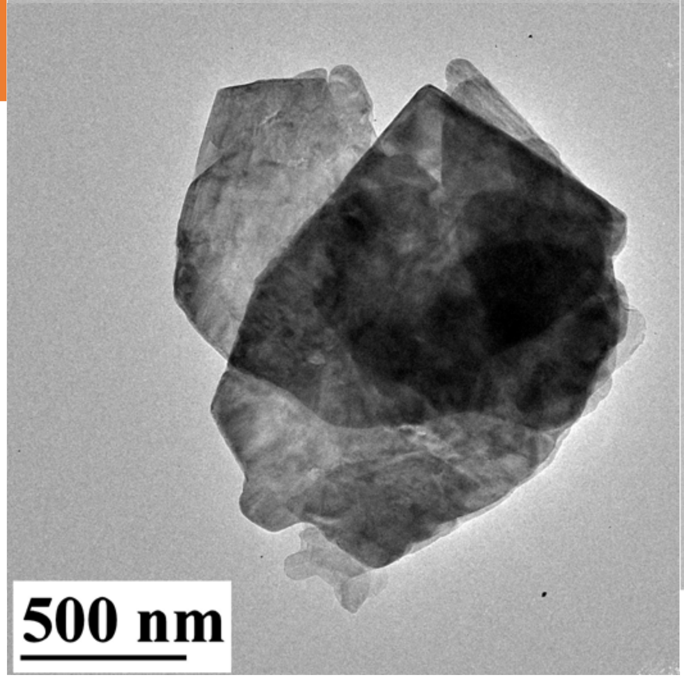

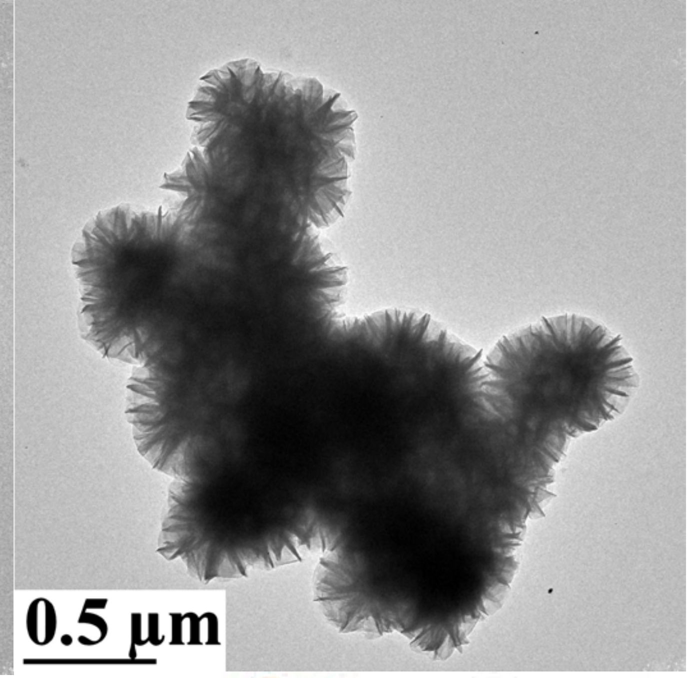

Mn^{7+}

H^+

Mn^{4+}
Mn^{3+}

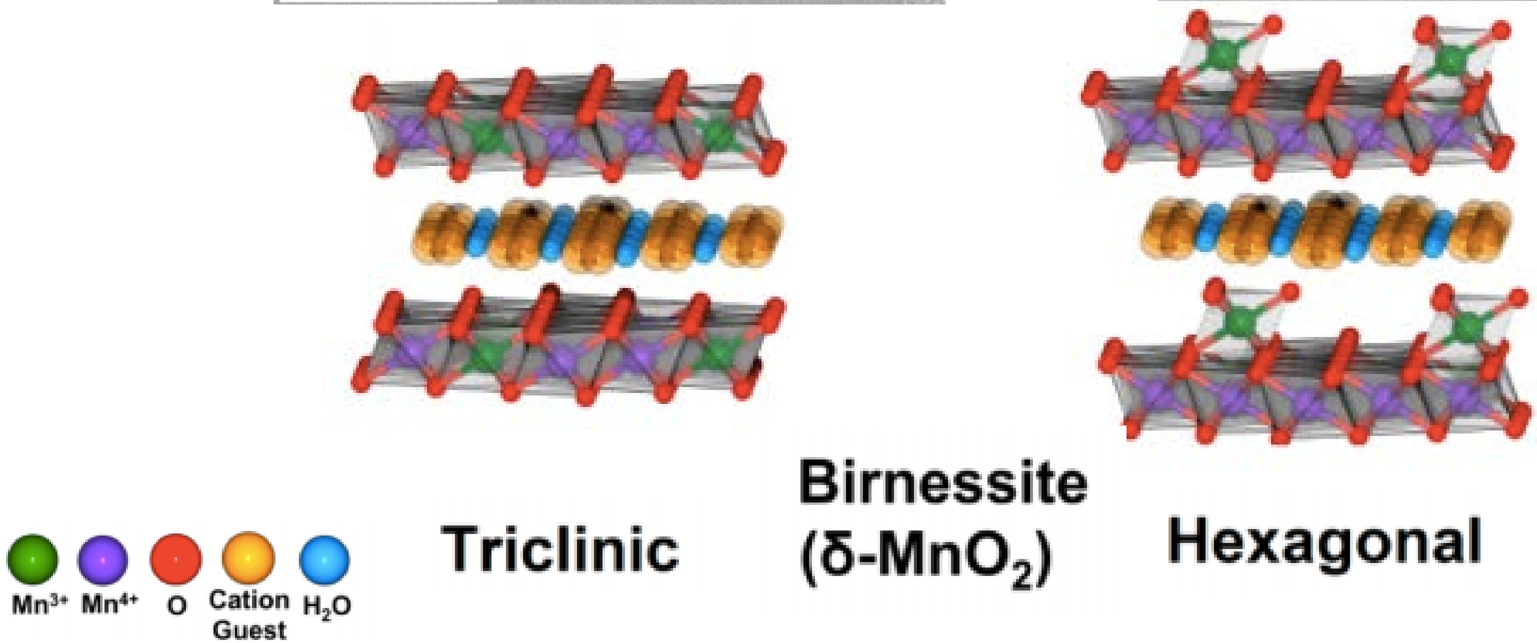

Smith, et. Al. *ACS Catal*. 2016, 6, 2089–2099
McKenzie, R. M. *Mineralogical Magazine.* 1971, 38.296, 493-502.
Yang and Wang. *Clays and Clay minerals* 50.1 (2002): 63-69.

Methods of Modifying Structure

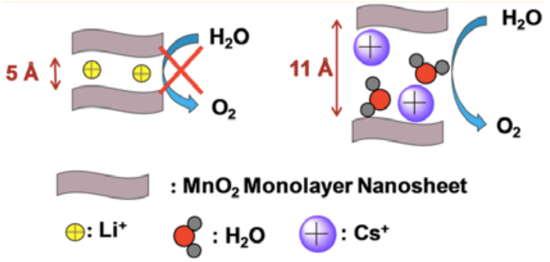

- Bilayer nanosheets
- Changing average oxidation state (synthesis)
- Intercalating metals (Co, Ni, Cu)
- Doping (Co)

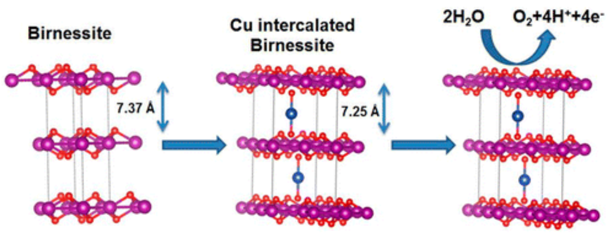

- Frustrated water in the interlayer space

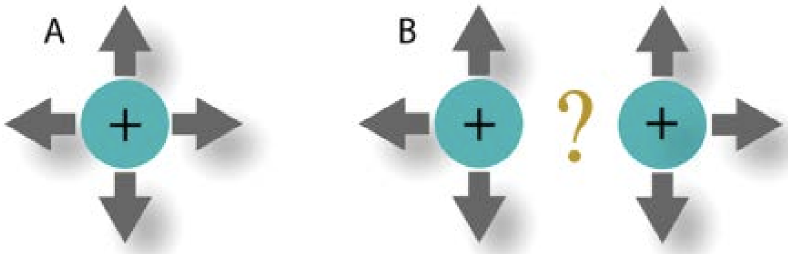

Remsing, R. et. al. J. Phys. Chem. Lett. 2015, 6, 4804−4808
McKendry, I, et.al 2015 Dalton Transactions

Thenuwara (2015) Thenuwara (2016) Thenuwara (2016)
Kang, Qing, et al. *JACS* 139.5 (2017): 1863-1870.

Active site

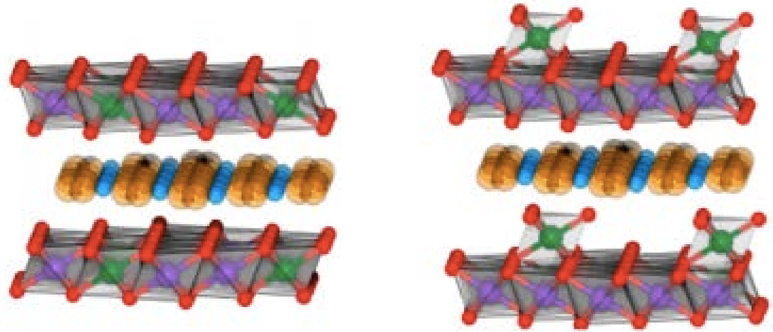

- Pinpointing
  - Corner shared manganese

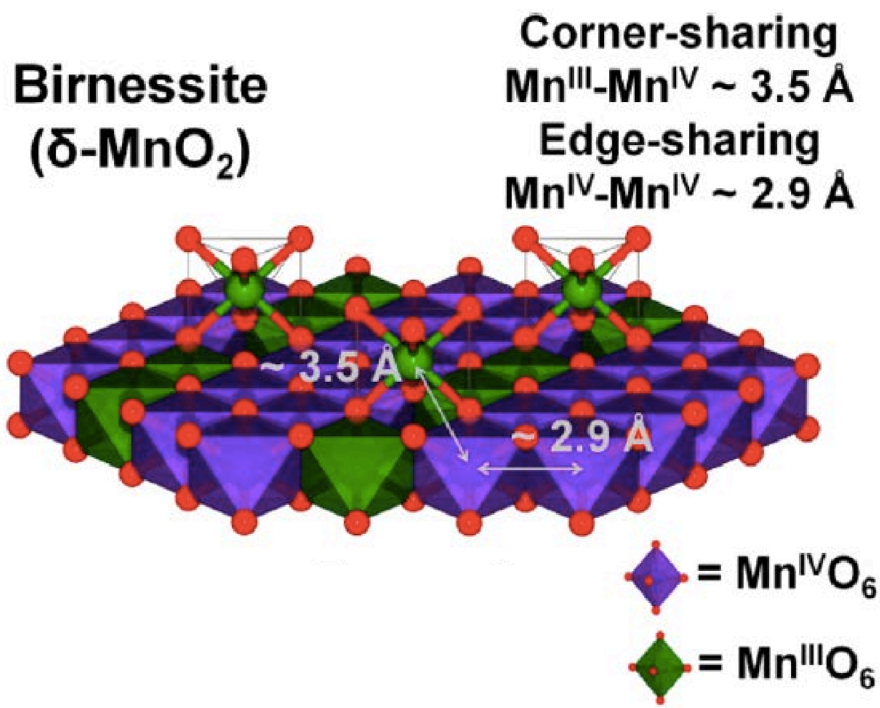

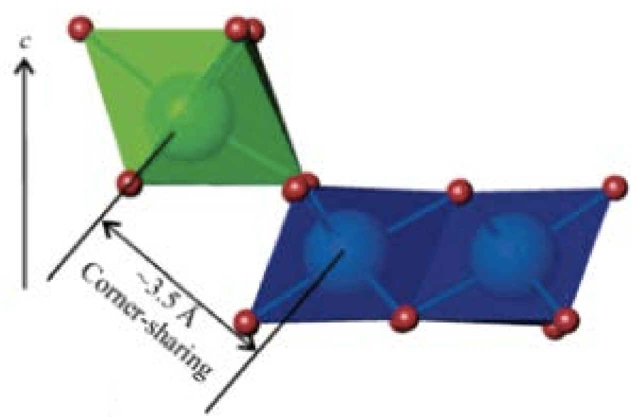

Smith, et. Al. *ACS Catal*. 2016, 6, 2089–2099

Active site

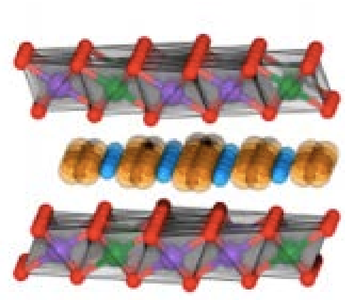

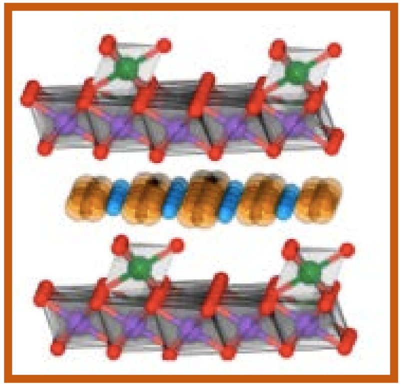

- Pinpointing
  - Corner shared manganese

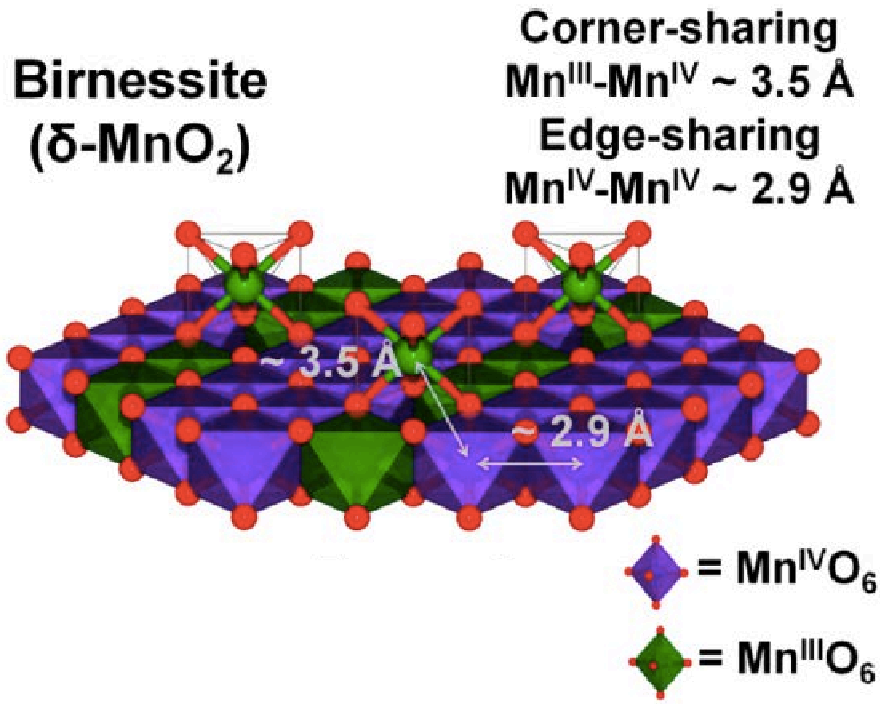

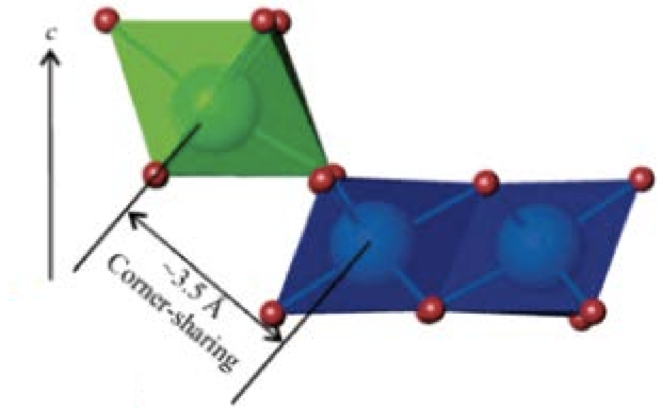

Smith, et. Al. *ACS Catal*. 2016, 6, 2089–2099

Motivation

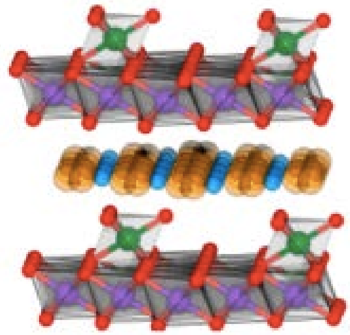

- Determine the site for water oxidation activity
  - Interlayer chemistry is key to water oxidation in birnessite
  - Why does birnessite behave the way it does?
- Improve and understand the water oxidation activity of birnessite
  - What happens during and after the chemistry

How do we do this?

TEM
Transmission Electron Microscopy

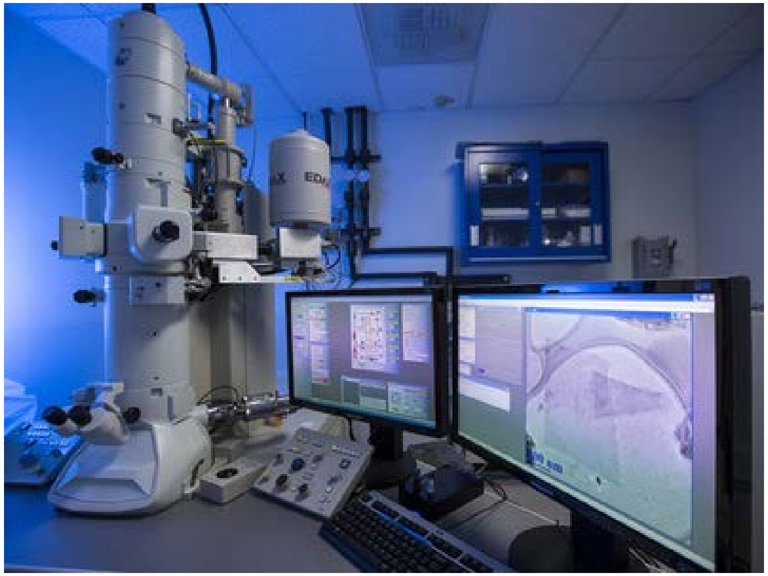

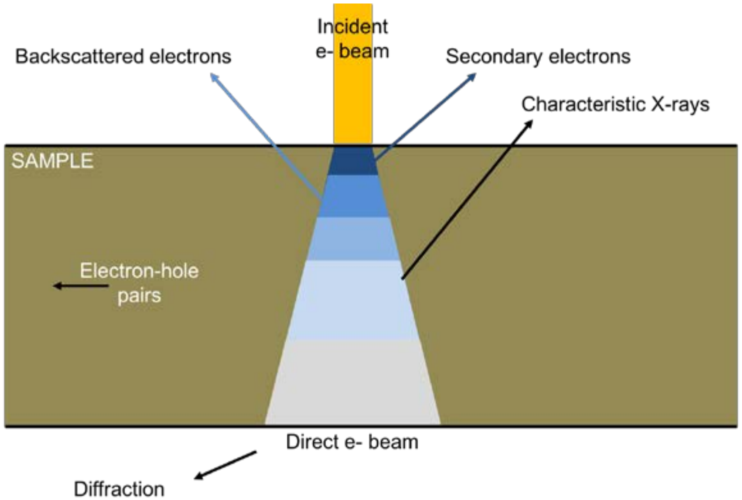

XRD
X-ray diffraction

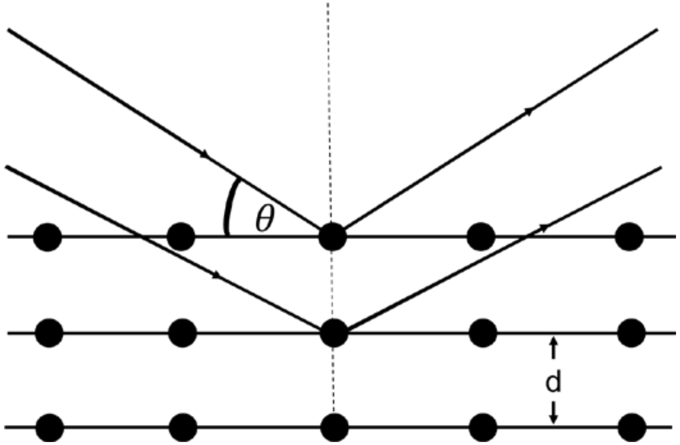

XPS
X-ray photoelectron spectroscopy

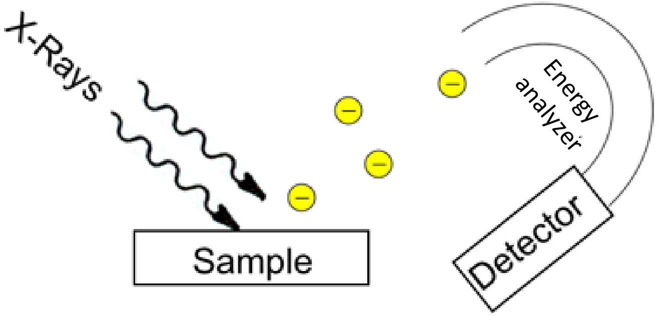

https://www.e20.ph.tum.de/en/techniques/photoelectron-spectroscopy/

TEM
Transmission Electron Microscopy

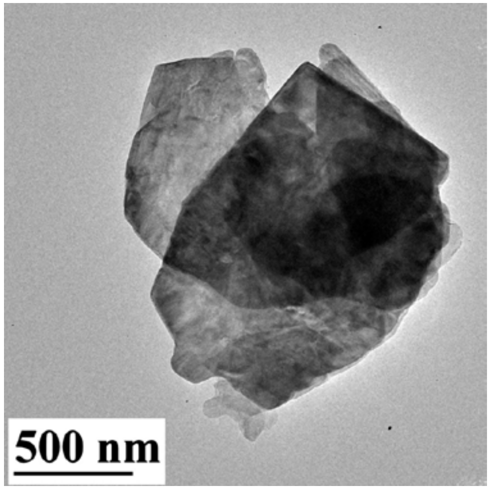

Triclinic

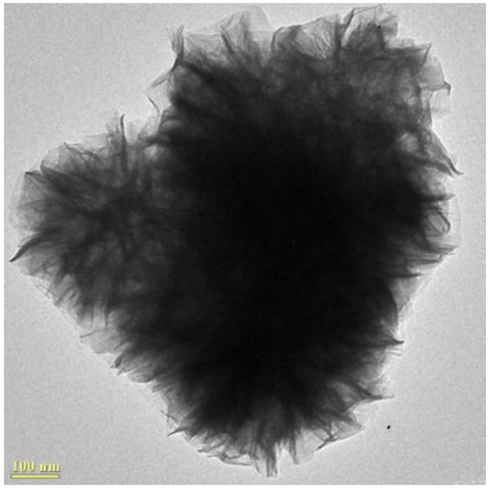

Hexagonal

XRD
X-ray diffraction

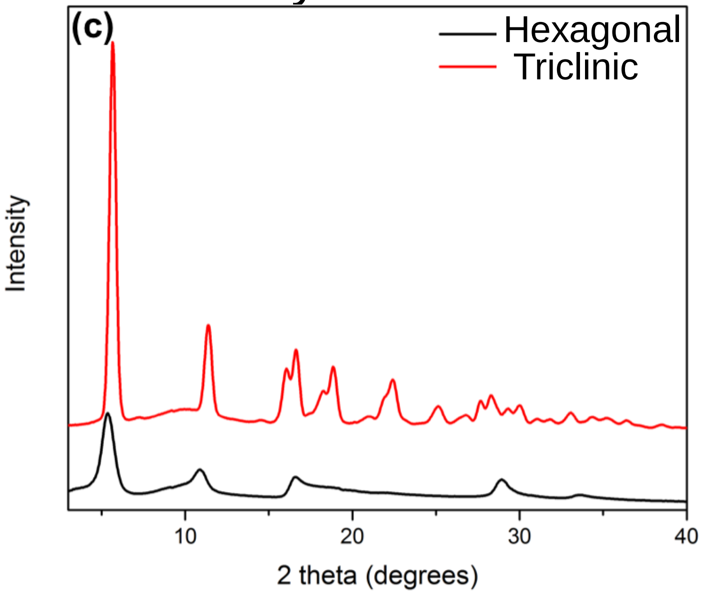

XPS
X-ray photoelectron spectroscopy

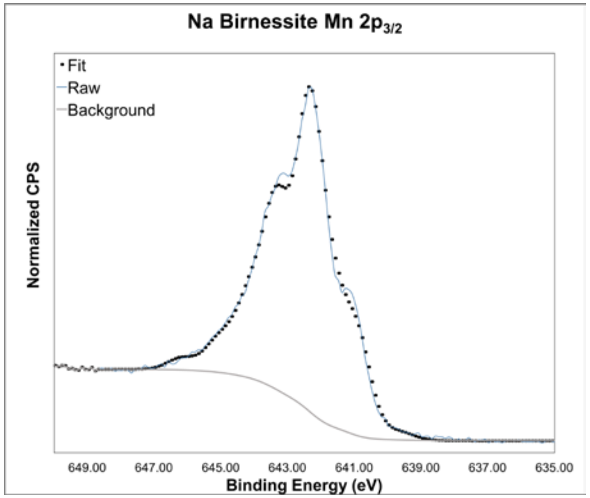

AOS 3.51

AOS 3.56

Accessing Activity

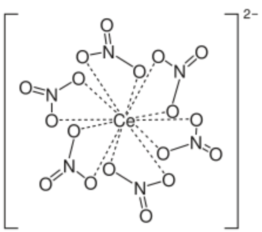

Ceric ammonium nitrate

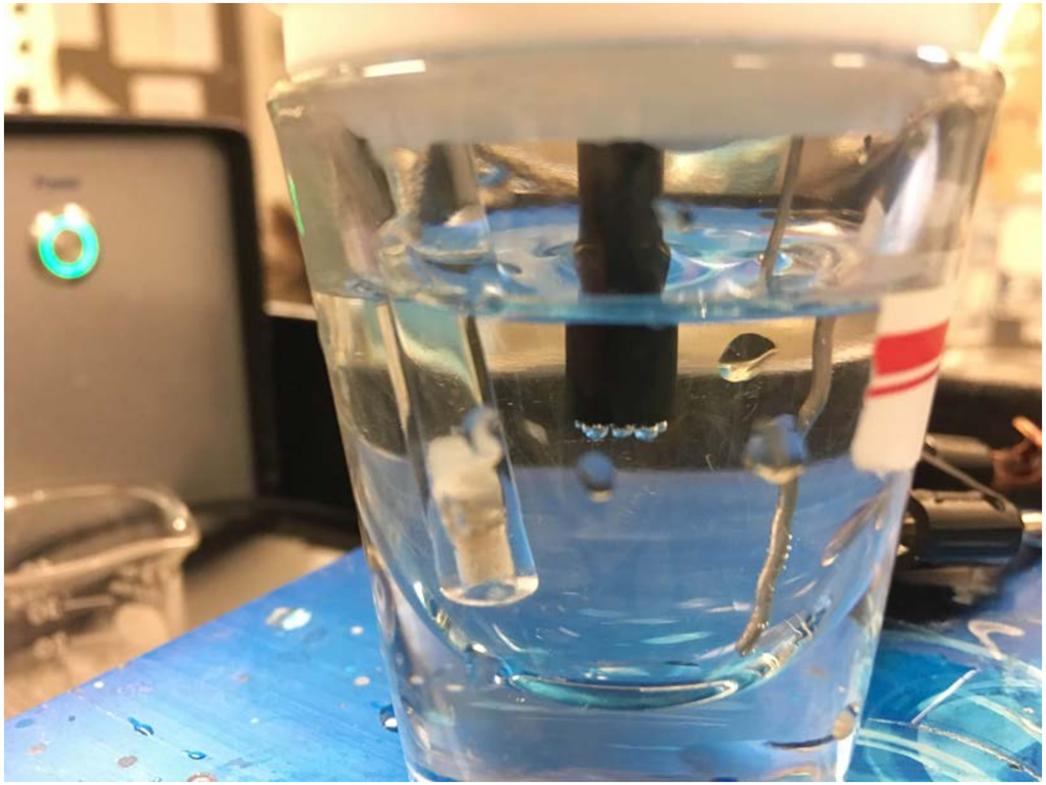

Electrochemistry

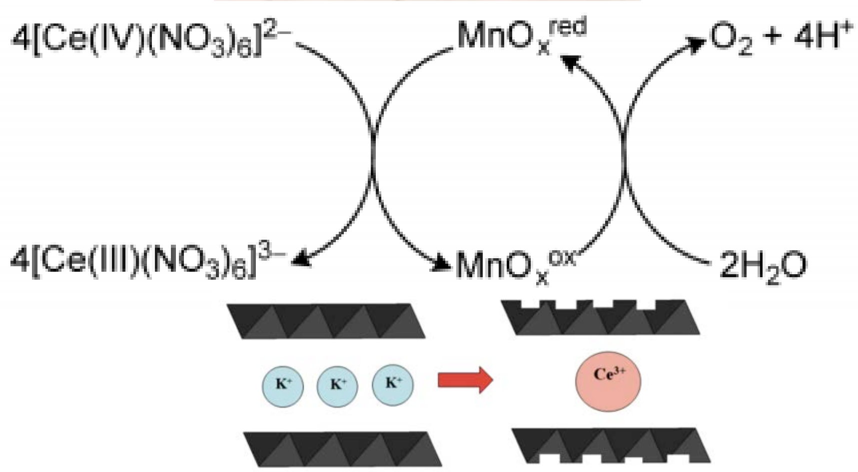

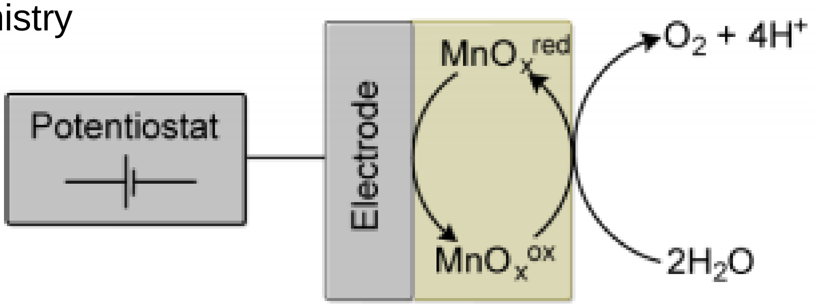

E = 1.23 V

Thermodynamic minimum =1.23 V and potential at which reaction actually occurs is the OVERPOTENTIAL

Najafpour, et al. *Dalton Transactions* 42.40 (2013): 14603-14611.

Characterization

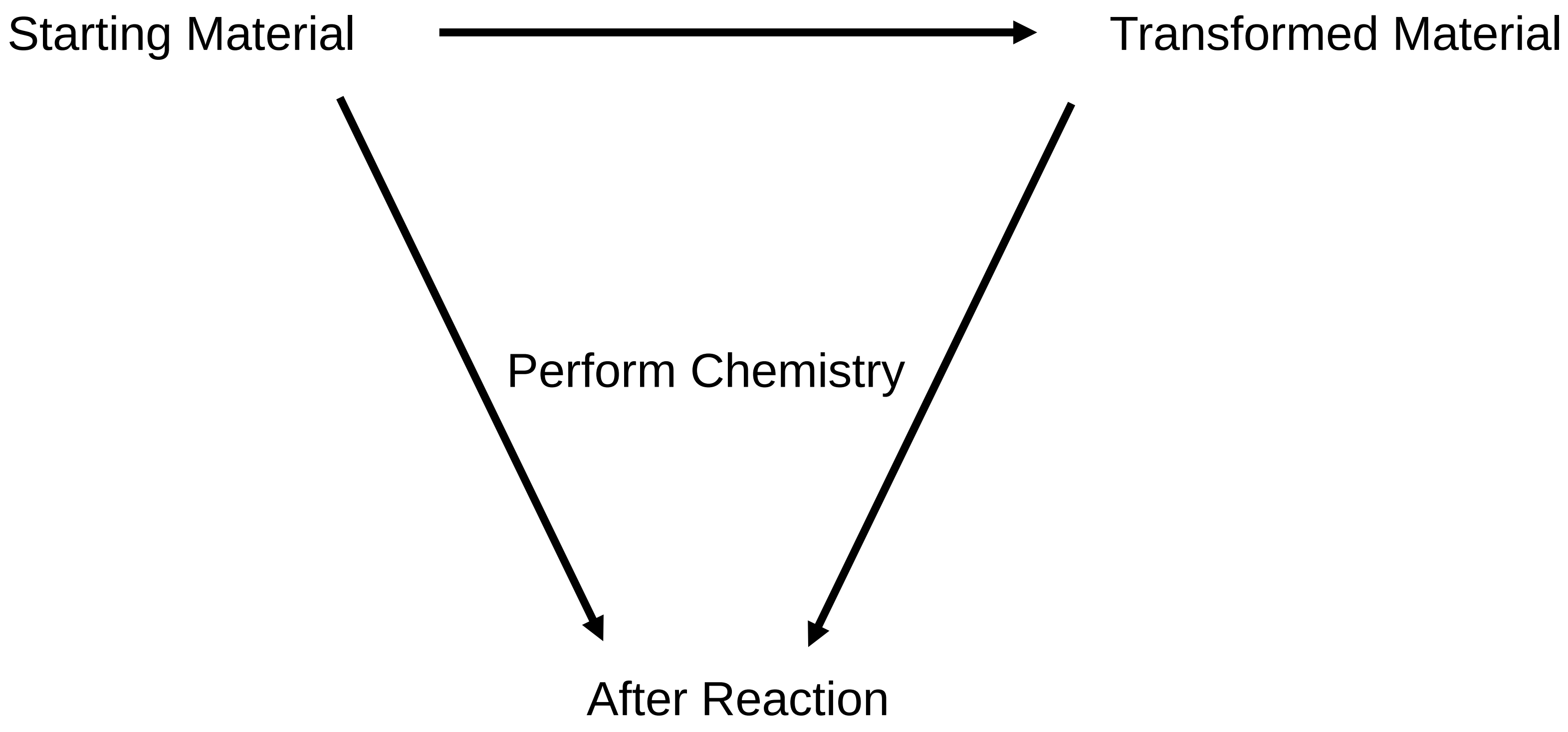

Investigation of birnessite interlayer

Exfoliation of bulk structure to investigate nanosheets

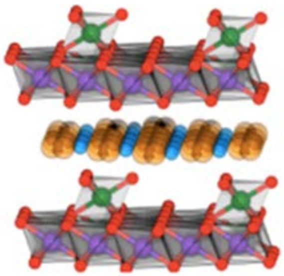

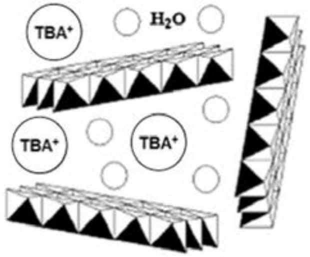

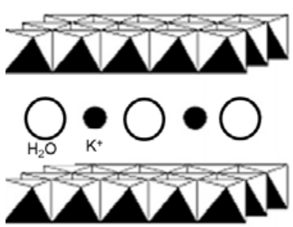

Modification of bulk structure

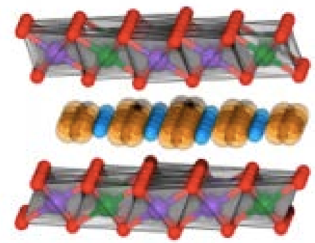

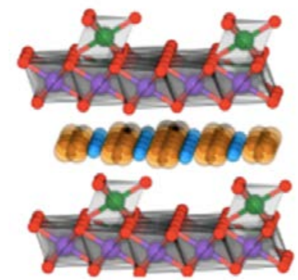

Investigation of birnessite interlayer

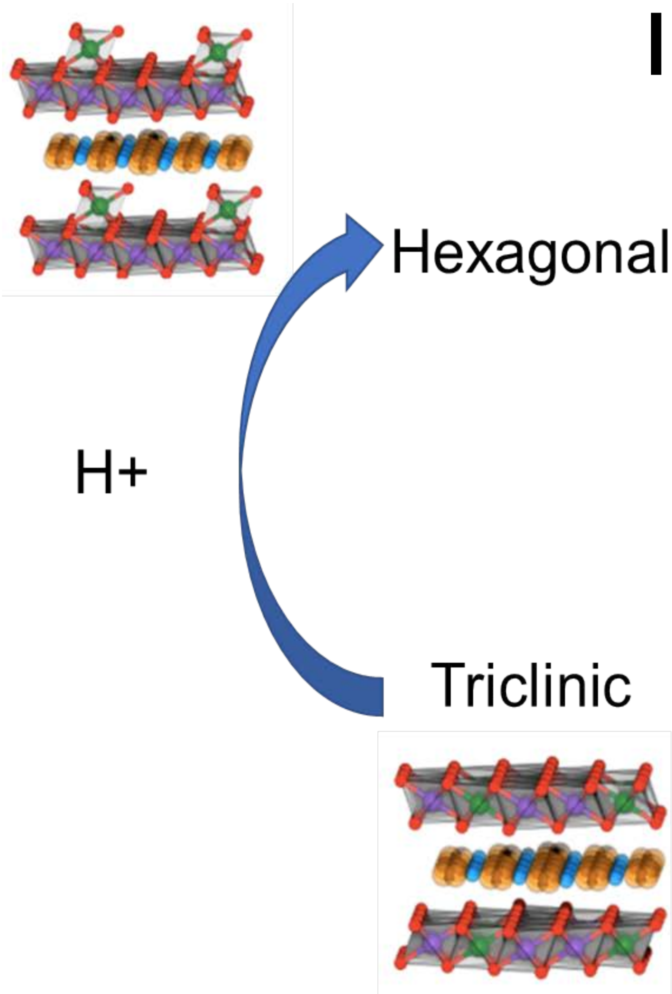

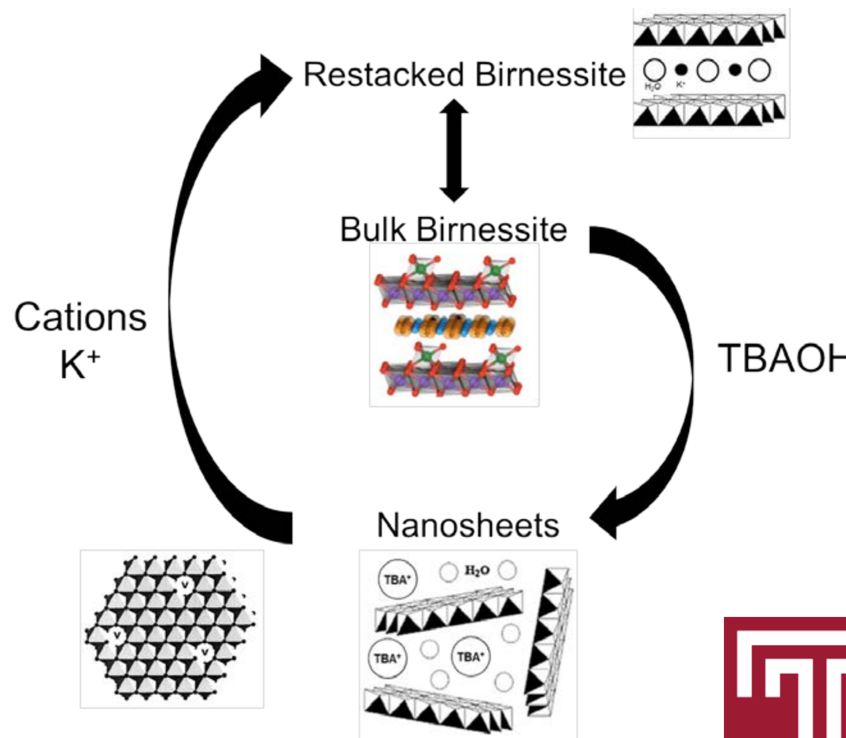

Investigation of birnessite interlayer

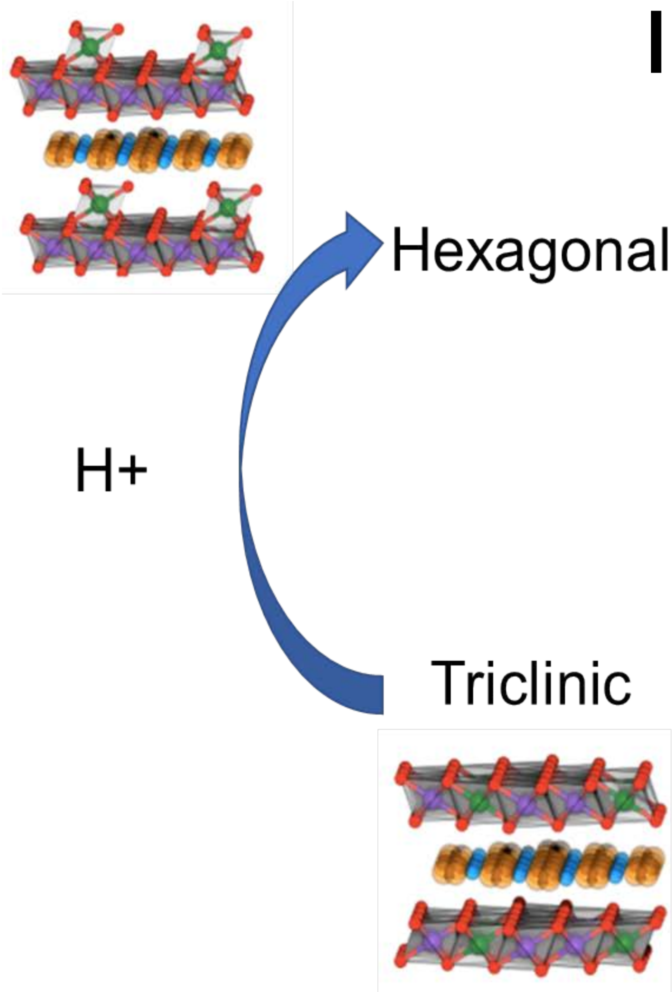

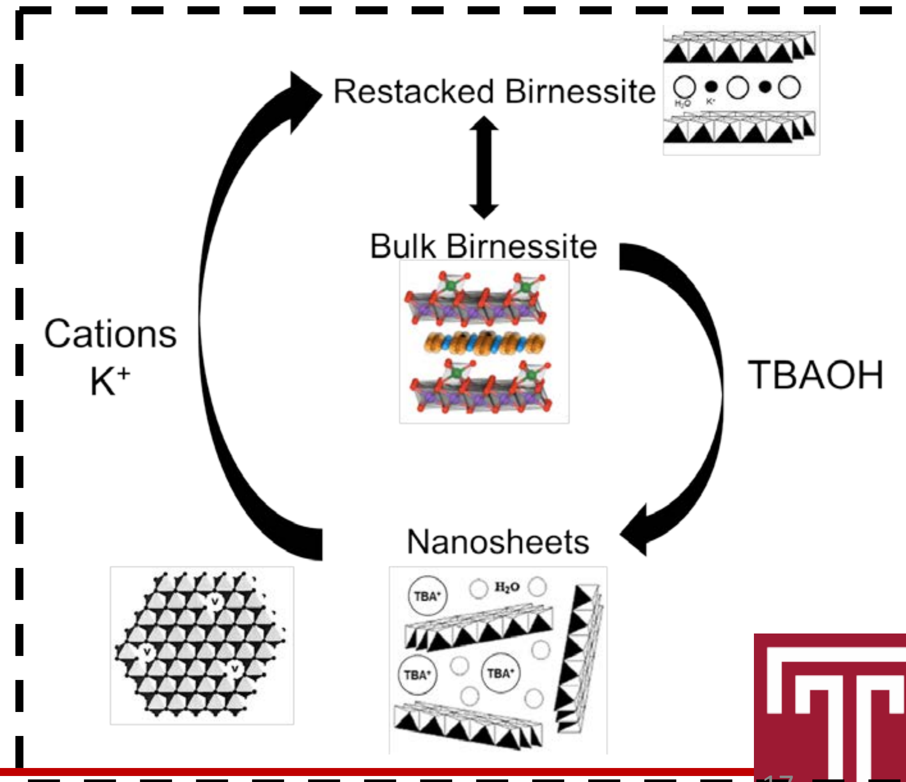

Exfoliation of bulk structure to investigate nanosheets

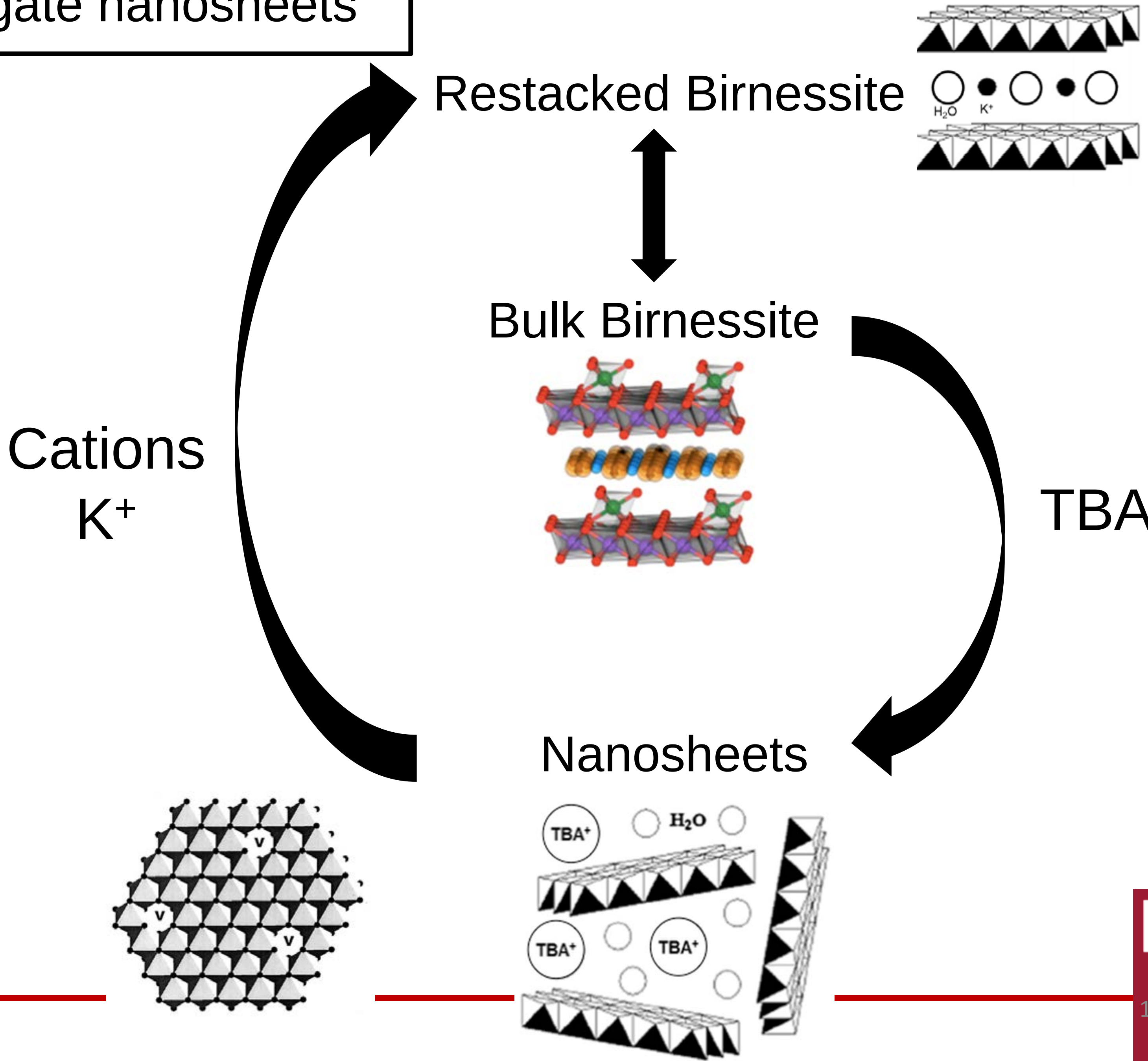

Exfoliation of bulk structure to investigate nanosheets

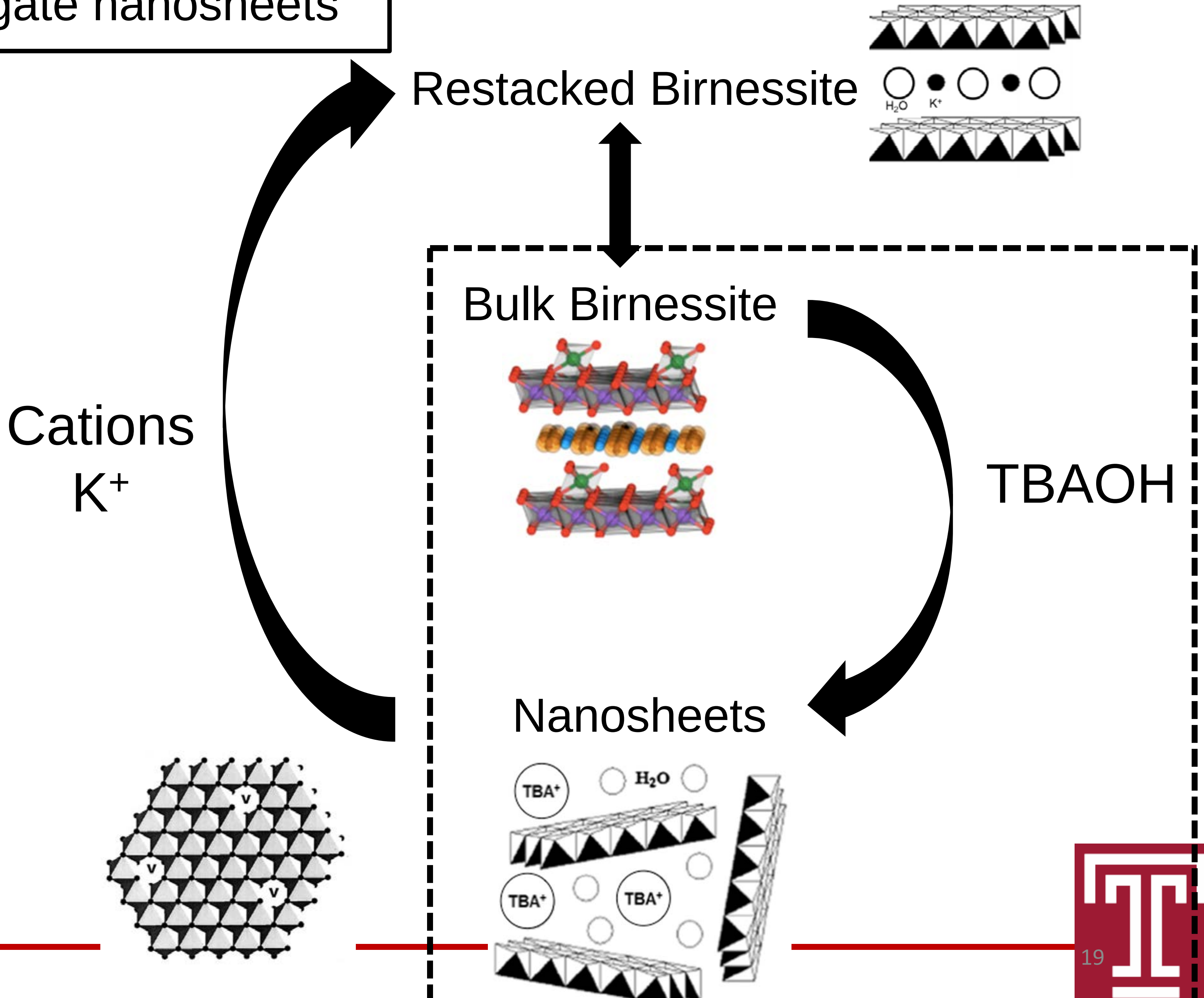

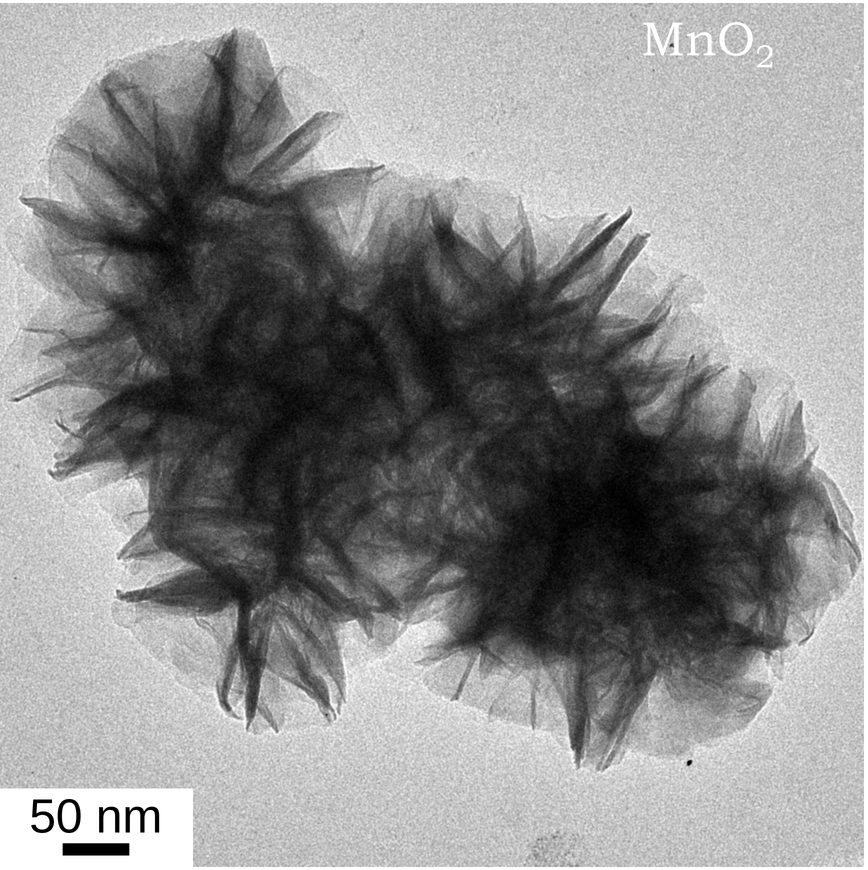

TBAOH

10 days

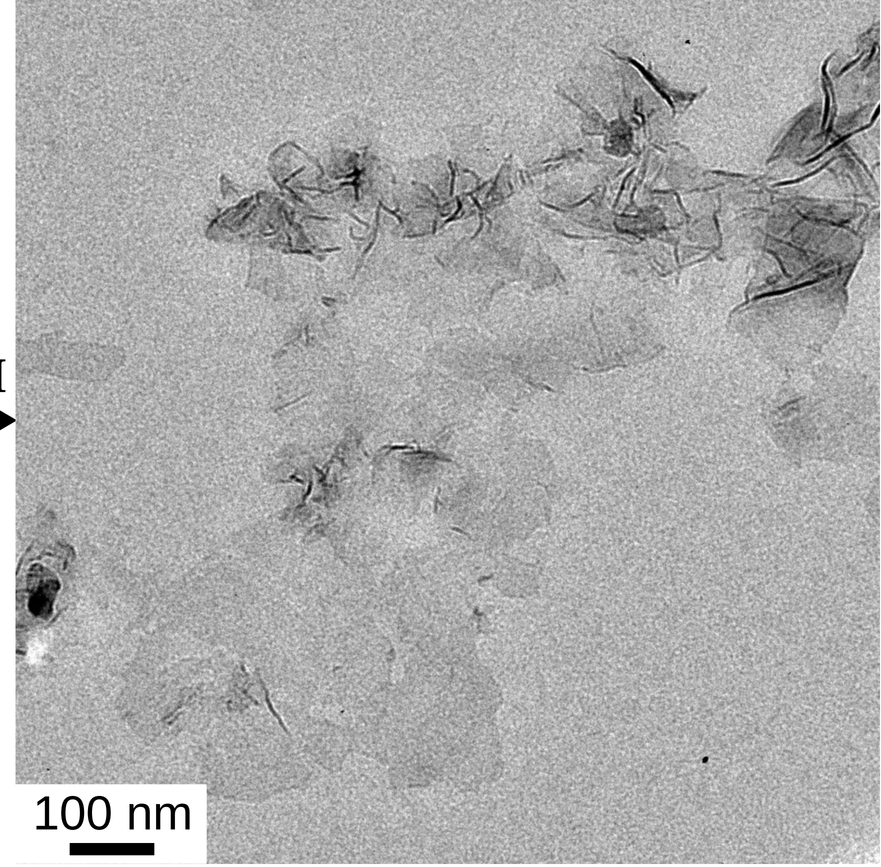

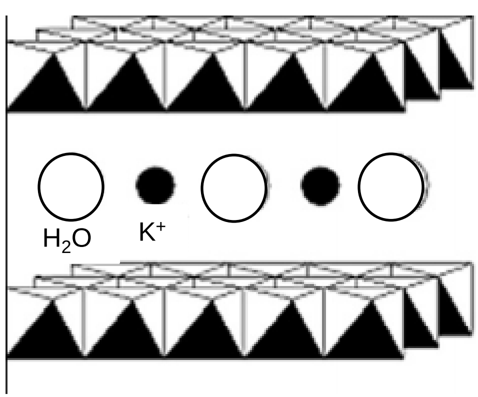

TBAOH

10 days

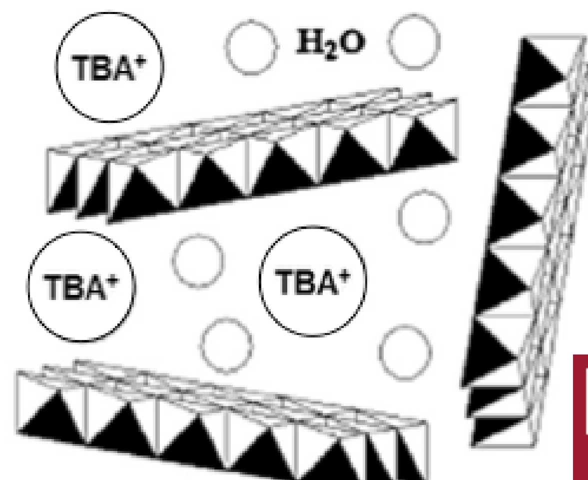

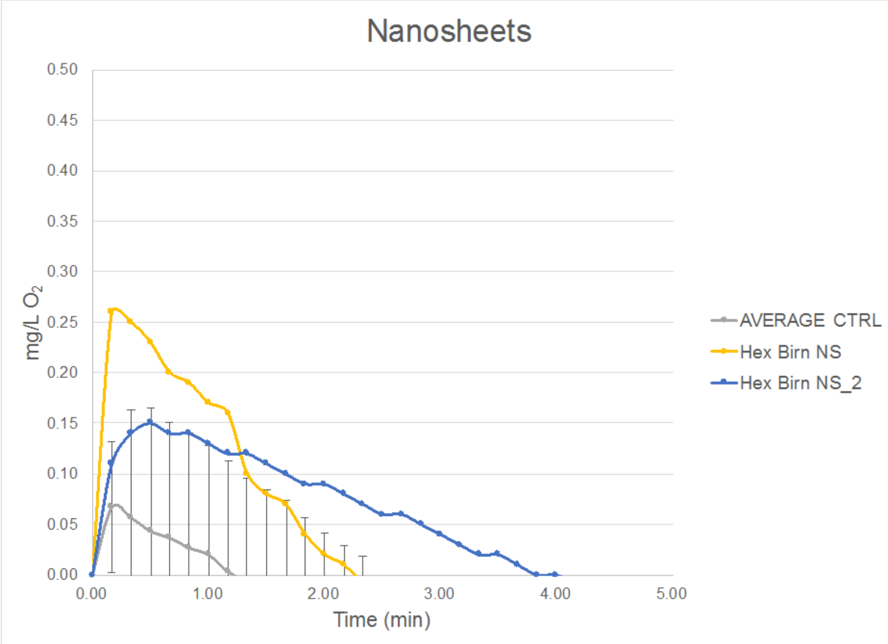

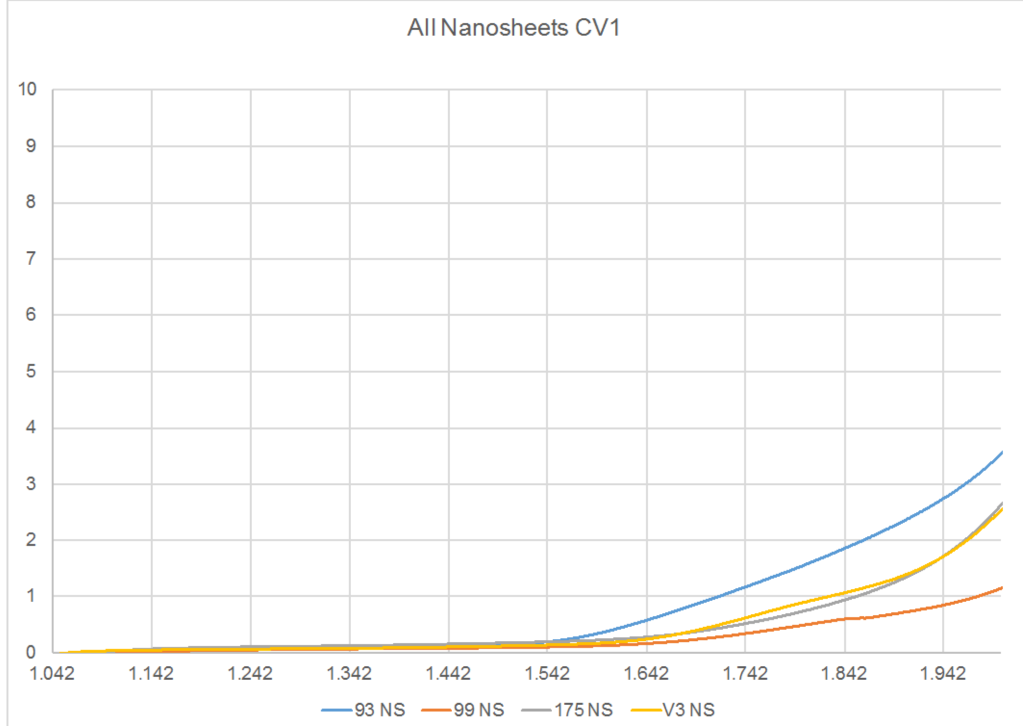

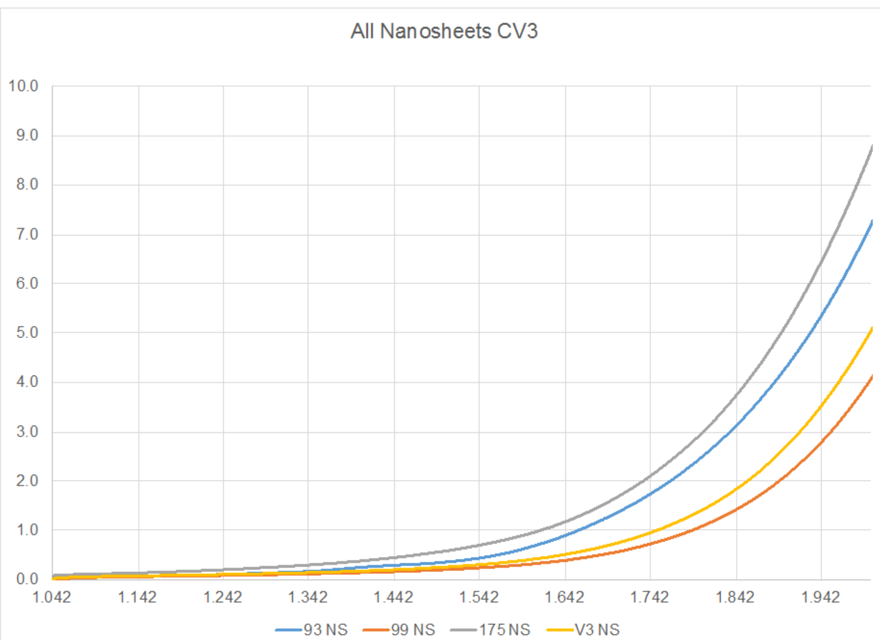

Suspended nanosheets do not demonstrate water oxidation activity

Exfoliation of bulk structure to investigate nanosheets

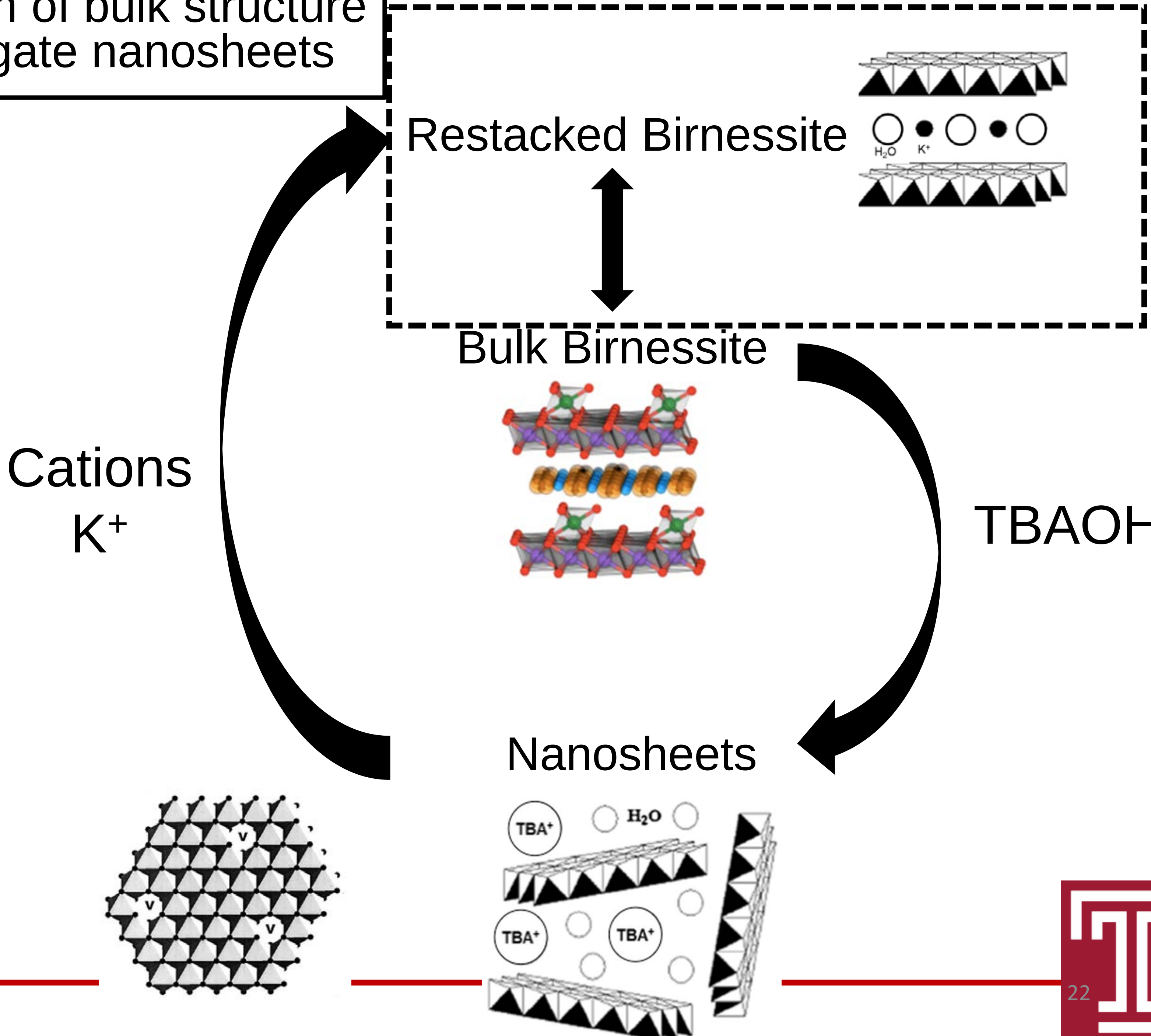

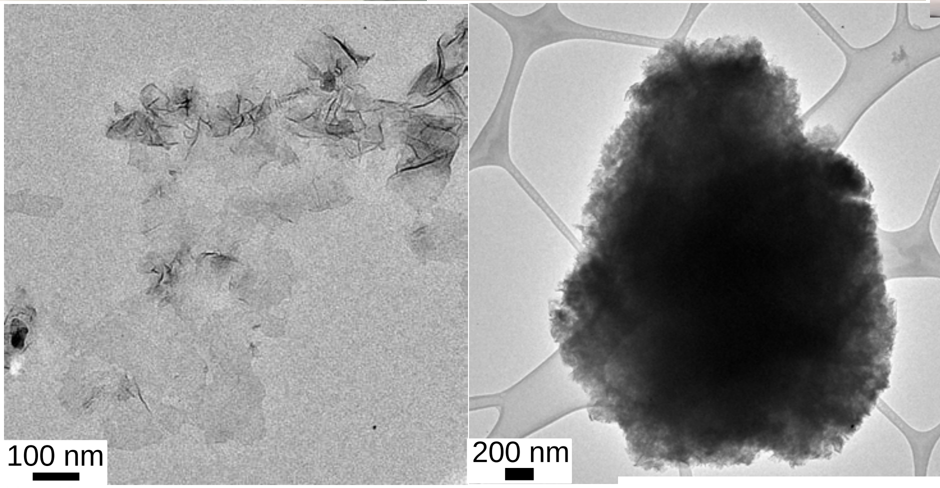
100 nm
200 nm

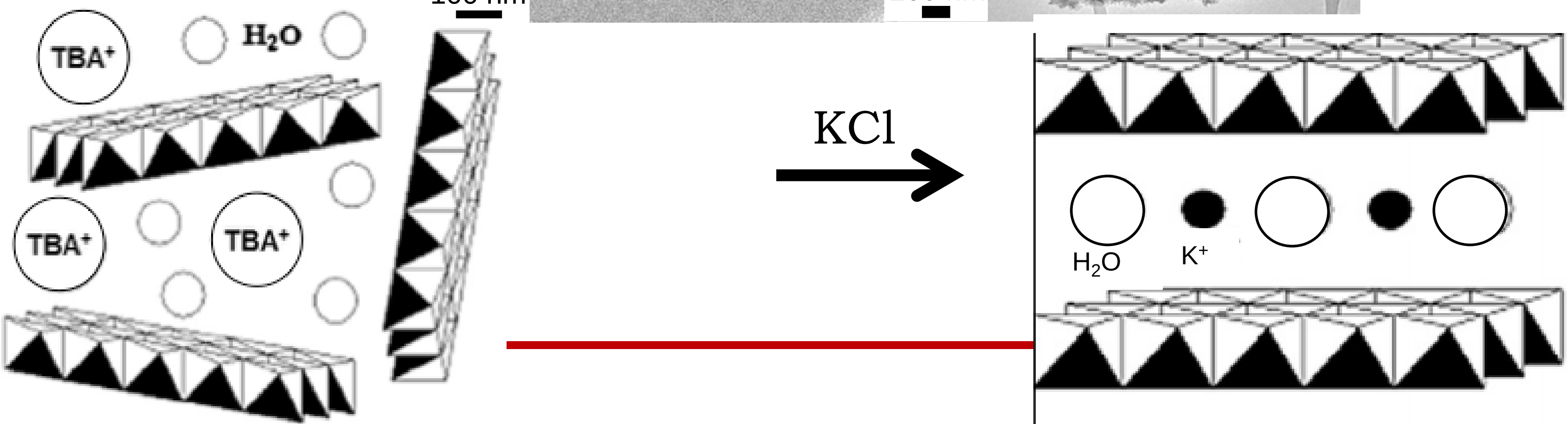
TBA+
H_2O
TBA+
TBA+
KCl
H_2O
K^+

Restacked samples

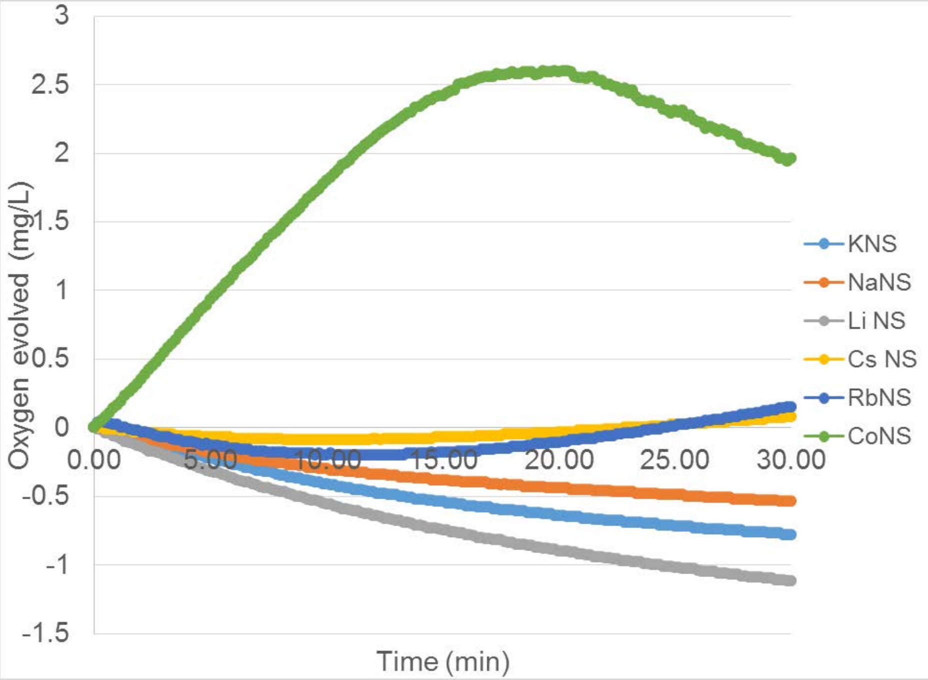

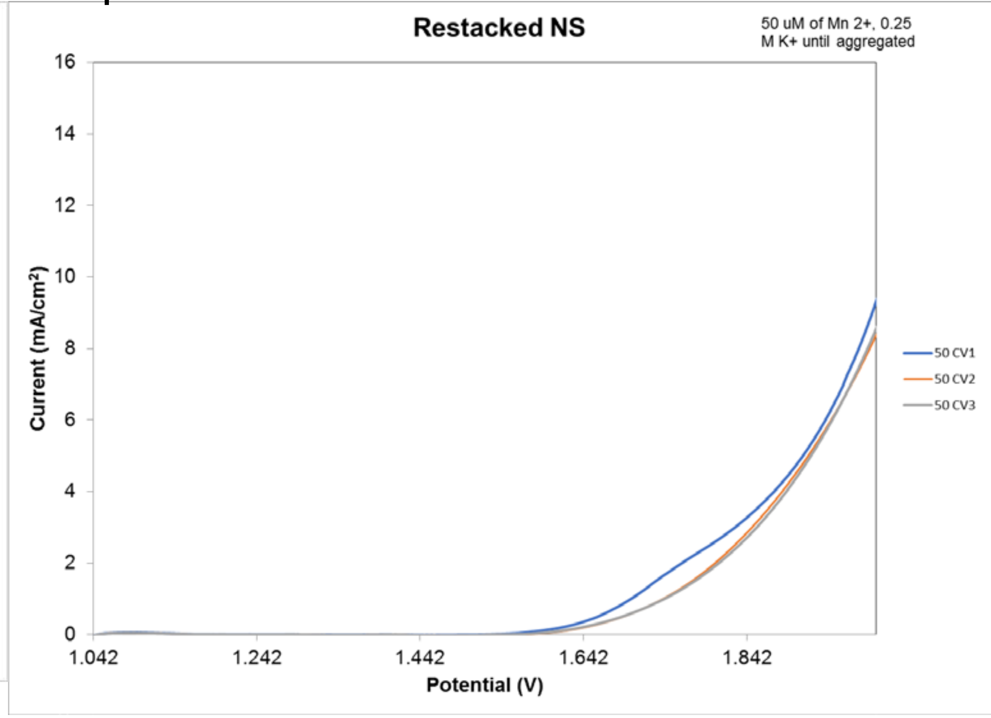

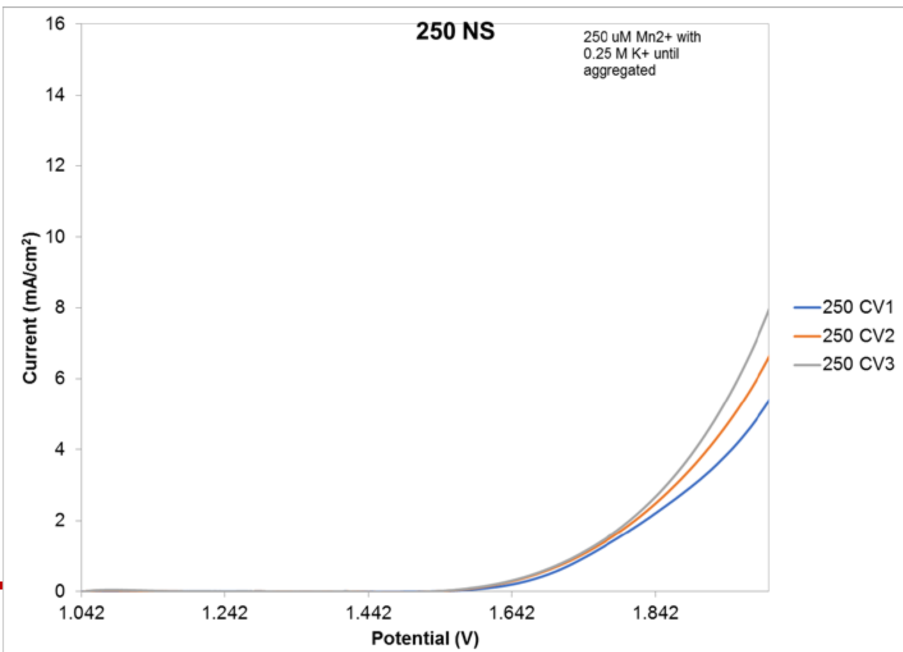

Sample	K/Mn
NS 50	0.313
SN 50	0.318
Hexagonal	0.124

Mn^{3+} is expelled from the interlayer, deactivating birnessite for water oxidation chemistry

Restacked samples

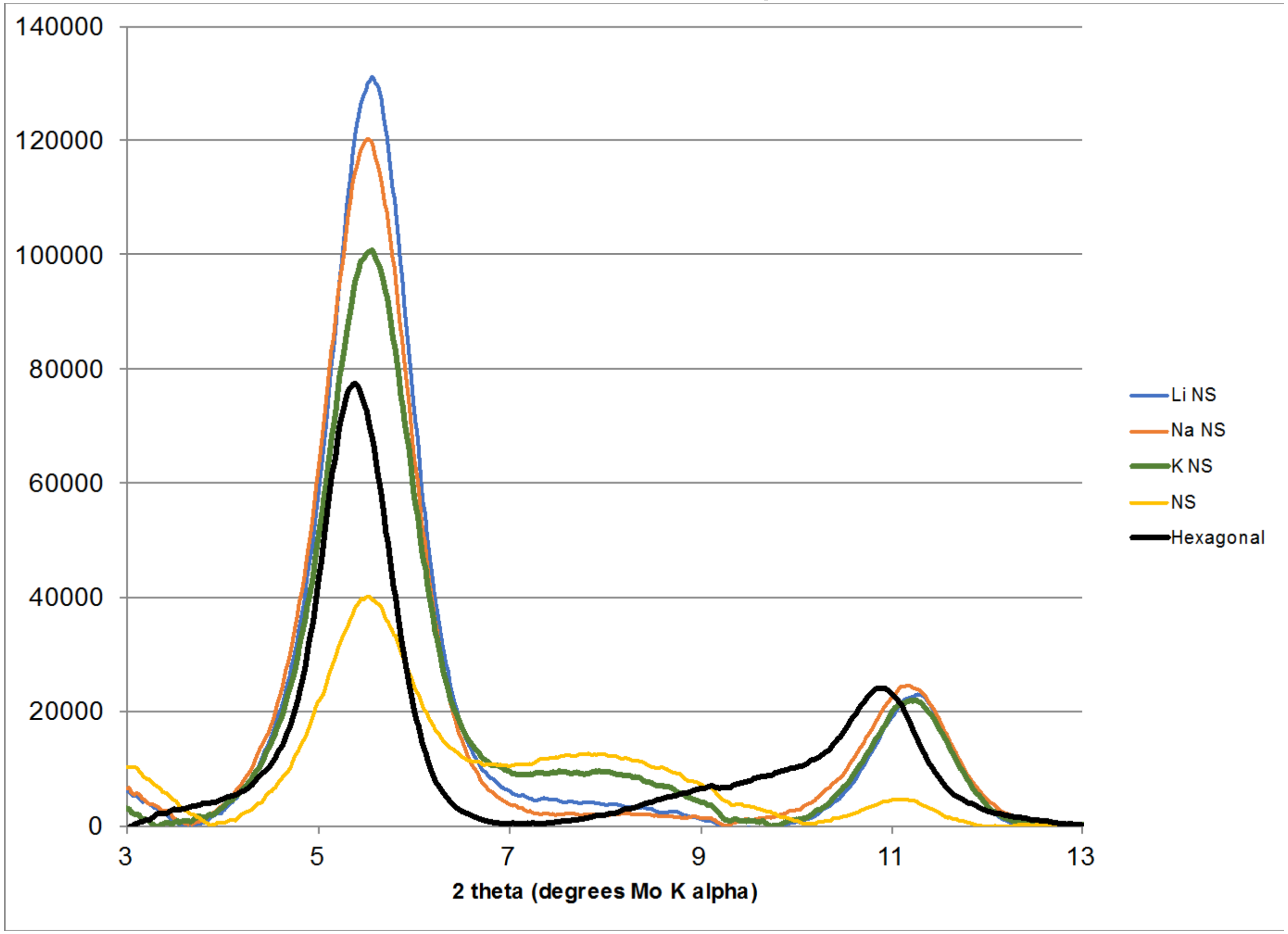

Shifts to higher 2 theta (lower d-space) indicate a contracting of interlayer space

	001	002	I_{001}/I_{002}
NS	7.47	3.68	2.56
K	7.39	3.65	2.82
Na	7.42	3.65	3.43
Li	7.37	3.63	3.67
Hexagonal	7.55	3.71	2.40

Increase of I_{001}/I_{002} indicate an increase in stacking order

Conclusion from work with nanosheets

- Nanosheet suspensions are not ideal for water oxidation
- Assembling nanosheets back into bulk birnessite can be thought of as Mn^{3+} free bulk birnessite
  - Mn^{3+} in the interlayer is key to water oxidation

- Work with bulk birnessite, manipulate bulk structure in order to improve and investigate water oxidation

Manipulation of birnessite interlayer

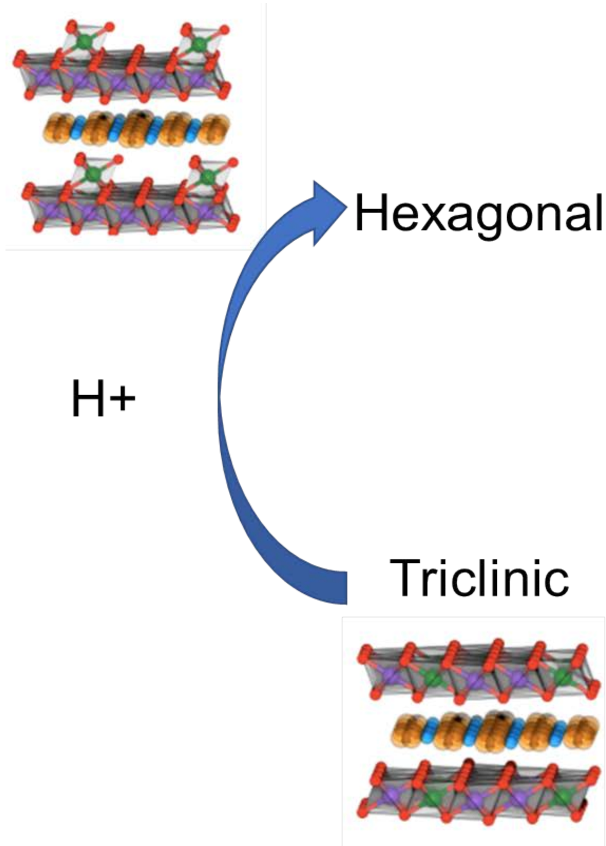

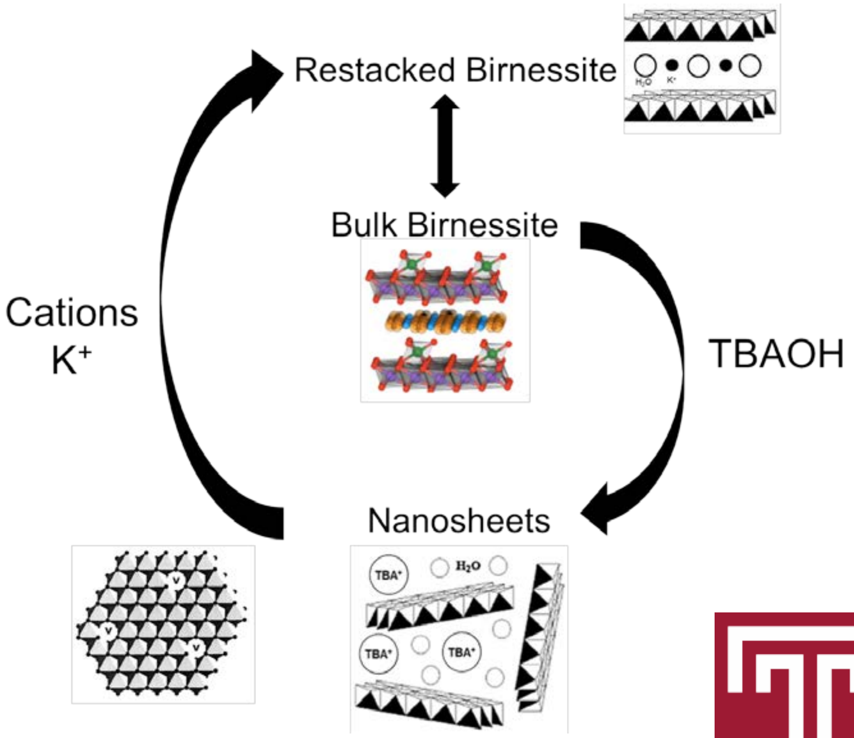

Manipulation of birnessite interlayer

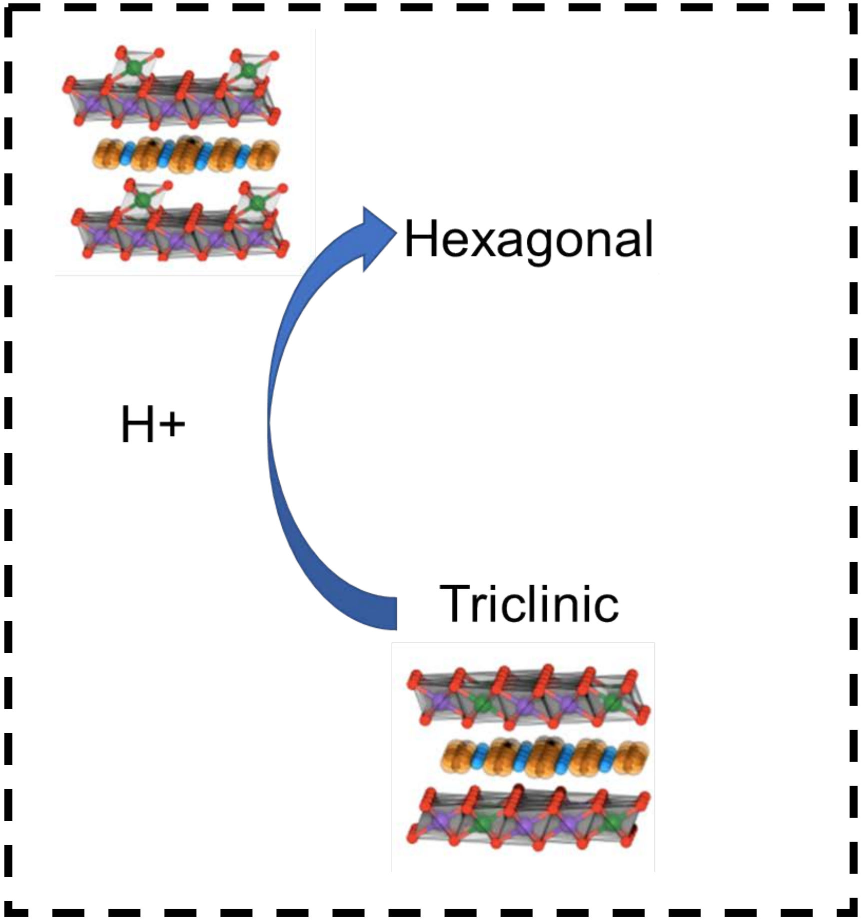

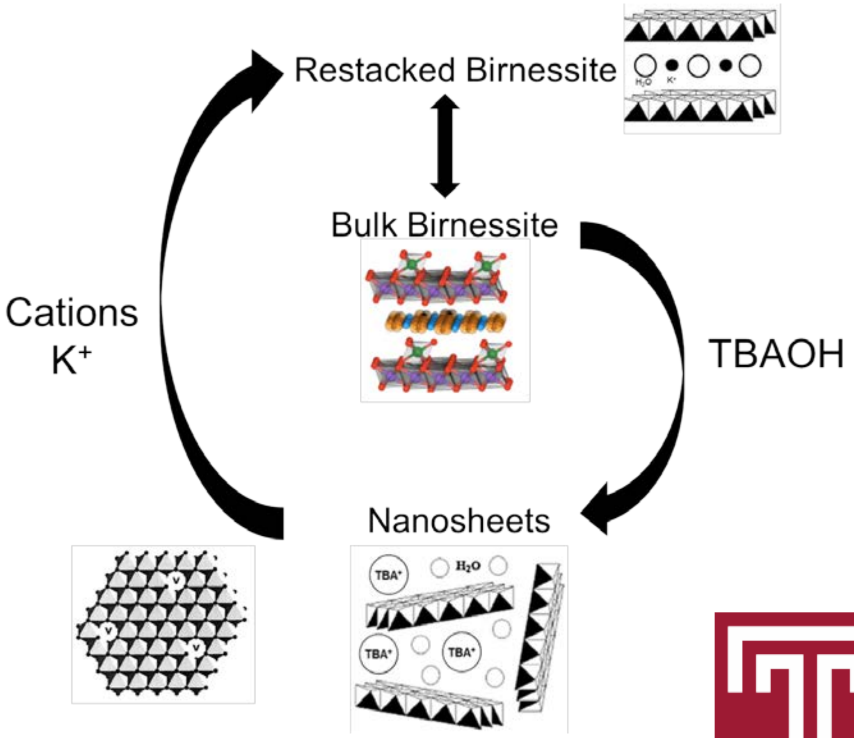

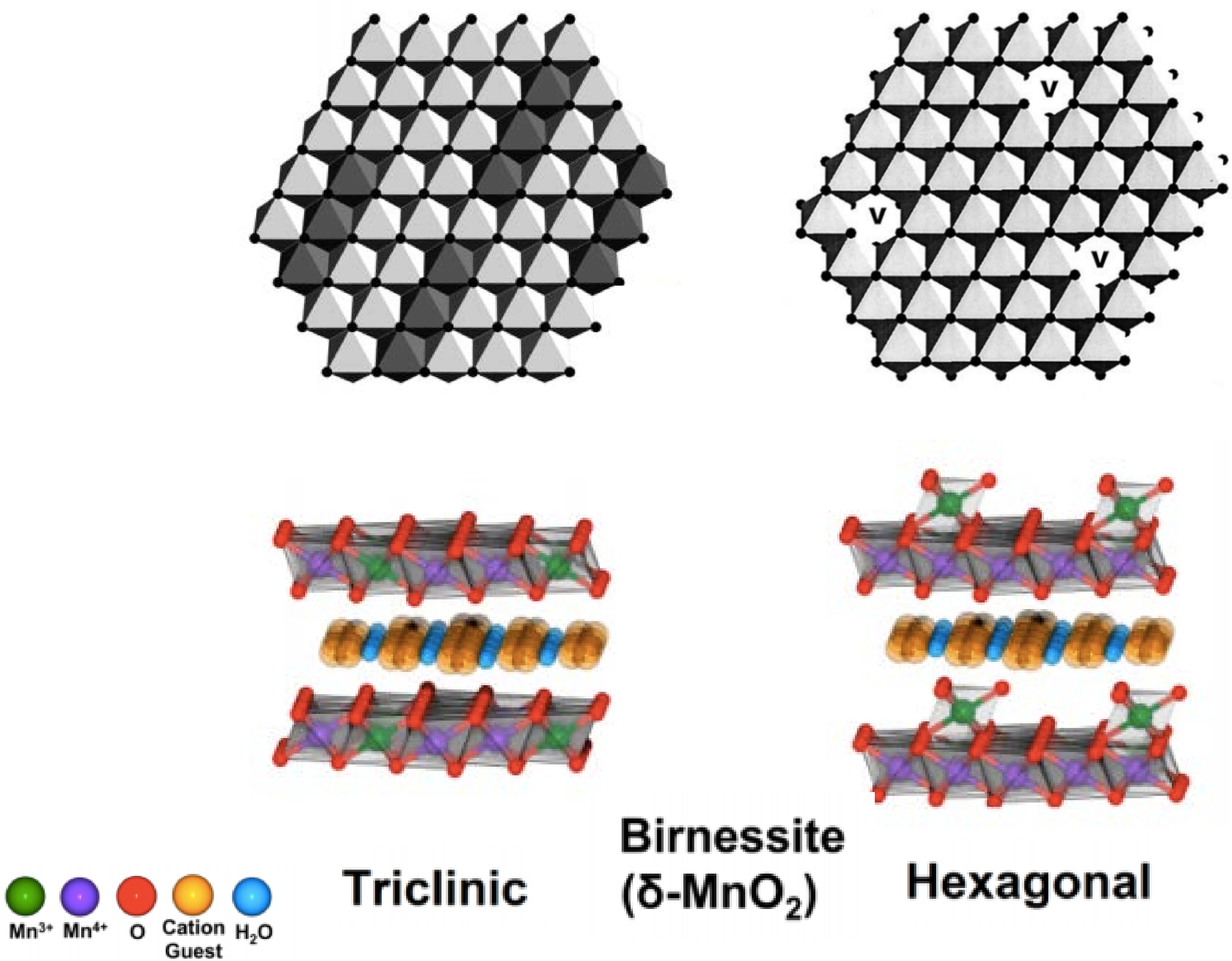

Smith, et. Al. *ACS Catal*. 2016, 6, 2089–2099
McKenzie, R. M. *Mineralogical Magazine.* 1971, 38.296, 493-502.
Yang and Wang. *Clays and Clay minerals* 50.1 (2002): 63-69.

Triclinic vs Hexagonal

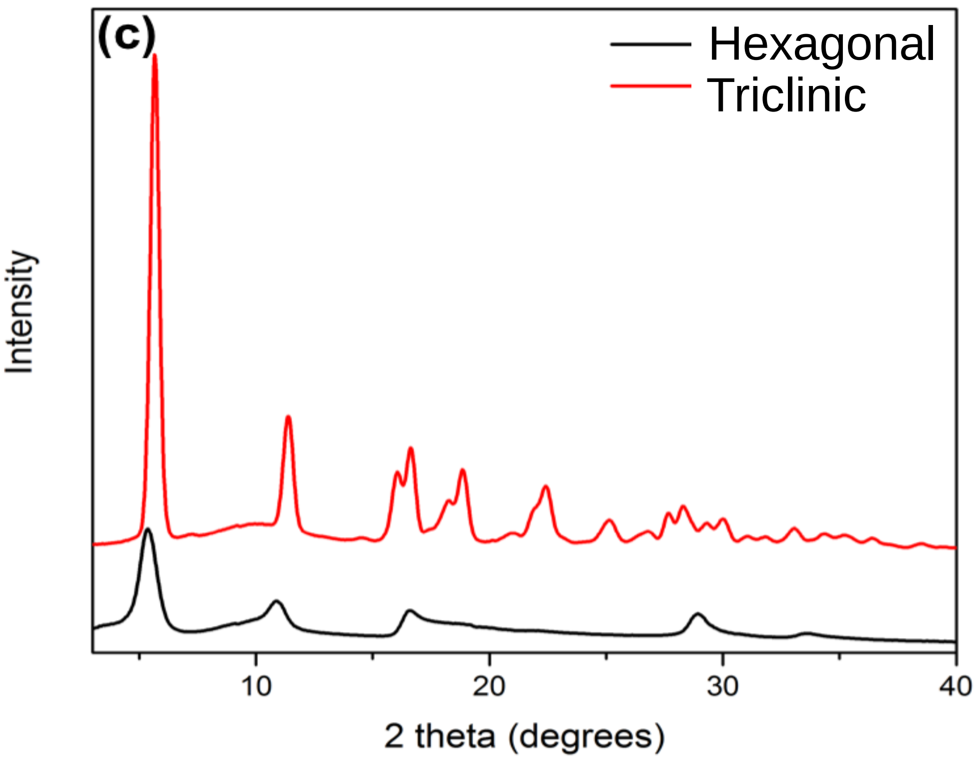

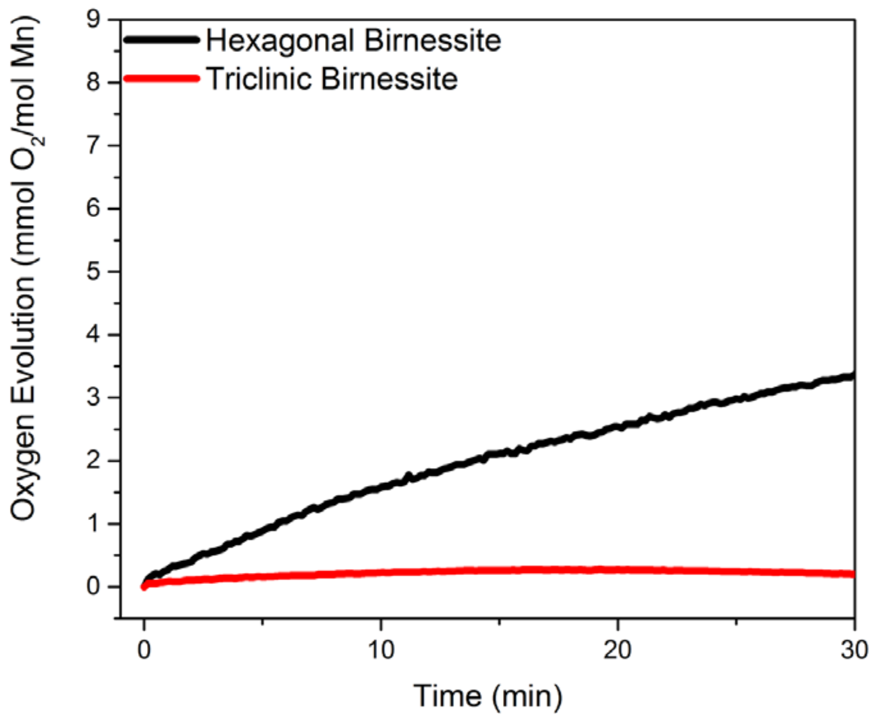

The Experiment

Transform Triclinic to Hexagonal with protons (acidic solution), measure oxygen evolution.

Experiment

- Triclinic Birnessite
  - pH 3, 18 h
  - pH 5, 18 h
  - pH 7, 18 h
- Compare to hexagonal birnessite

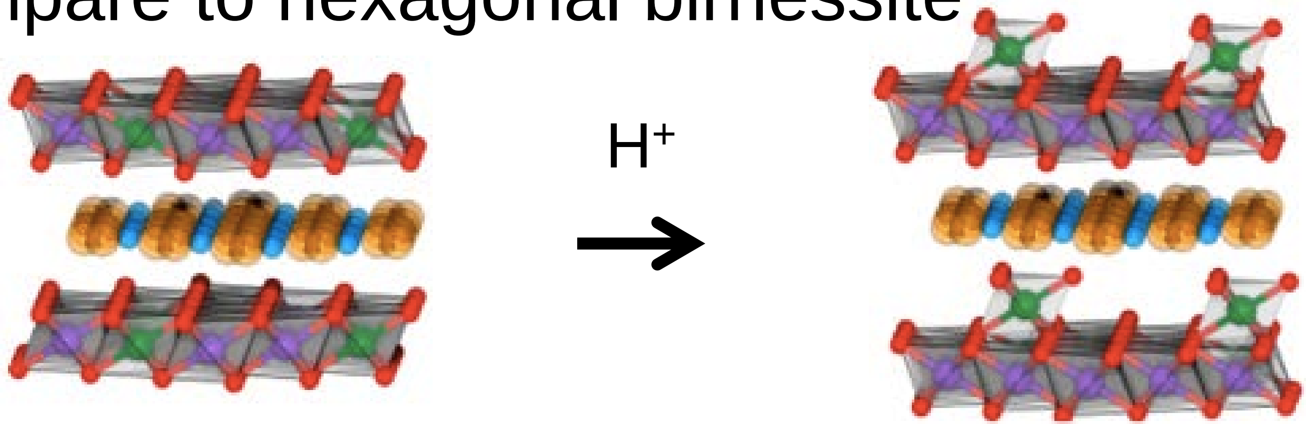

Triclinic

Hexagonal

Migration of Mn^{3+} into the interlayer

1)

H^+ →

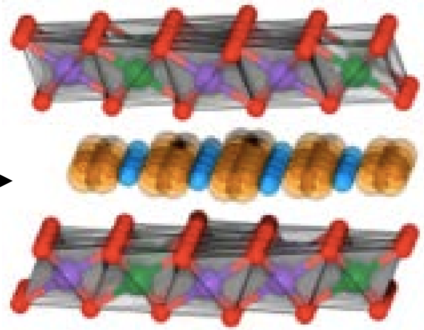

$1/3\ Na^+$ →

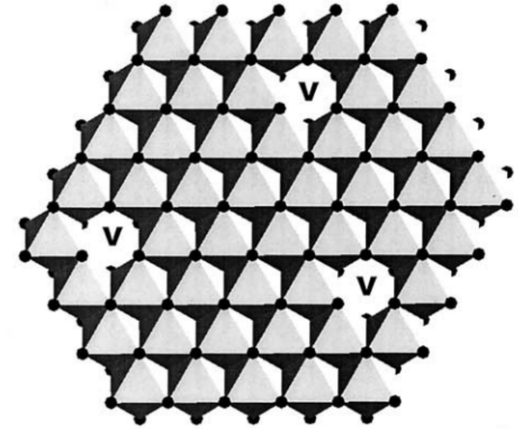

1/3 of Mn^{3+} undergoes disproportionation to Mn^{2+} and Mn^{4+}

Remaining Na^+

2) H^+ →

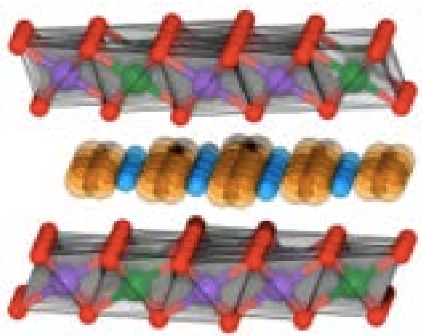

→ 1/2 Mn^{3+}_{sheet} migrates into interlayer

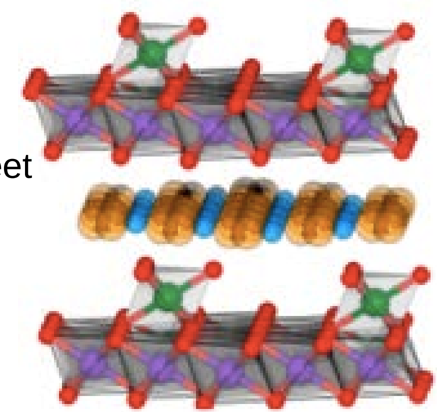

Mn^{2+} can re-adsorb above or below vacant sites

Lanson, et.al.American Mineralogist, Volume 85, pages 826–838, 2000
Villalobos, et.al. Geochimica et Cosmochimica Acta, Vol. 67, No. 14, pp. 2649–2662, 2003

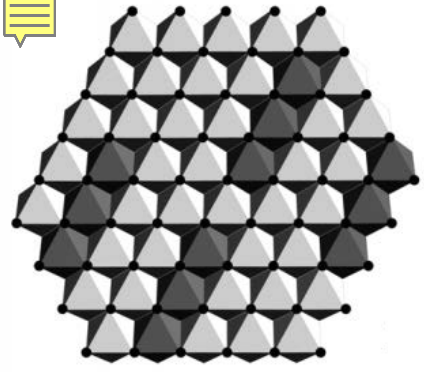

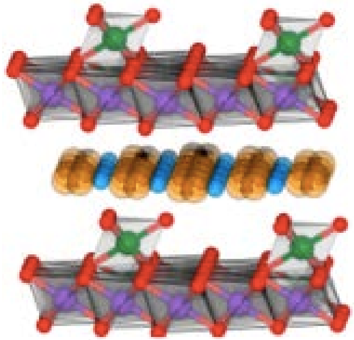

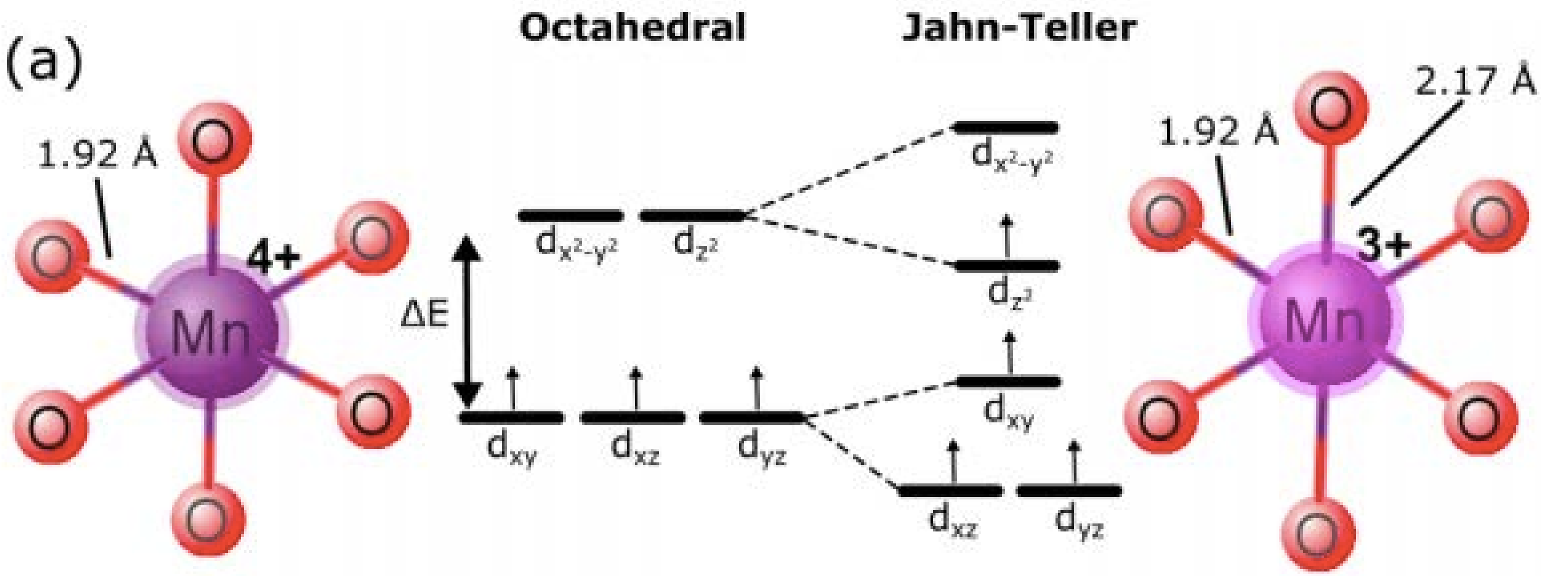

Disproportionation and migration of Mn^{3+} cations release the steric layer strain from the Jahn-Teller distortion in the former Mn^{3+} rich rows.

Lucht, et.al. J. Phys. Chem. C 2015, 119, 22838–22846
Lanson, Bruno, et al. *American Mineralogist* 85.5-6 (2000): 826-838.

Experiment

- Stir Triclinic birnessite in acidic water for 18 hr
- Hypothesis: Interlayer Mn^{3+} in transformed sample improves water oxidation

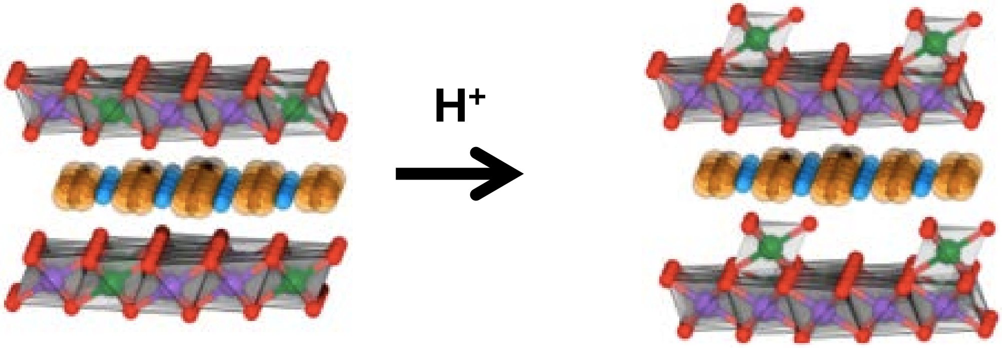

Characterization

After transformation, before chemistry

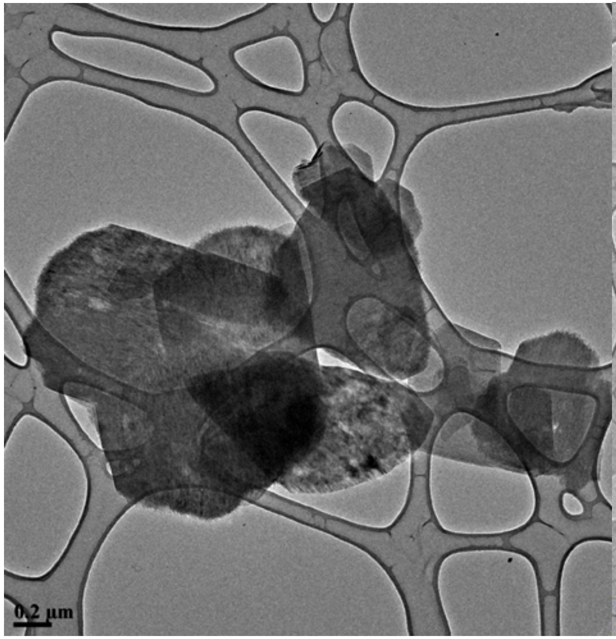

Triclinic birnessite,
pH 3, 18 hrs

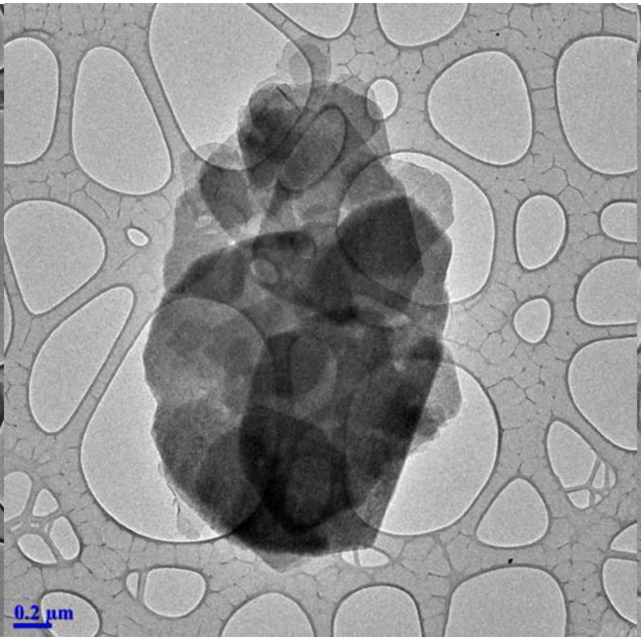

Triclinic birnessite,
pH 5 18 hr

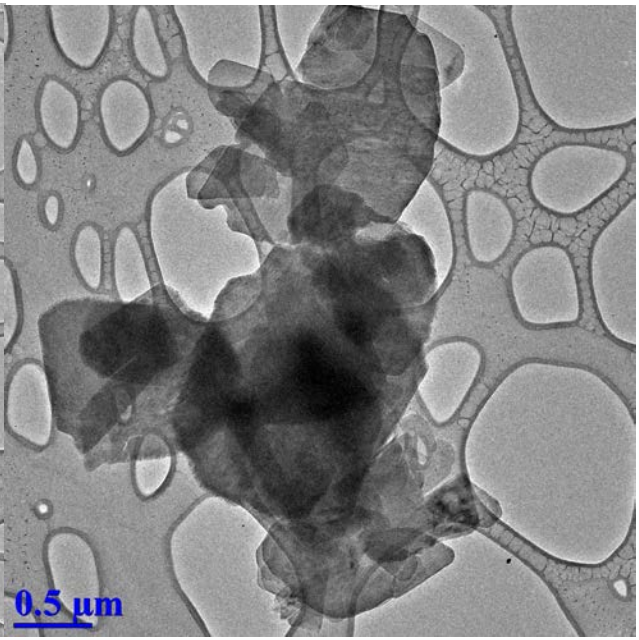

Triclinic birnessite,
pH 7 18 hr

Morphology is retained.

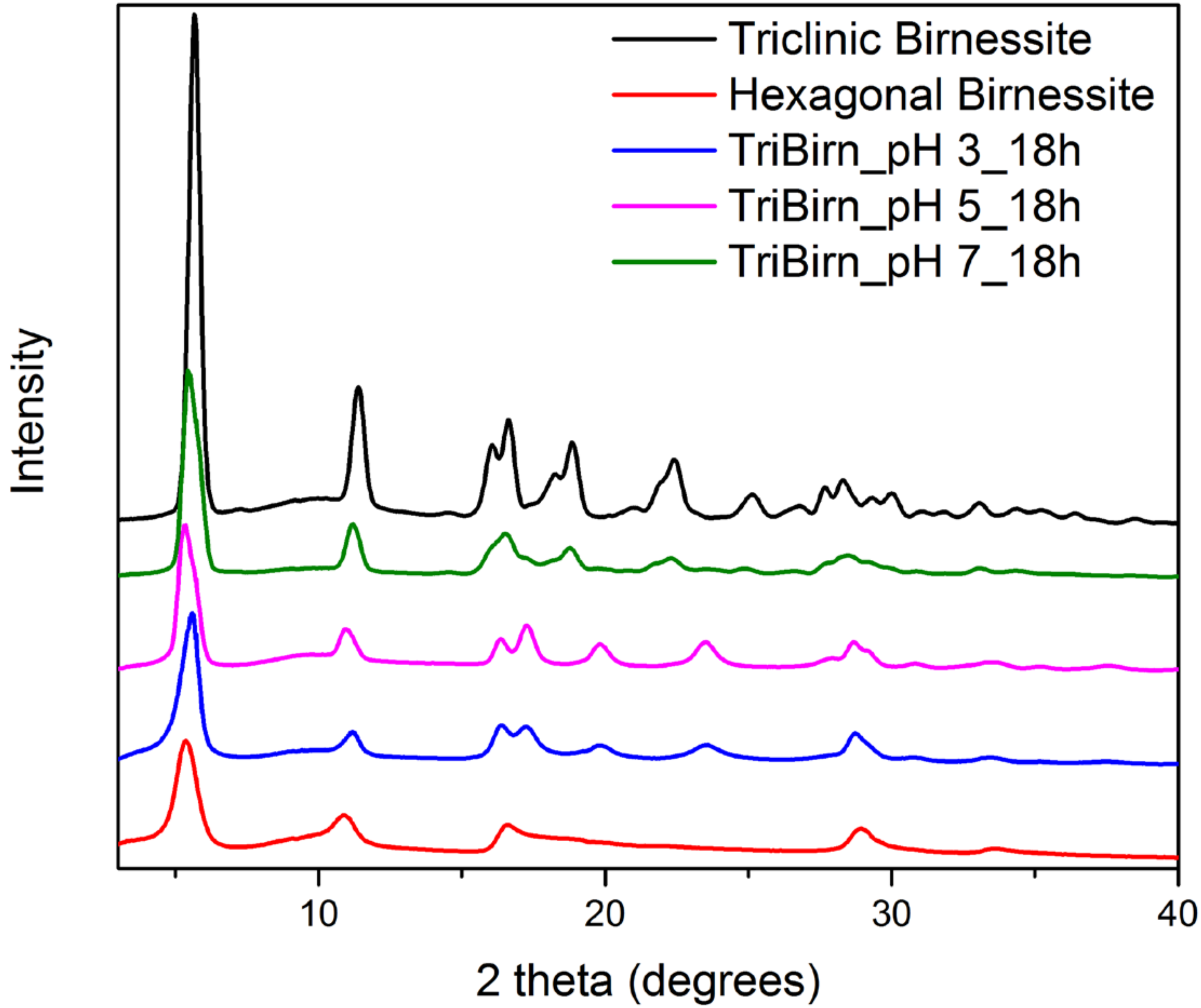

Ling, Florence T., et al. *Chemical Geology* 416 (2015): 1-10.

XRD Discussion

Shifts to lower 2 theta (higher d-space) indicate an expanding of interlayer space

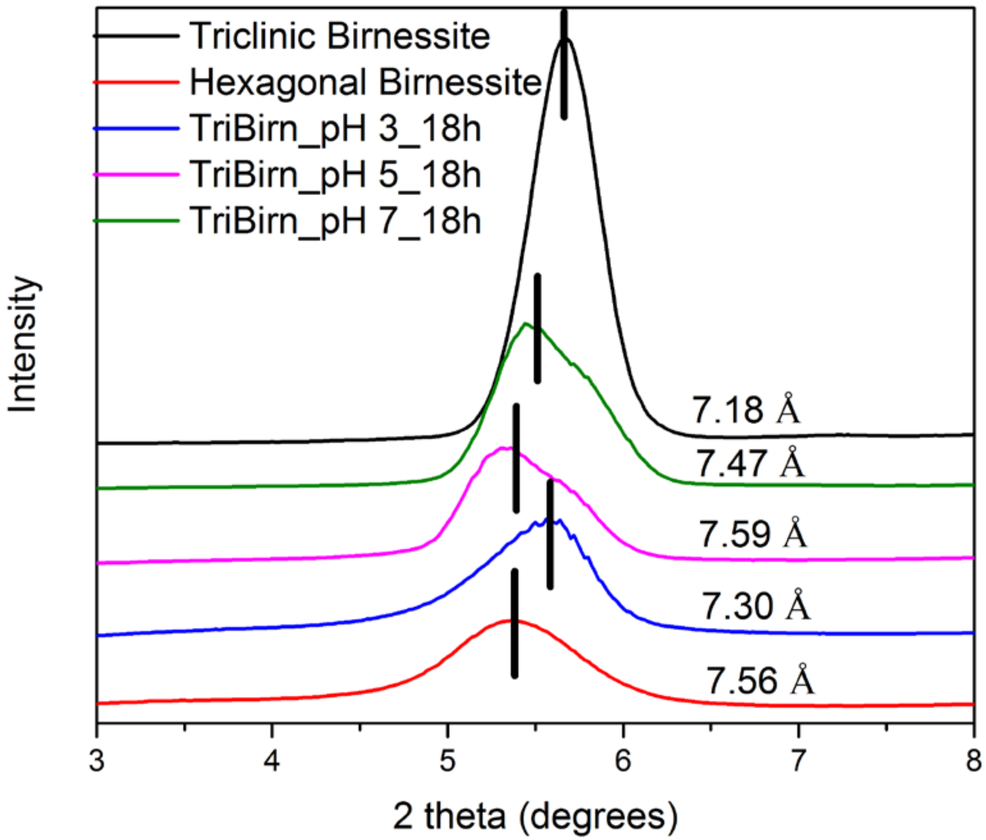

Sample	Na/Mn
Triclinic Birnessite	0.37
pH 3	0.024
pH 5	0.091
pH 7	0.27

Na^+ removal causes charge to be balanced by Mn^{3+} and H^+

Mn^{3+} causing repulsion between the sheets?

XRD Discussion

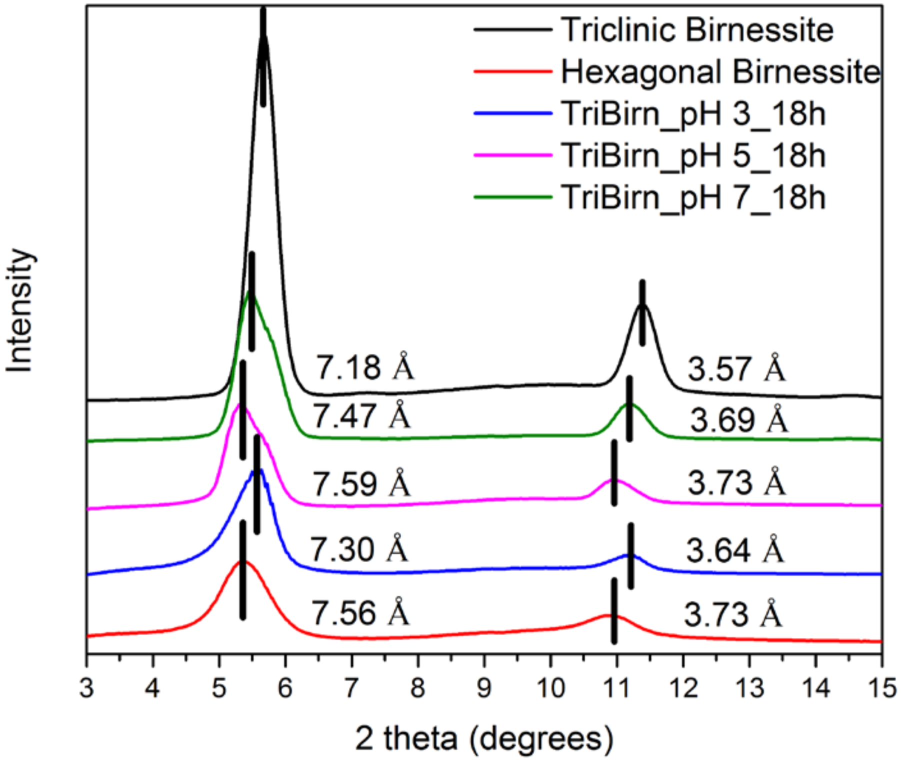

Sample	I_{001}	I_{002}	I_{001}/I_{002}
Triclinic Birnessite	550150	157008	3.50
Hexagonal Birnessite	134640	55876	2.41
pH 3	168969	44414	3.80
pH 5	161441	51993	3.10
pH 7	225008	62414	3.60

Decrease of I_{001} indicate a decrease in stacking order

Water oxidation chemistry

Experiments

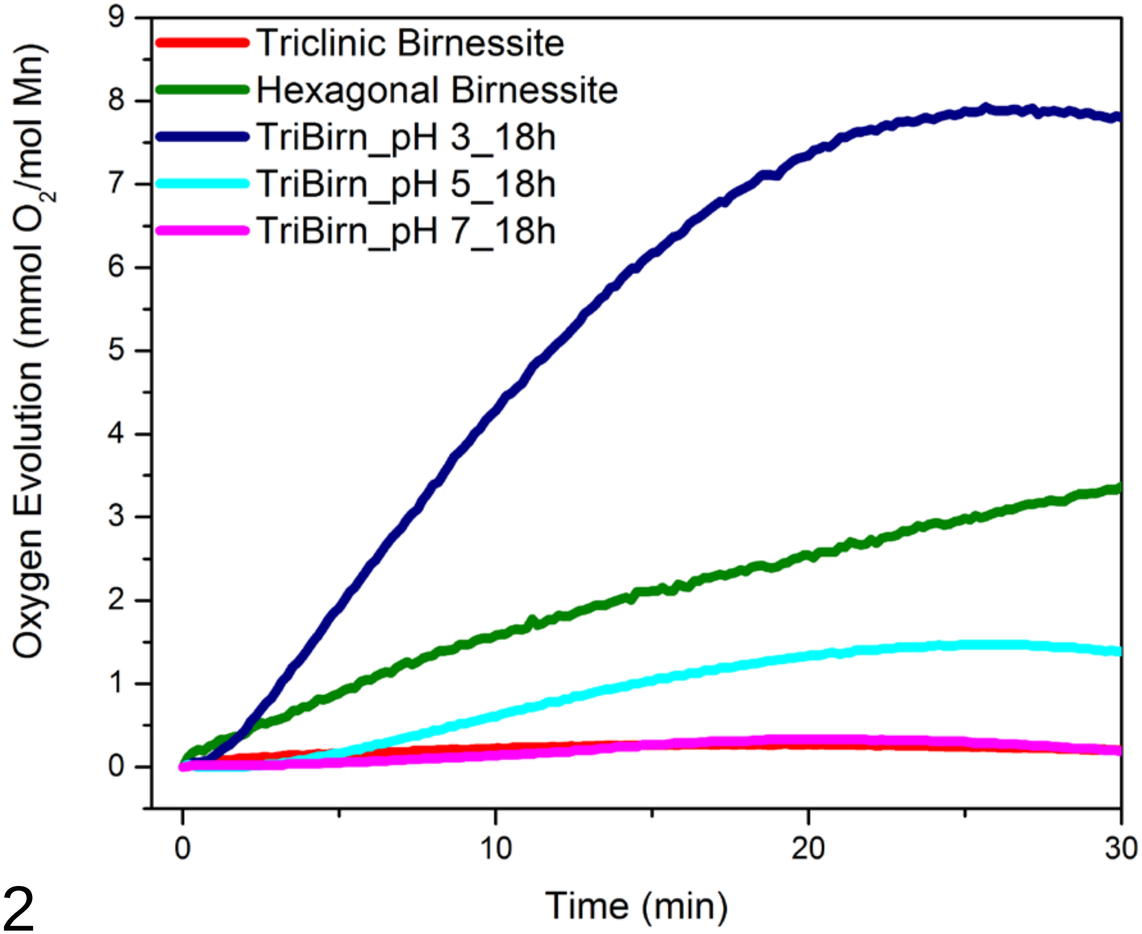

pH =2

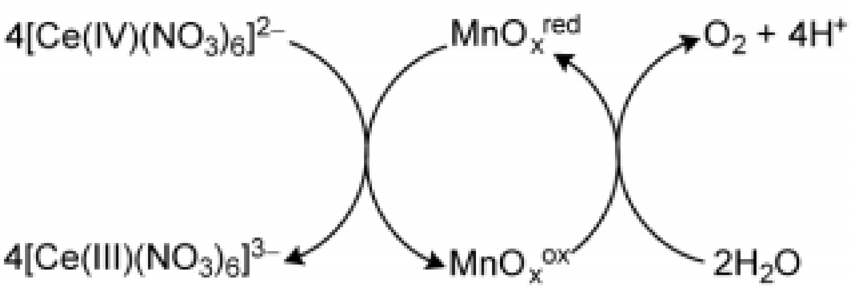

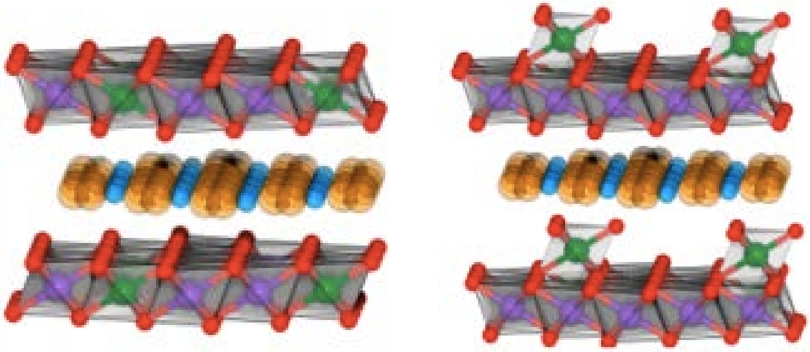

Najafpour, et al. *Dalton Transactions* 42.40 (2013): 14603-14611.

Pokhrel, et.al. J. Am. Chem. Soc. 2015, 137, 8384−8387

Electrochemistry

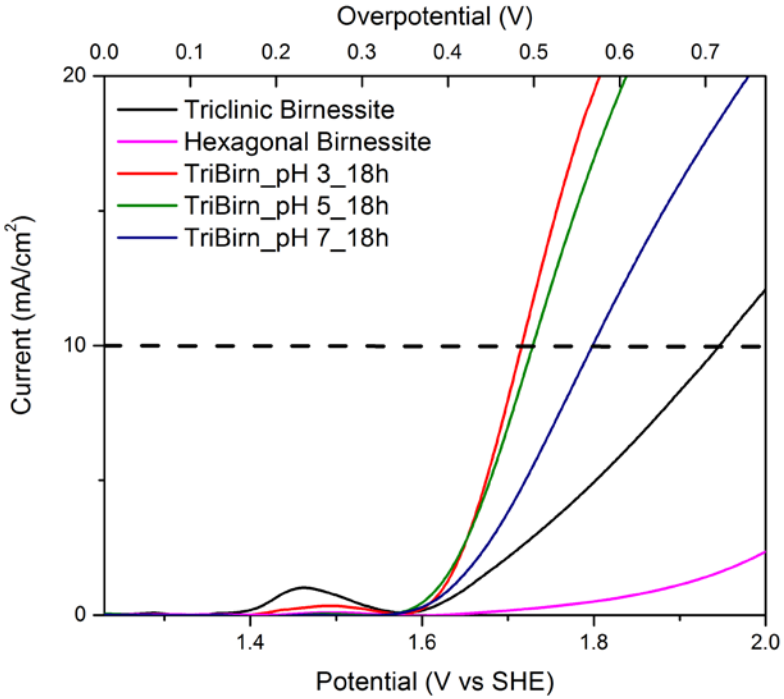

Overpotential at 10 mA/cm^2

Sample	CV 1	CV2
Triclinic Birnessite	710 mV	710 mV
Hexagonal Birnessite	--	--
pH 3	490 mV	500 mV
pH 5	510 mV	550 mV
pH 7	570 mV	550 mV

pH = 14

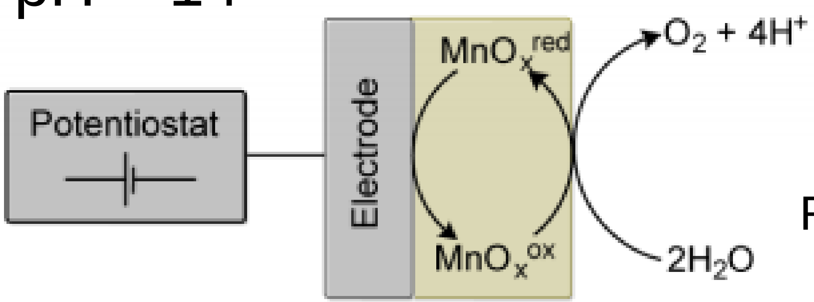

Reference

Counter

Najafpour, et al. *Dalton Transactions* 42.40 (2013): 14603-14611.

Pokhrel, et.al. J. Am. Chem. Soc. 2015, 137, 8384−8387

Electrochemistry

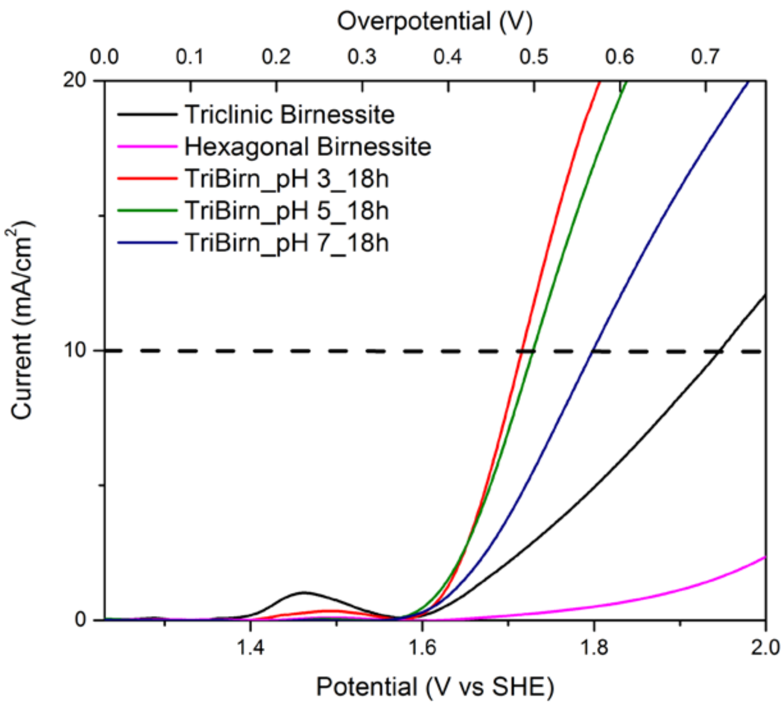

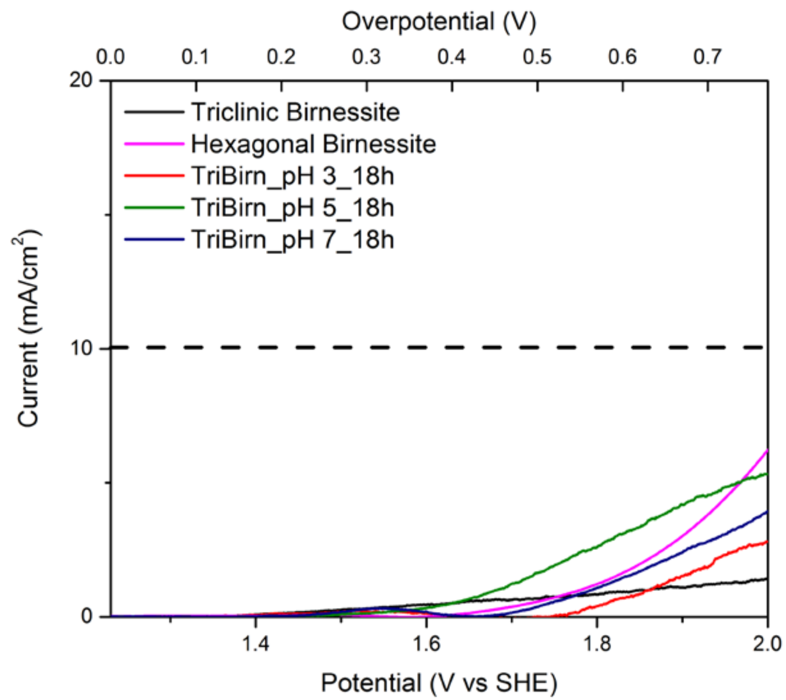

pH = 14

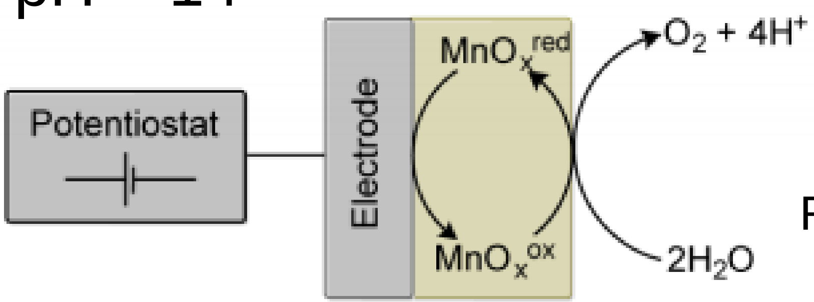

Reference

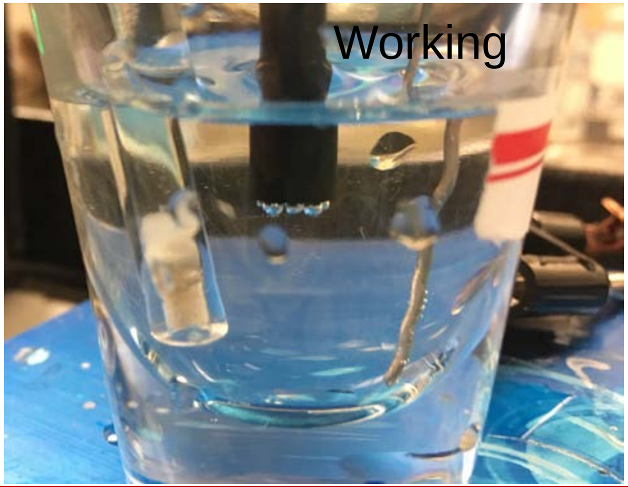

Counter

Najafpour, et al. *Dalton Transactions* 42.40 (2013): 14603-14611.

Pokhrel, et.al. J. Am. Chem. Soc. 2015, 137, 8384−8387

Sample	Overpotential
Cu-birnessite	490 mV
Ni-birnessite	400 mV
Co-birnessite	360 mV

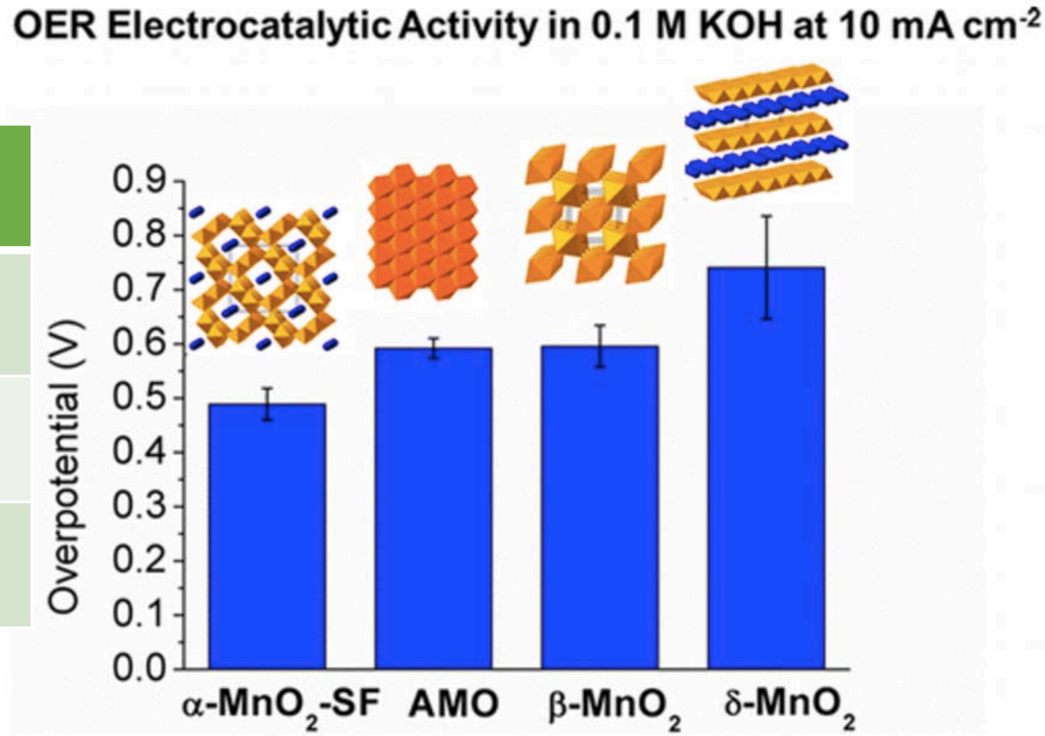

Sample	CV 1	CV2
Triclinic Birnessite	710 mV	710 mV
Hexagonal Birnessite	--	--
pH 3	490 mV	500 mV
pH 5	510 mV	550 mV
pH 7	570 mV	550 mV

Meng, et.al. J. Am. Chem. Soc., **2014**, *136* (32), pp 11452–11464 Thenuwara, Akila C., et al. "*Angewandte Chemie International Edition* (2016):10381
Thenuwara, Akila C., et al. *Langmuir* 31.46 (2015): 12807-12813. Thenuwara, Akila C., et al. *ACS Catalysis* 6.11 (2016): 7739-7743.

Ceric Experiment

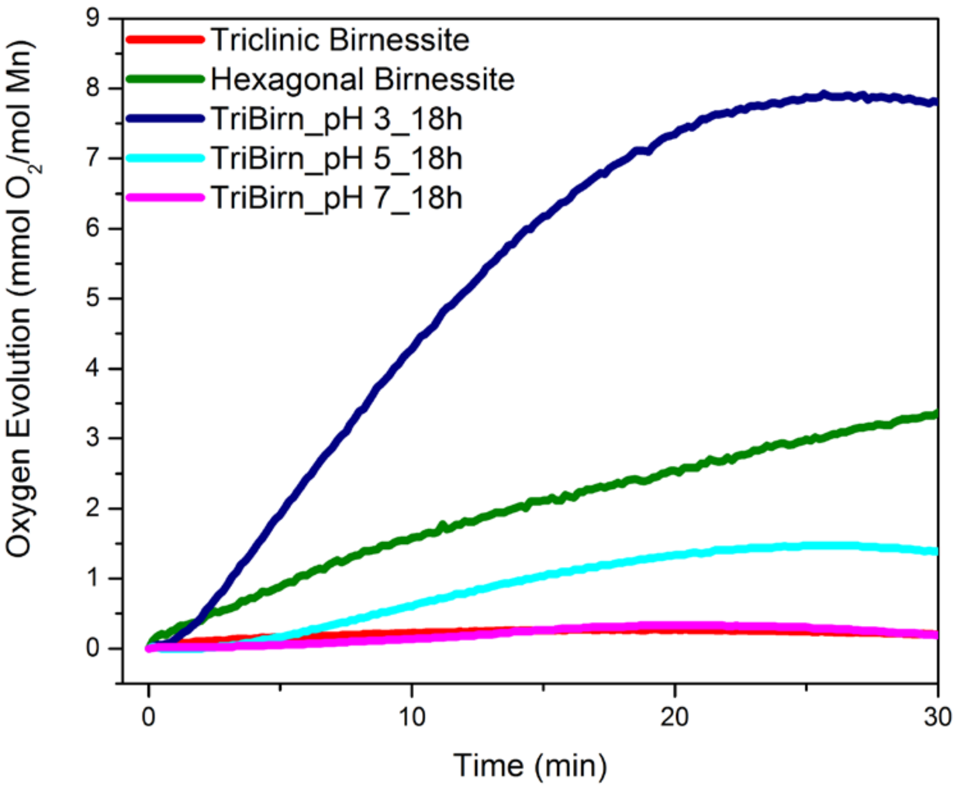

Electrochemistry

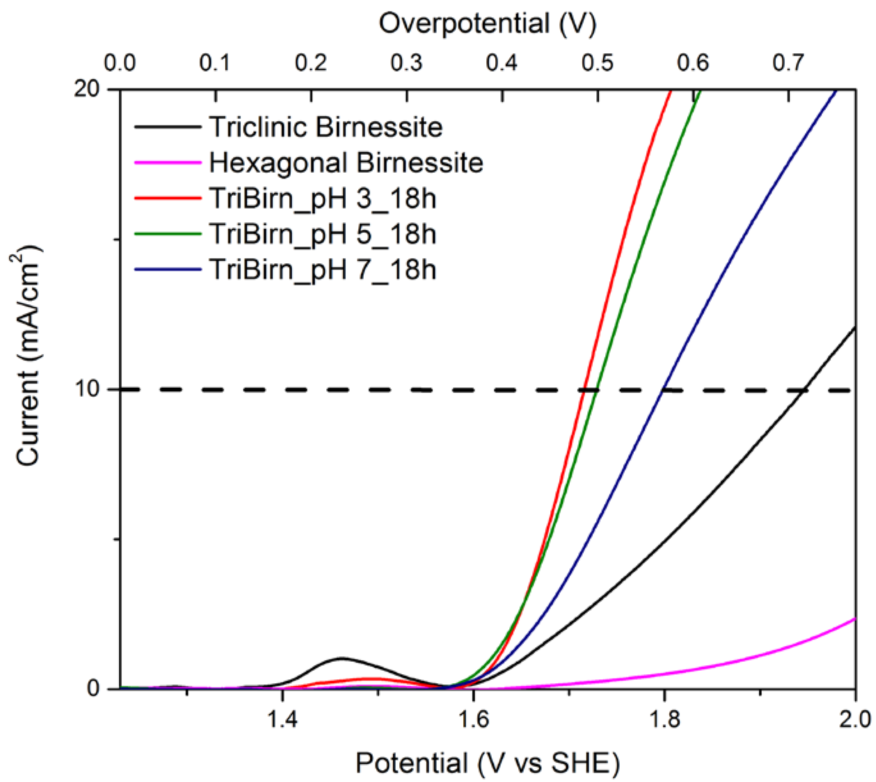

Overall trend is the same: pH 3 is best performing

Hexagonal is active for ceric but not for electrochemistry

Birnessite samples (triclinic transformed to hexagonal at pH 3 and 5 as well as hexagonal sample) Stability testing **STATIC.** *Constant current (5mA).*

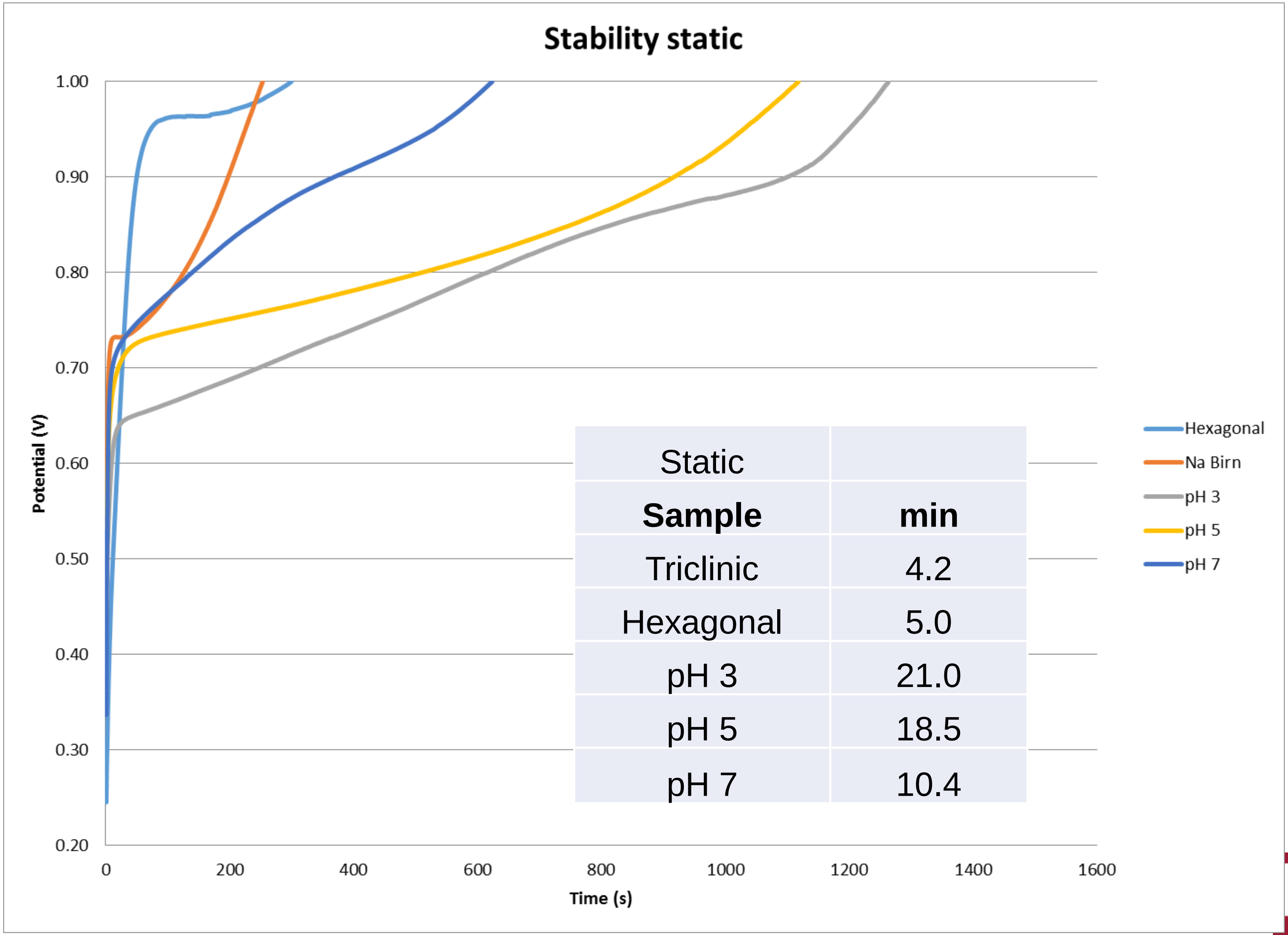

Static	
Sample	**min**
Triclinic	4.2
Hexagonal	5.0
pH 3	21.0
pH 5	18.5
pH 7	10.4

Characterization

After electrochemisty/ceric experiments

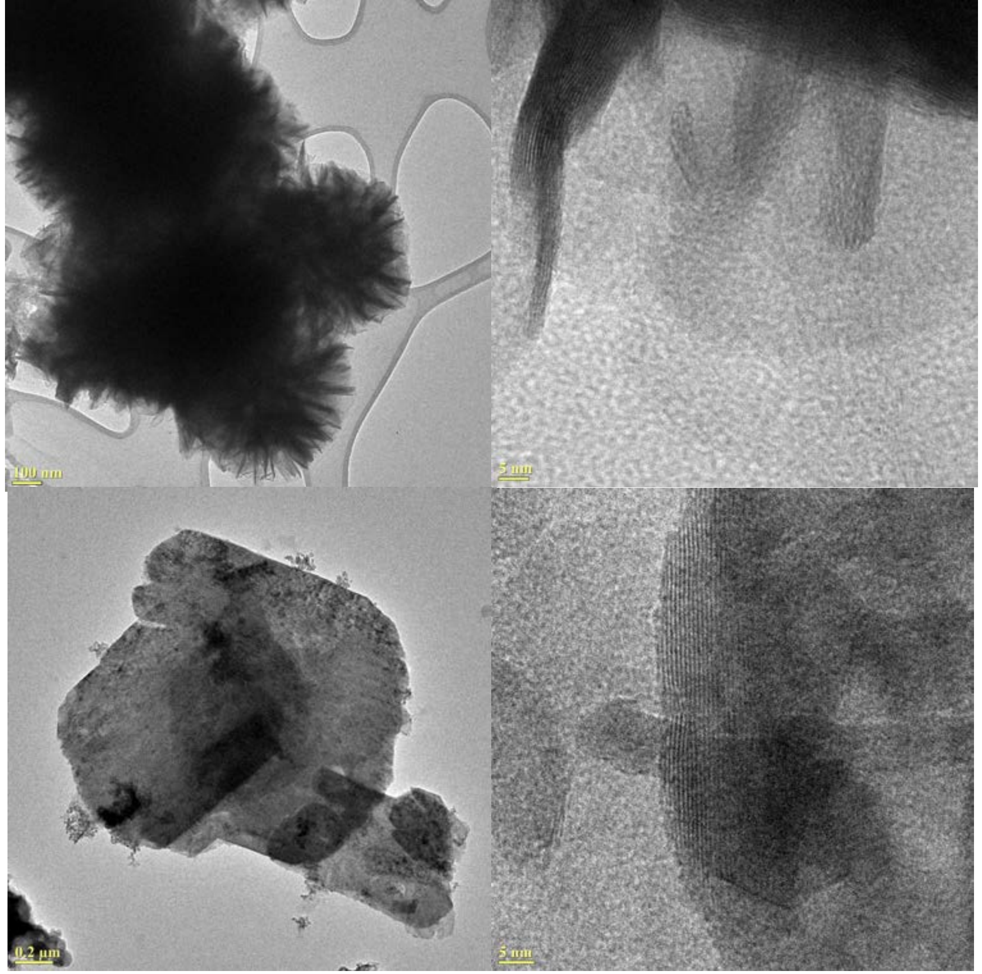

Sample	K/Mn
NS 50	0.312
SN 50	0.317
Hexagonal	0.124
Hexagonal TBA	0.082
Hexagonal after echem	0.176

Mn^{3+} removed from interlayer and replaced by K?

After Electrochemistry Characterization

Tri Birn	Tri Birn Af echem	pH 3	pH 3 af echem	pH 5	pH 5 af e chem	Hexagonal	Hex af echem
7.13	7.09	7.28	7.00	7.30	7.05	7.55	7.39
3.56	3.55	3.63	3.49	3.64	3.53	3.71	3.63

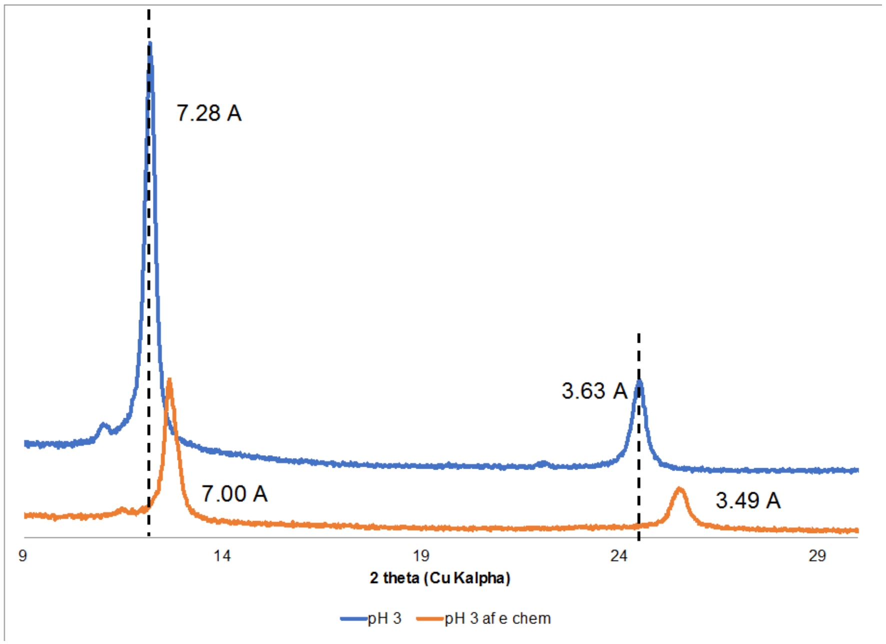

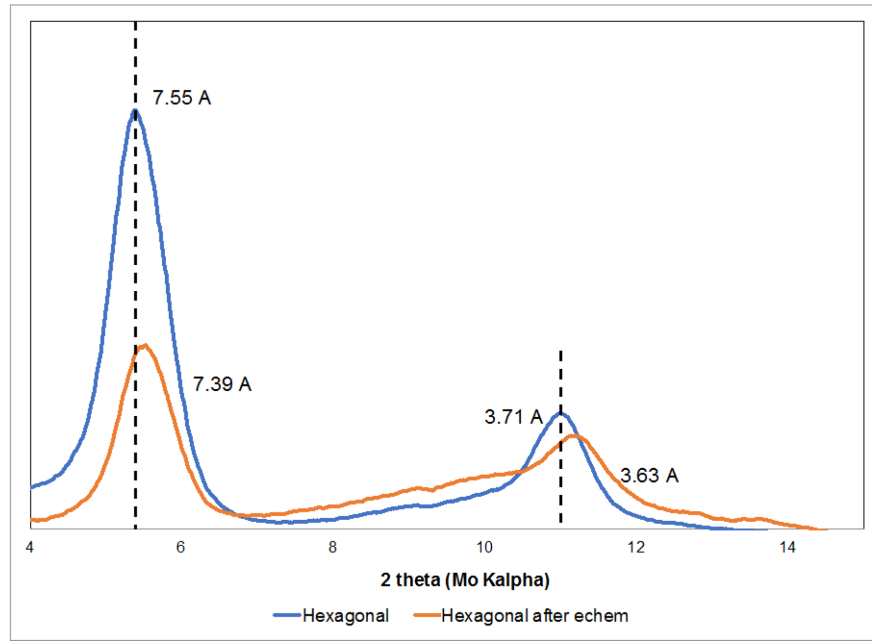

Shifts to higher 2 theta (lower d-space) indicate a contracting of interlayer space

Mn^{3+} removal?

XPS Characterization

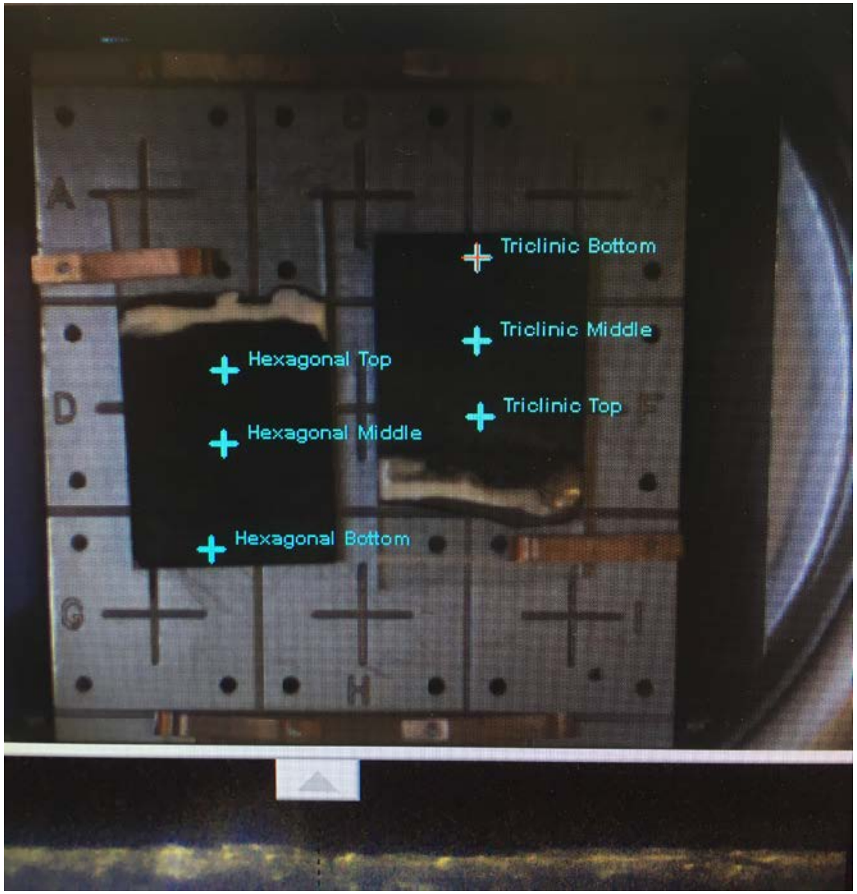

Hexagonal	
Before Electrochem	After Electrochem
3.47	3.51

Triclinic	
Before Electrochem	After Electrochem
3.45	3.52

Very small increase in surface AOS

More Mn(IV)?

Conclusions

- Interlayer species is key to activity
  - Mn^{3+} must be contained between sheets to create unique environment
  - Previously inactive phase can be activated by inducing migration of Mn^{3+} into the interlayer
- Post catalysis characterization indicates possible removal of Mn^{3+} from the interlayer space
- Future work
  - Characterization of post-electrochemistry samples

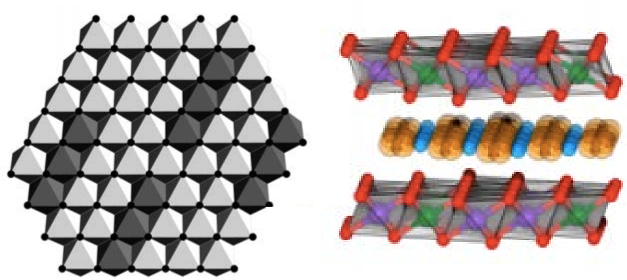

$$2\,H_2O \rightarrow O_2 + 4H^+ + 4e^-$$

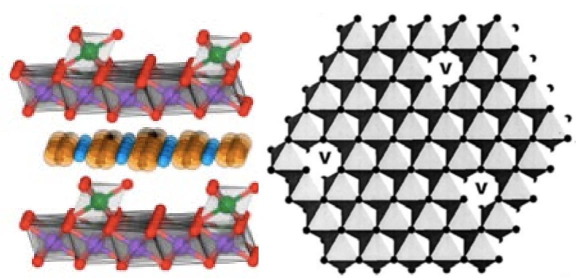

Acknowledgements

- Dr. Daniel Strongin
- Dr. Michael Zdilla
- Dr. Eric Borguet
- Akila Thenuwara
- Nuwan Attanayake
- Ian McKendry
- Qing Kang
- Loranne Vernisse
- Yaroslav Aulin
- Rick Remsing
- Haowei Peng

Questions?

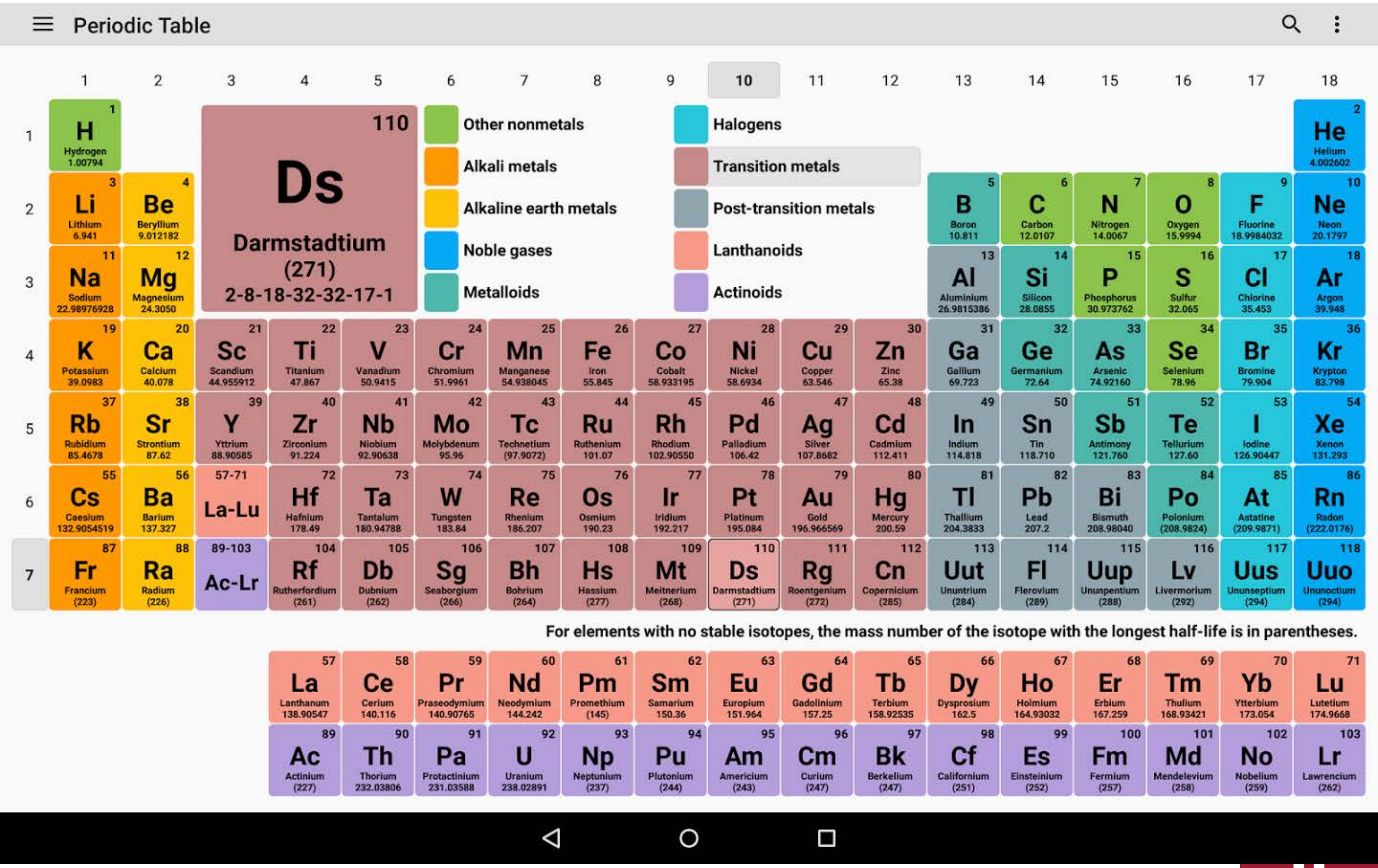

Periodic Table

110 Ds Darmstadtium (271) 2-8-18-32-32-17-1

Other nonmetals · Alkali metals · Alkaline earth metals · Noble gases · Metalloids · Halogens · Transition metals · Post-transition metals · Lanthanoids · Actinoids

	1	2	3	4	5	6	7	8	9	10	11	12	13	14	15	16	17	18
1	1 H Hydrogen 1.00794																	2 He Helium 4.002602
2	3 Li Lithium 6.941	4 Be Beryllium 9.012182											5 B Boron 10.811	6 C Carbon 12.0107	7 N Nitrogen 14.0067	8 O Oxygen 15.9994	9 F Fluorine 18.9984032	10 Ne Neon 20.1797
3	11 Na Sodium 22.98976928	12 Mg Magnesium 24.3050											13 Al Aluminium 26.9815386	14 Si Silicon 28.0855	15 P Phosphorus 30.973762	16 S Sulfur 32.065	17 Cl Chlorine 35.453	18 Ar Argon 39.948
4	19 K Potassium 39.0983	20 Ca Calcium 40.078	21 Sc Scandium 44.955912	22 Ti Titanium 47.867	23 V Vanadium 50.9415	24 Cr Chromium 51.9961	25 Mn Manganese 54.938045	26 Fe Iron 55.845	27 Co Cobalt 58.933195	28 Ni Nickel 58.6934	29 Cu Copper 63.546	30 Zn Zinc 65.38	31 Ga Gallium 69.723	32 Ge Germanium 72.64	33 As Arsenic 74.92160	34 Se Selenium 78.96	35 Br Bromine 79.904	36 Kr Krypton 83.798
5	37 Rb Rubidium 85.4678	38 Sr Strontium 87.62	39 Y Yttrium 88.90585	40 Zr Zirconium 91.224	41 Nb Niobium 92.90638	42 Mo Molybdenum 95.96	43 Tc Technetium (97.9072)	44 Ru Ruthenium 101.07	45 Rh Rhodium 102.90550	46 Pd Palladium 106.42	47 Ag Silver 107.8682	48 Cd Cadmium 112.411	49 In Indium 114.818	50 Sn Tin 118.710	51 Sb Antimony 121.760	52 Te Tellurium 127.60	53 I Iodine 126.90447	54 Xe Xenon 131.293
6	55 Cs Caesium 132.9054519	56 Ba Barium 137.327	57-71 La-Lu	72 Hf Hafnium 178.49	73 Ta Tantalum 180.94788	74 W Tungsten 183.84	75 Re Rhenium 186.207	76 Os Osmium 190.23	77 Ir Iridium 192.217	78 Pt Platinum 195.084	79 Au Gold 196.966569	80 Hg Mercury 200.59	81 Tl Thallium 204.3833	82 Pb Lead 207.2	83 Bi Bismuth 208.98040	84 Po Polonium (208.9824)	85 At Astatine (209.9871)	86 Rn Radon (222.0176)
7	87 Fr Francium (223)	88 Ra Radium (226)	89-103 Ac-Lr	104 Rf Rutherfordium (261)	105 Db Dubnium (262)	106 Sg Seaborgium (266)	107 Bh Bohrium (264)	108 Hs Hassium (277)	109 Mt Meitnerium (268)	110 Ds Darmstadtium (271)	111 Rg Roentgenium (272)	112 Cn Copernicium (285)	113 Uut Ununtrium (284)	114 Fl Flerovium (289)	115 Uup Ununpentium (288)	116 Lv Livermorium (292)	117 Uus Ununseptium (294)	118 Uuo Ununoctium (294)

For elements with no stable isotopes, the mass number of the isotope with the longest half-life is in parentheses.

57 La Lanthanum 138.90547	58 Ce Cerium 140.116	59 Pr Praseodymium 140.90765	60 Nd Neodymium 144.242	61 Pm Promethium (145)	62 Sm Samarium 150.36	63 Eu Europium 151.964	64 Gd Gadolinium 157.25	65 Tb Terbium 158.92535	66 Dy Dysprosium 162.5	67 Ho Holmium 164.93032	68 Er Erbium 167.259	69 Tm Thulium 168.93421	70 Yb Ytterbium 173.054	71 Lu Lutetium 174.9668
89 Ac Actinium (227)	90 Th Thorium 232.03806	91 Pa Protactinium 231.03588	92 U Uranium 238.02891	93 Np Neptunium (237)	94 Pu Plutonium (244)	95 Am Americium (243)	96 Cm Curium (247)	97 Bk Berkelium (247)	98 Cf Californium (251)	99 Es Einsteinium (252)	100 Fm Fermium (257)	101 Md Mendelevium (258)	102 No Nobelium (259)	103 Lr Lawrencium (262)

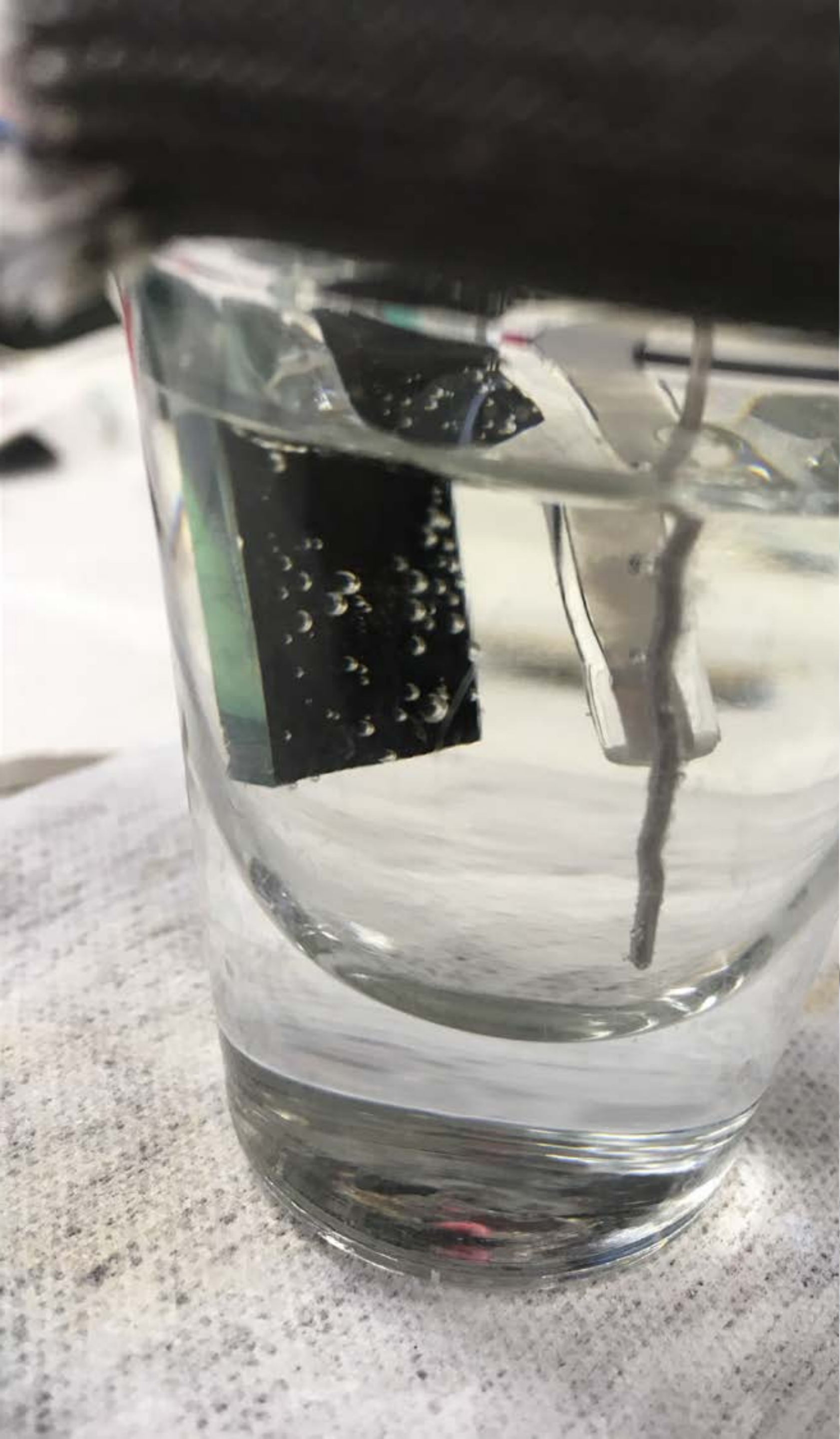
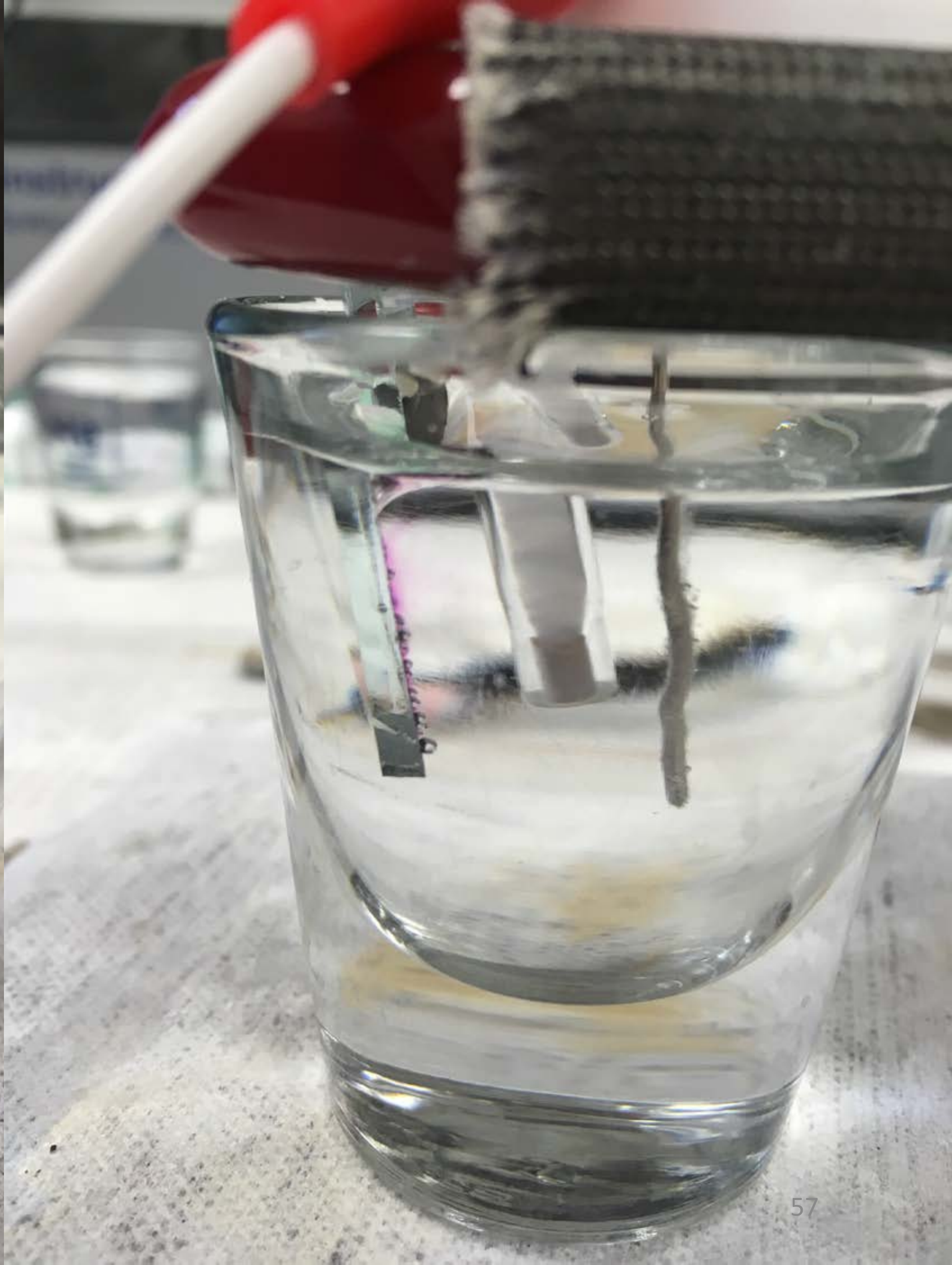

CONTROL EXPT: KMnO4 in 1M KOH with time

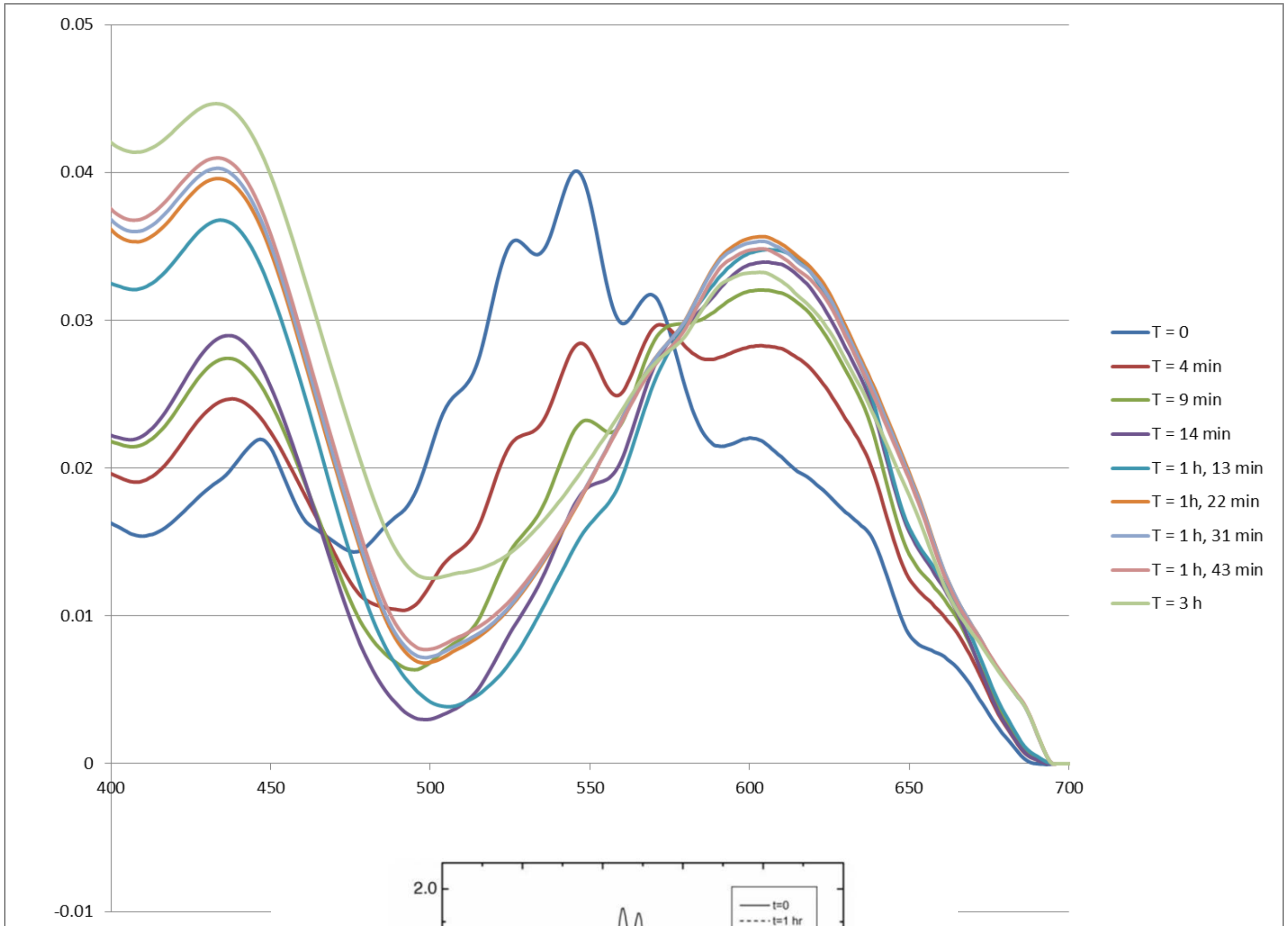

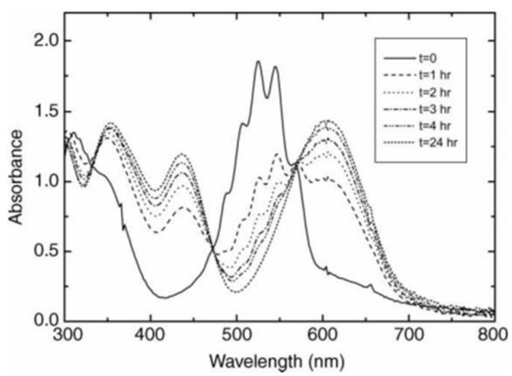

Figure 1. UV-Visible spectral changes for permanganate conversion to manganate as a function of time in 3.0 M NaOH.

Mn 7+ → Mn 6+
The formation of a manganate(VI) intermediate was also consistent with the green color observed as the reaction proceeded [30]
The appearance of two isosbestic points at wavelengths 575 and 473 nm during the courses of the reactions indicates the interconversion of Mn(VII) to both Mn(VI) and Mn(IV), as MnO2, respectively

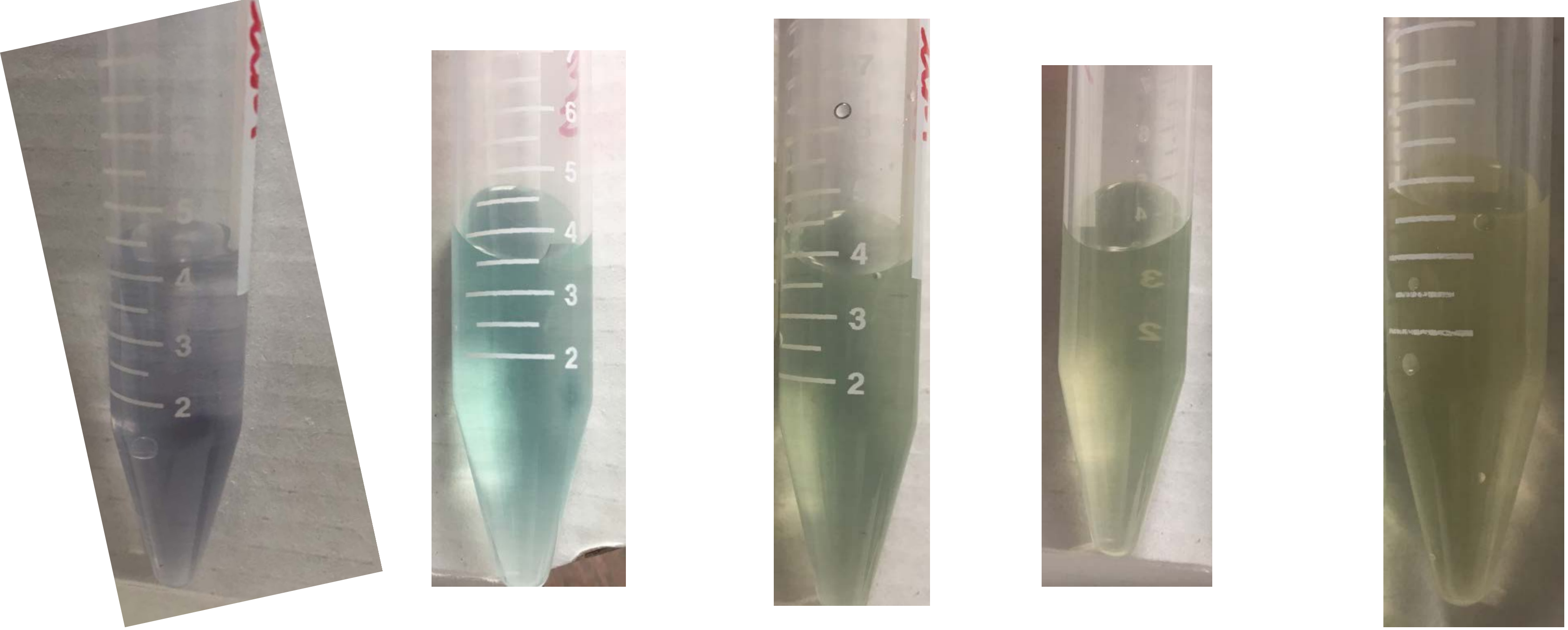

T 1 min

T 4 h

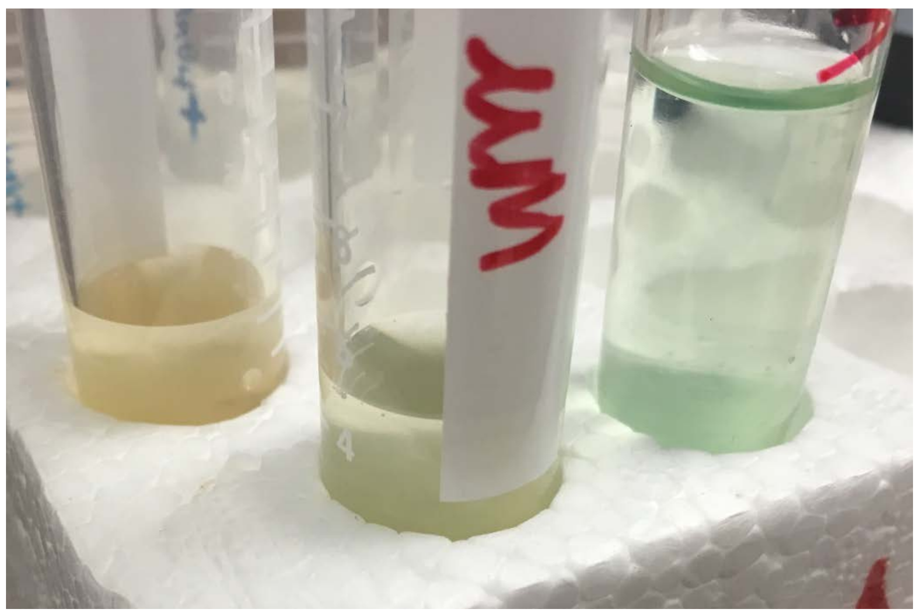

UV-vis Raw data Baseline corrected using manual baseline in Origin

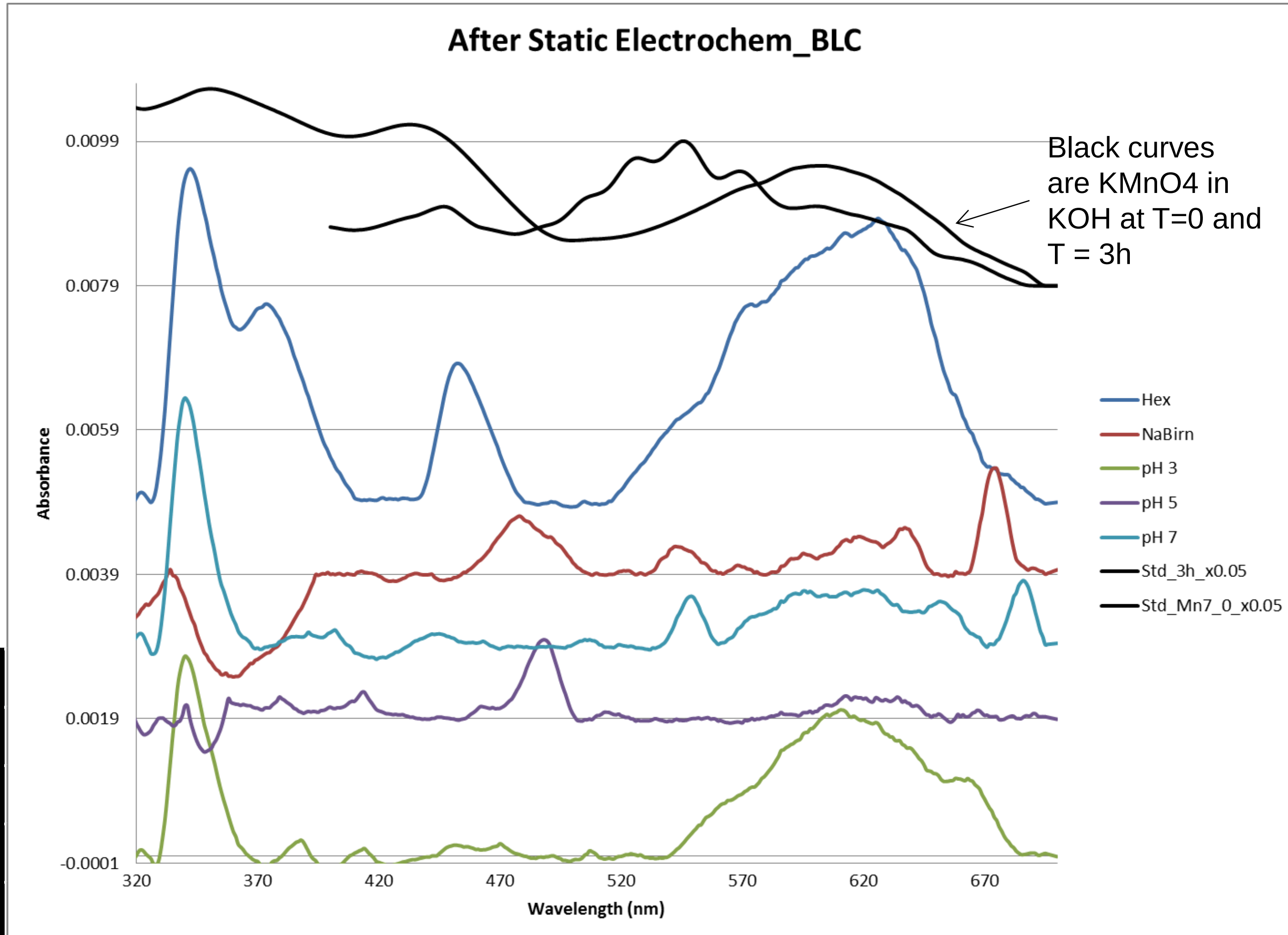

	620 T 1h
	uM
Hexagonal	6.96
pH 3	3.17
pH 5	-0.05
pH 7	2.97
Triclinic	0.42

Supernatant after reaction with ceric

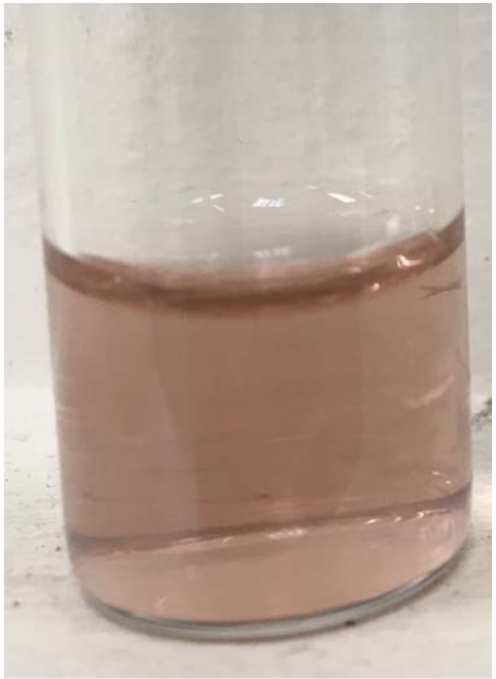

Sample	uM permanganate (525 nm)
Triclinic	29.7
Hexagonal	2.40
pH 3	5.20
pH 5	4.16
pH 7	15.77

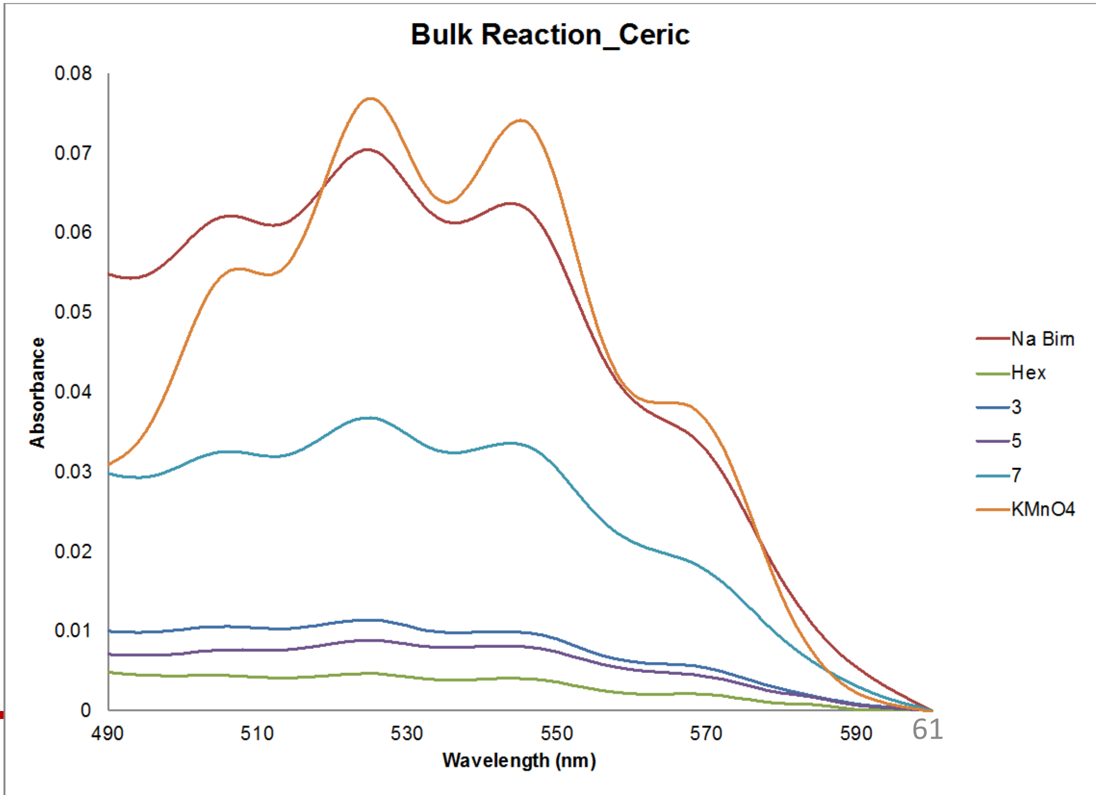

Sample	uM Mn7+ (525 nm)
Triclinic	29.7
Hexagonal	2.40
pH 3	5.20
pH 5	4.16
pH 7	15.77

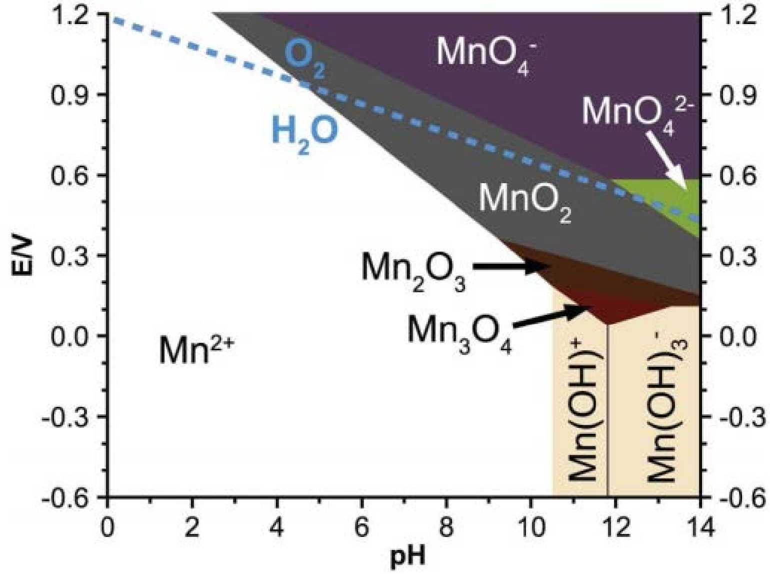

	620 T 1h
	uM
Hexagonal	6.96
pH 3	3.17
pH 5	-0.05
pH 7	2.97
Triclinic	0.42

Sample	Ce4+ uM Mn^{7+}/mg (525 nm)	EChem uM Mn^{6+}/mg (620 nm)
Triclinic	2.47	--
Hexagonal	0.22	4.97
pH 3	0.52	2.26
pH 5	0.38	--
pH 7	1.58	2.12

Opposing trends for higher oxidation state production

Wiechen, M, et.al. Dalton Trans., 2012, 41, 21–31

Ceric permanganate production

$$3Ce(IV) + MnO_2(s) + 2H_2O \rightarrow 3Ce(III) + MnO_4^- + 4H^+$$

The MnO_4^- probably originates from oxidation of Mn(II) adsorbed to the surface of oxide because this reaction is thermodynamically easier than the oxidation of MnO_2 to MnO_4^-.

$$2MnO_4^- + 3Mn(II) + 2H_2O \rightarrow 5MnO_2(s) + 4H^+$$

Sample	Ce^{4+} uM Mn^{7+}/mg (525 nm)
Triclinic	2.47
Hexagonal	0.22
pH 3	0.52
pH 5	0.38
pH 7	1.58

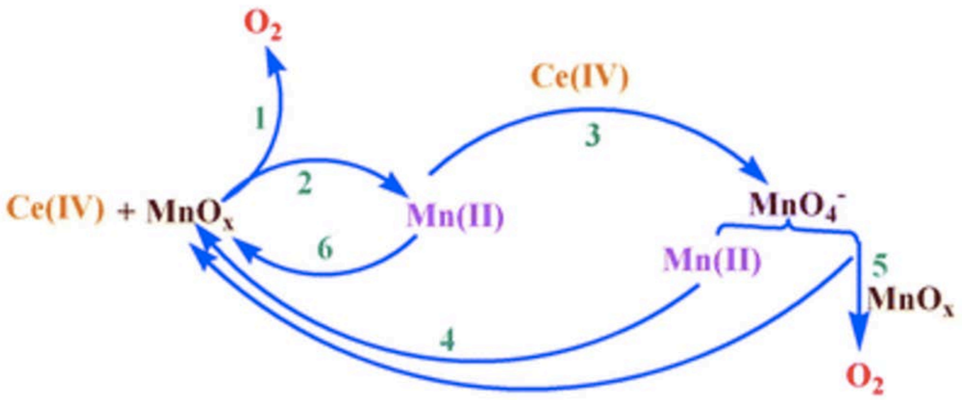

Najafpour, M, et.al. Dalton Trans., 2013, **42**, 14603-14611

Electrochemical Permanganate Production

Sample	uM Mn^{6+}/mg (620 nm)
Triclinic	--
Hexagonal	4.97
pH 3	2.26
pH 5	--
pH 7	2.12

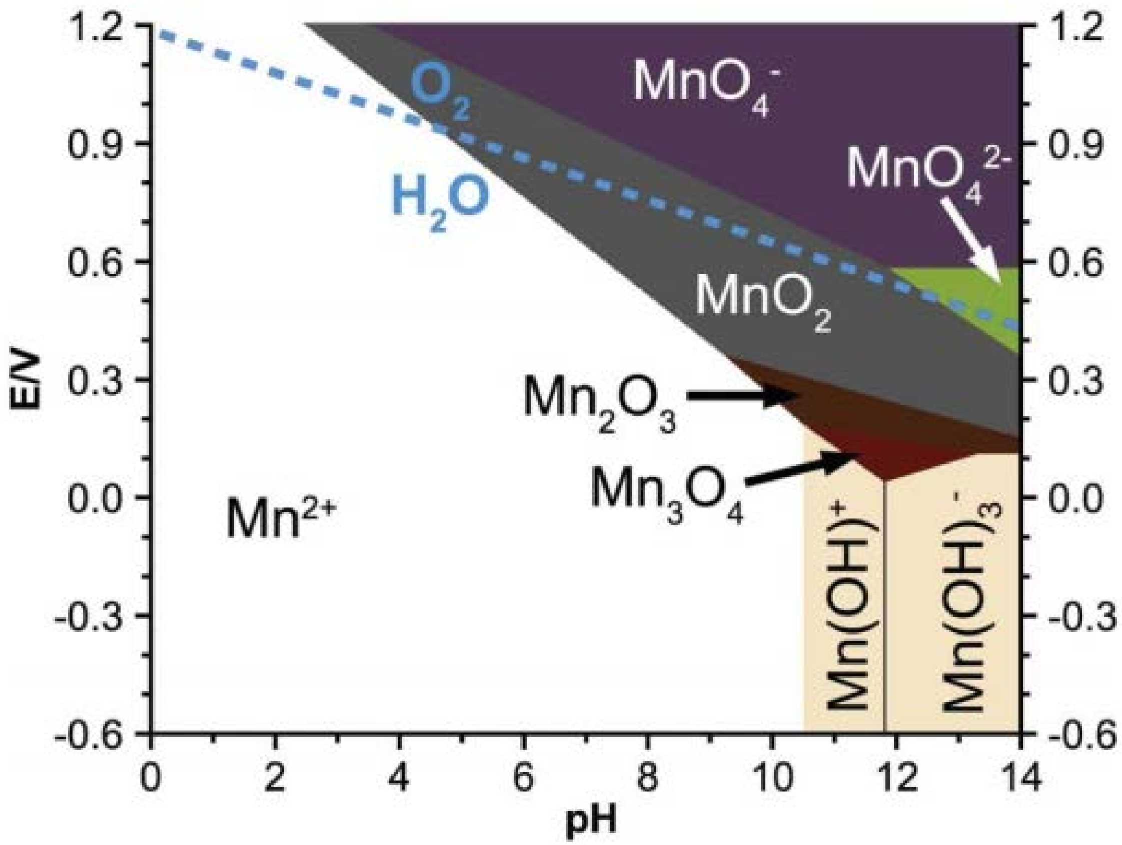

Wiechen, M, et.al. Dalton Trans., 2012, 41, 21–31

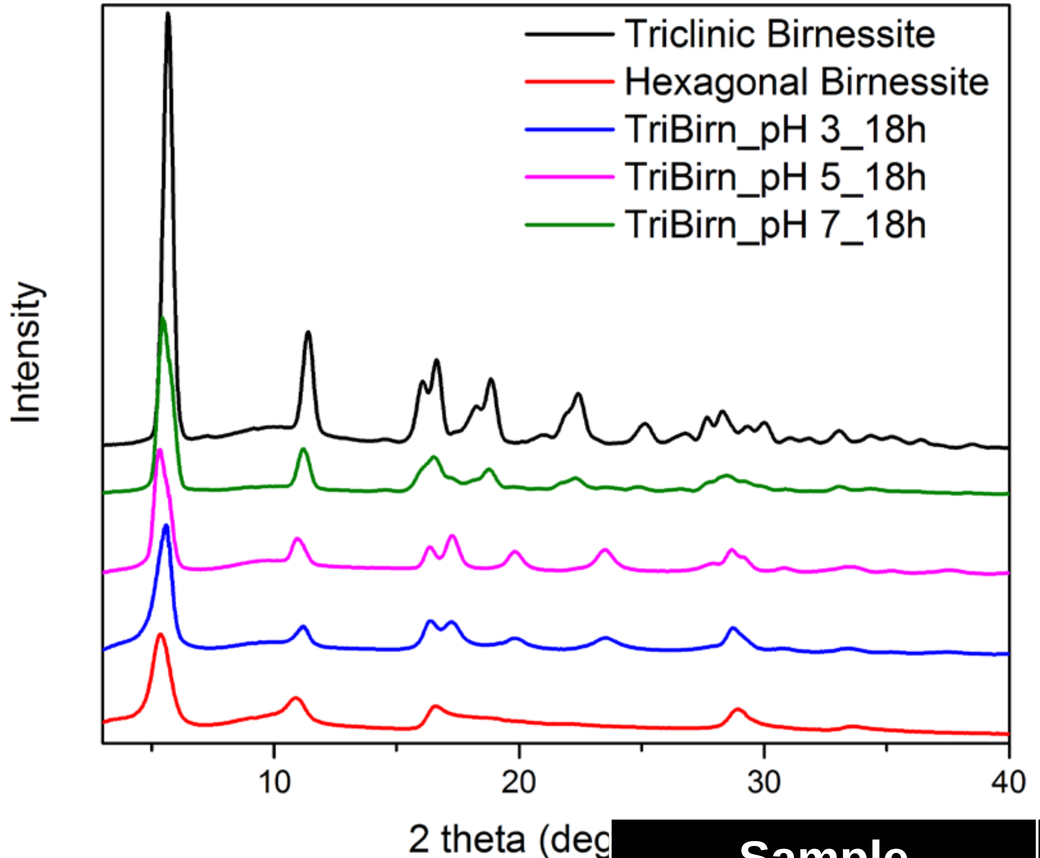

Sample	AOS (XPS)	AOS (Titration)
Triclinic Birnessite	3.51	3.45
pH 3	3.54	3.92
pH 5	3.49	3.94
pH 7	3.46	3.84
Hexagonal	3.63	3.70

Cox, et.al. *Science*. 2014. 345. 6198. 804-808.

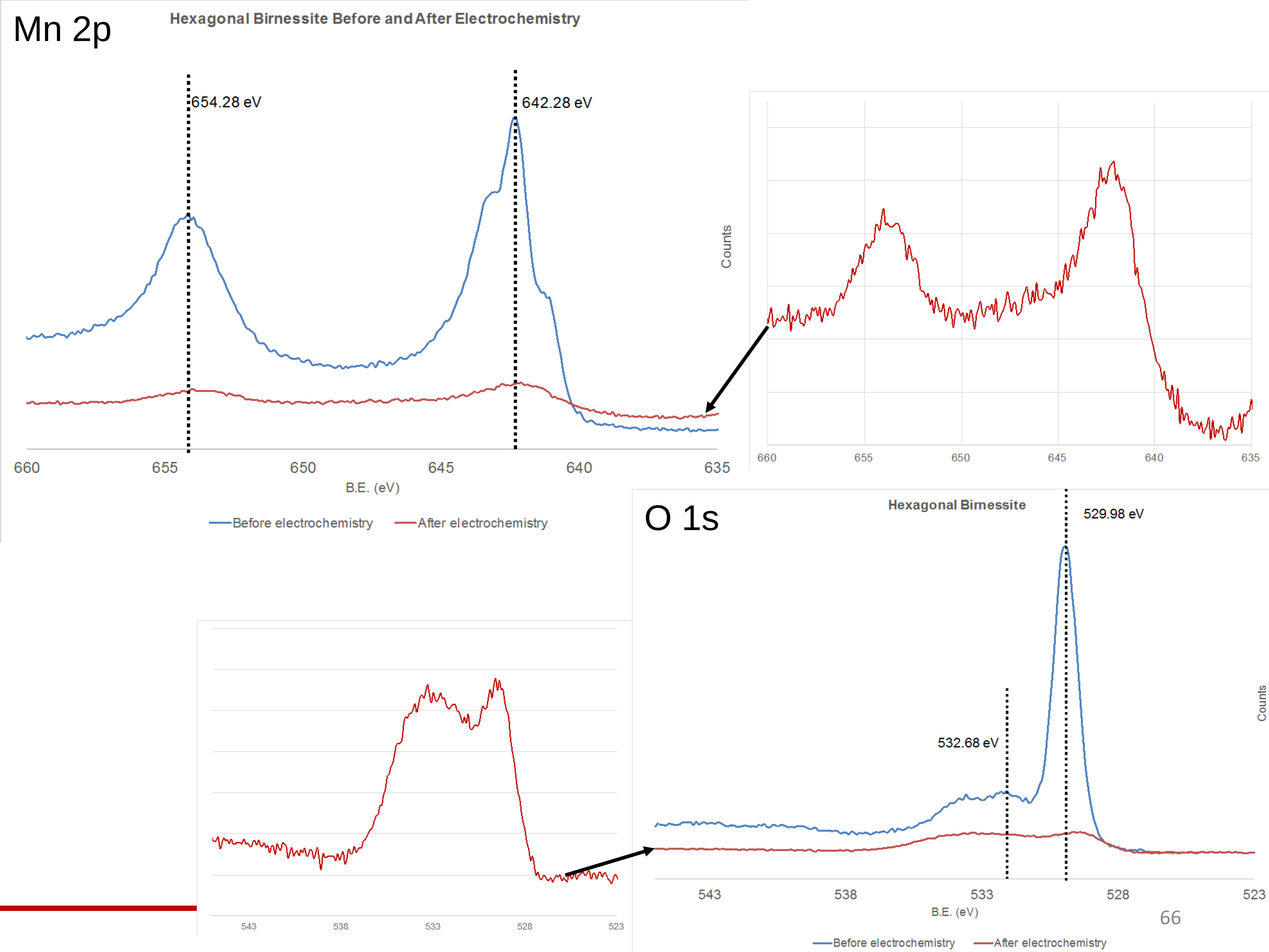

Mn 2p
Hexagonal Birnessite Before and After Electrochemistry
654.28 eV
642.28 eV
660
655
650
645
640
635
B.E. (eV)
Before electrochemistry
After electrochemistry
Counts
660
655
650
645
640
635
O 1s
Hexagonal Birnessite
529.98 eV
532.68 eV
543
538
533
528
523
B.E. (eV)
Before electrochemistry
After electrochemistry
Counts
543
538
533
528
523

Possible explanations

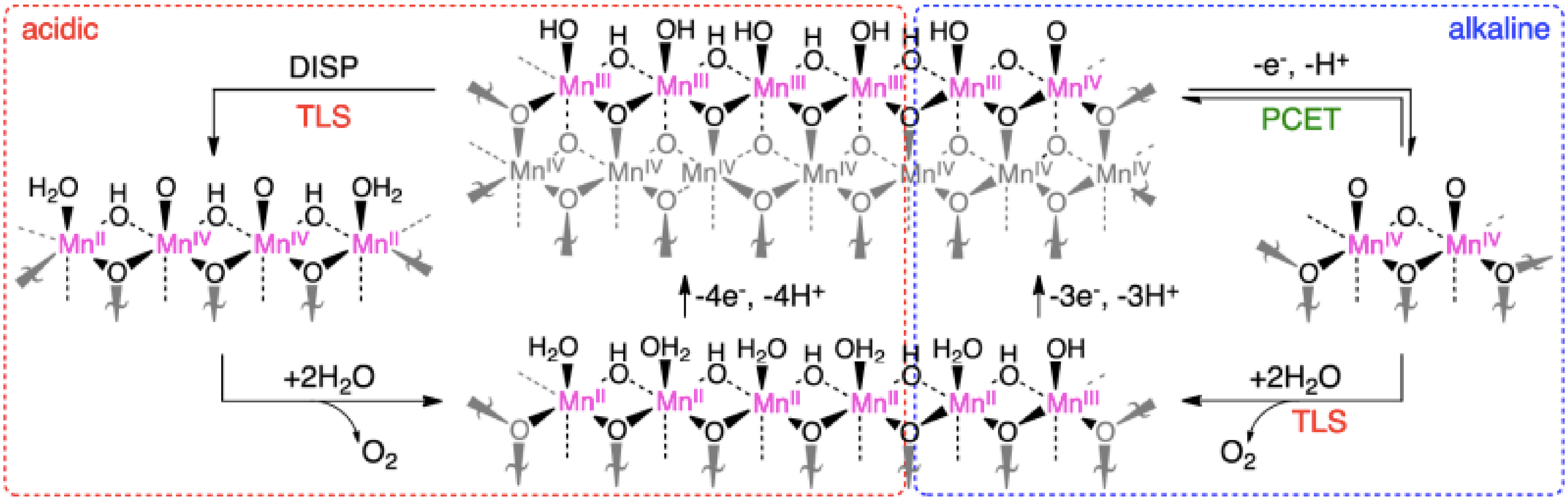

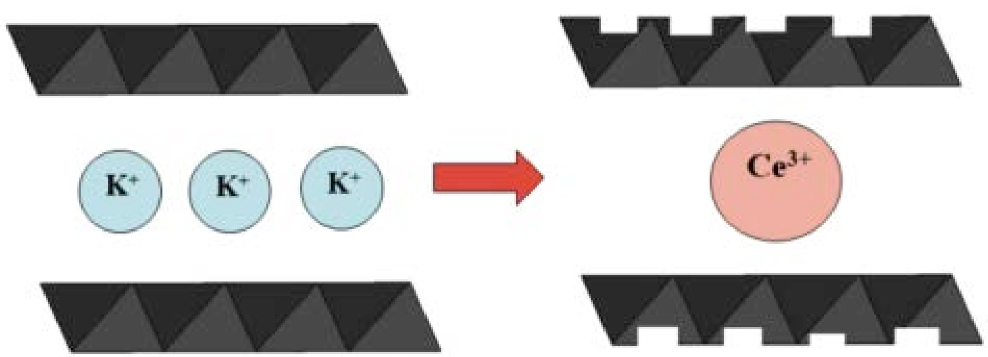

Najafpour, et al. *Dalton Transactions* 42.40 (2013): 14603-14611.
Huynh, et.al. *J. Am. Chem. Soc.* (2014), 136, 6002-6010

Modification of bulk structure

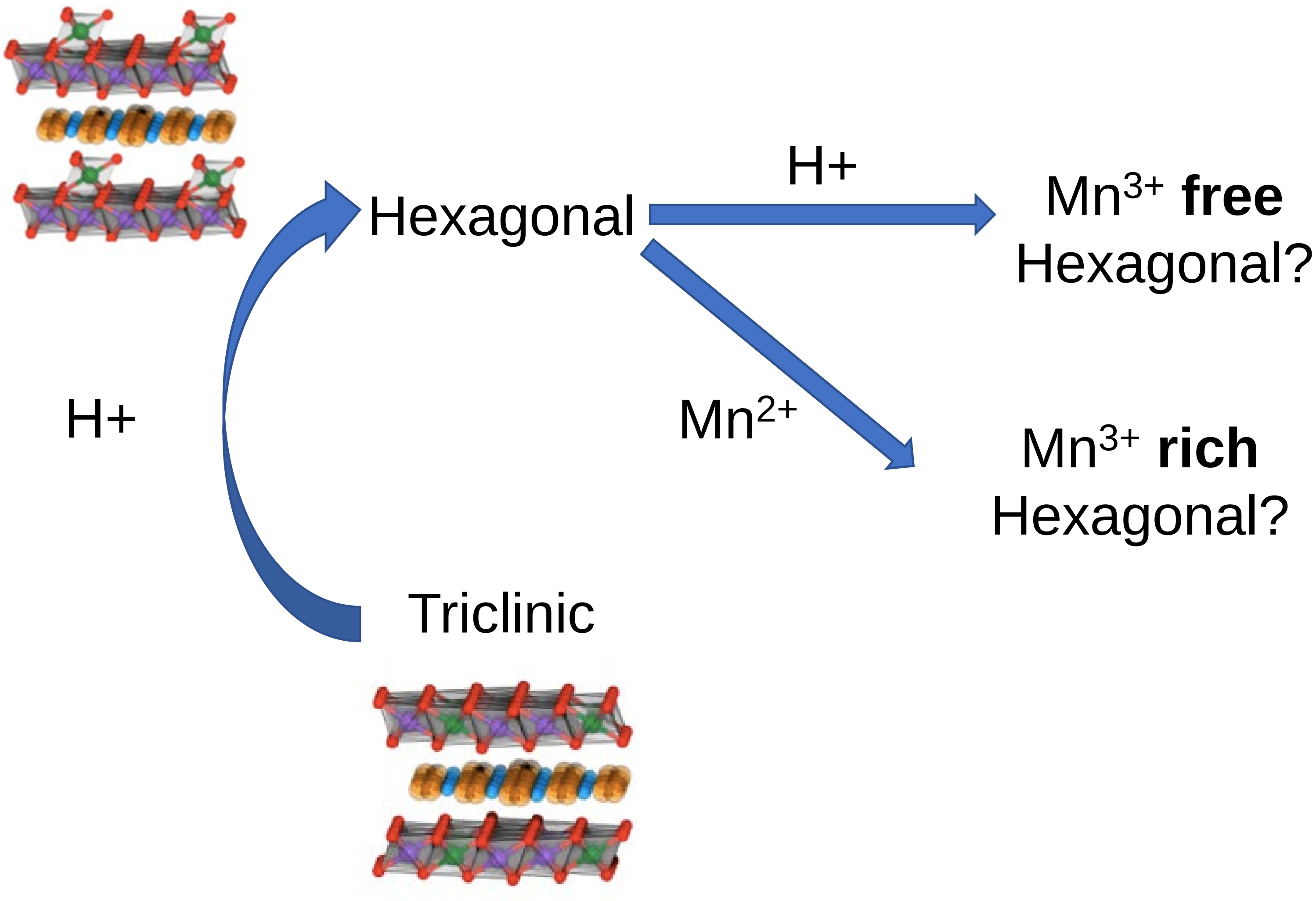

Modification of bulk structure

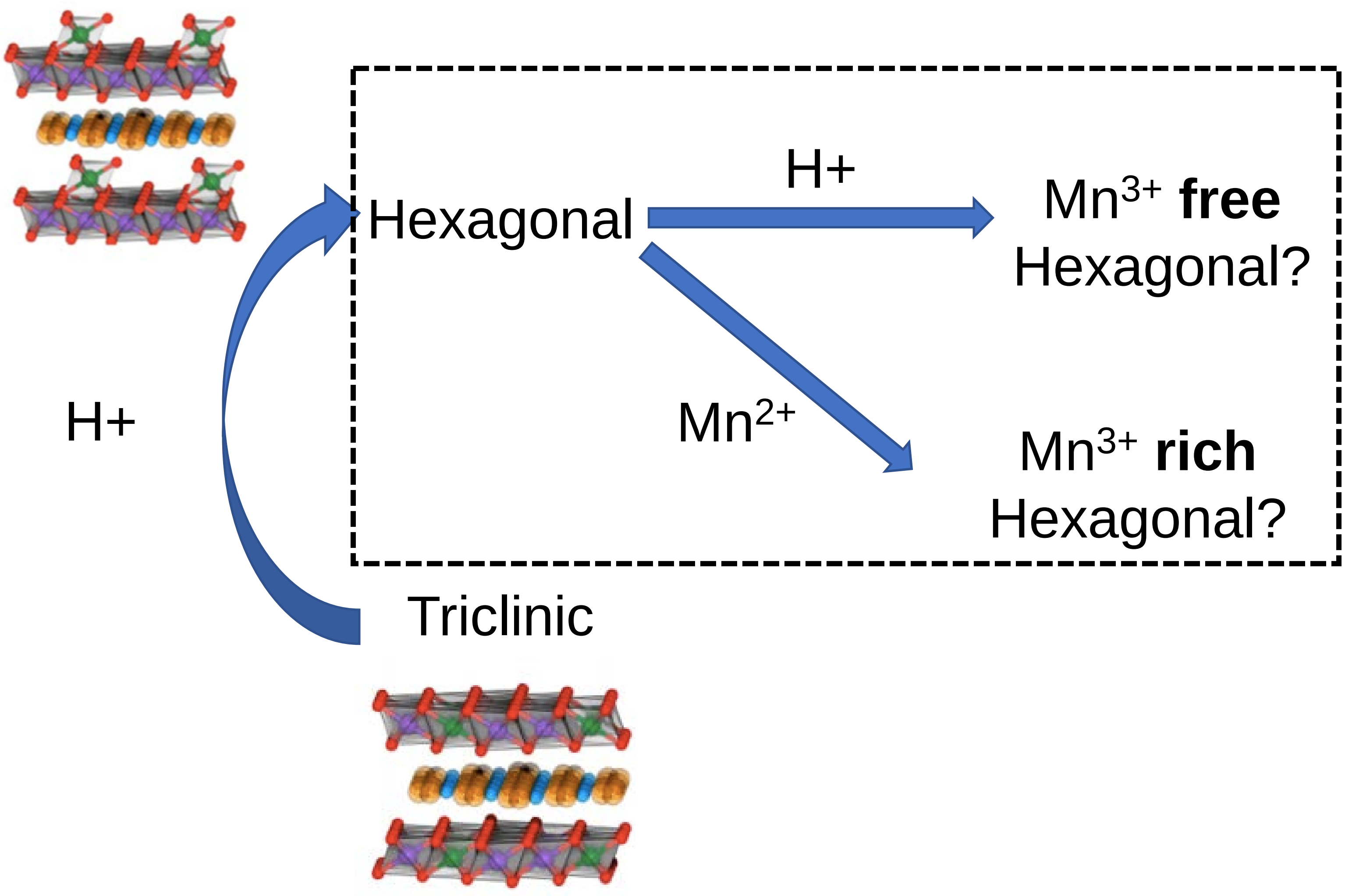

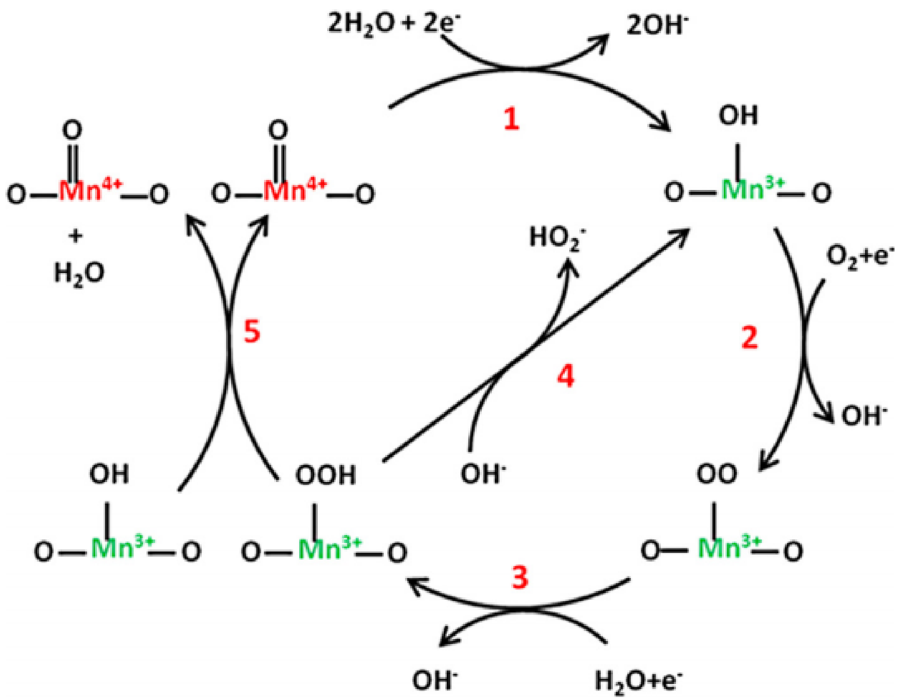

2H₂O + 2e⁻
2OH⁻
1
OH
O—Mn³⁺—O
O₂+e⁻
2
OH⁻
OO
O—Mn³⁺—O
3
OH⁻
H₂O+e⁻
OOH
O—Mn³⁺—O
4
HO₂⁻
OH⁻
5
OH
O—Mn³⁺—O
O
O—Mn⁴⁺—O
+
H₂O

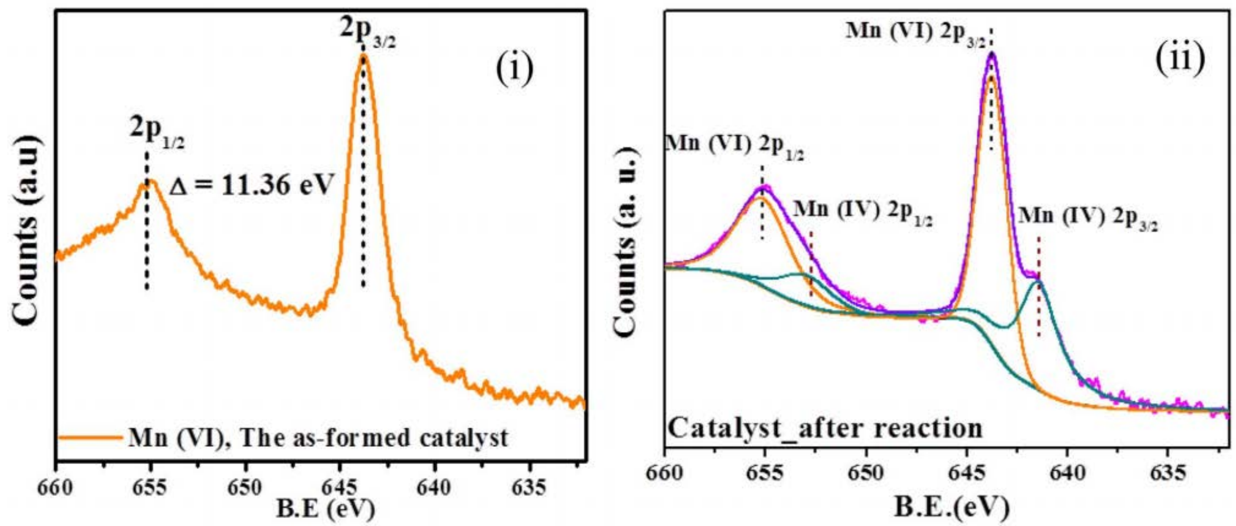

(i)
2p3/2
2p1/2
Δ = 11.36 eV
Counts (a.u)
Mn (VI), The as-formed catalyst
660 655 650 645 640 635
B.E (eV)
(ii)
Mn (VI) 2p3/2
Mn (VI) 2p1/2
Mn (IV) 2p1/2
Mn (IV) 2p3/2
Counts (a. u.)
Catalyst_after reaction
660 655 650 645 640 635
B.E.(eV)

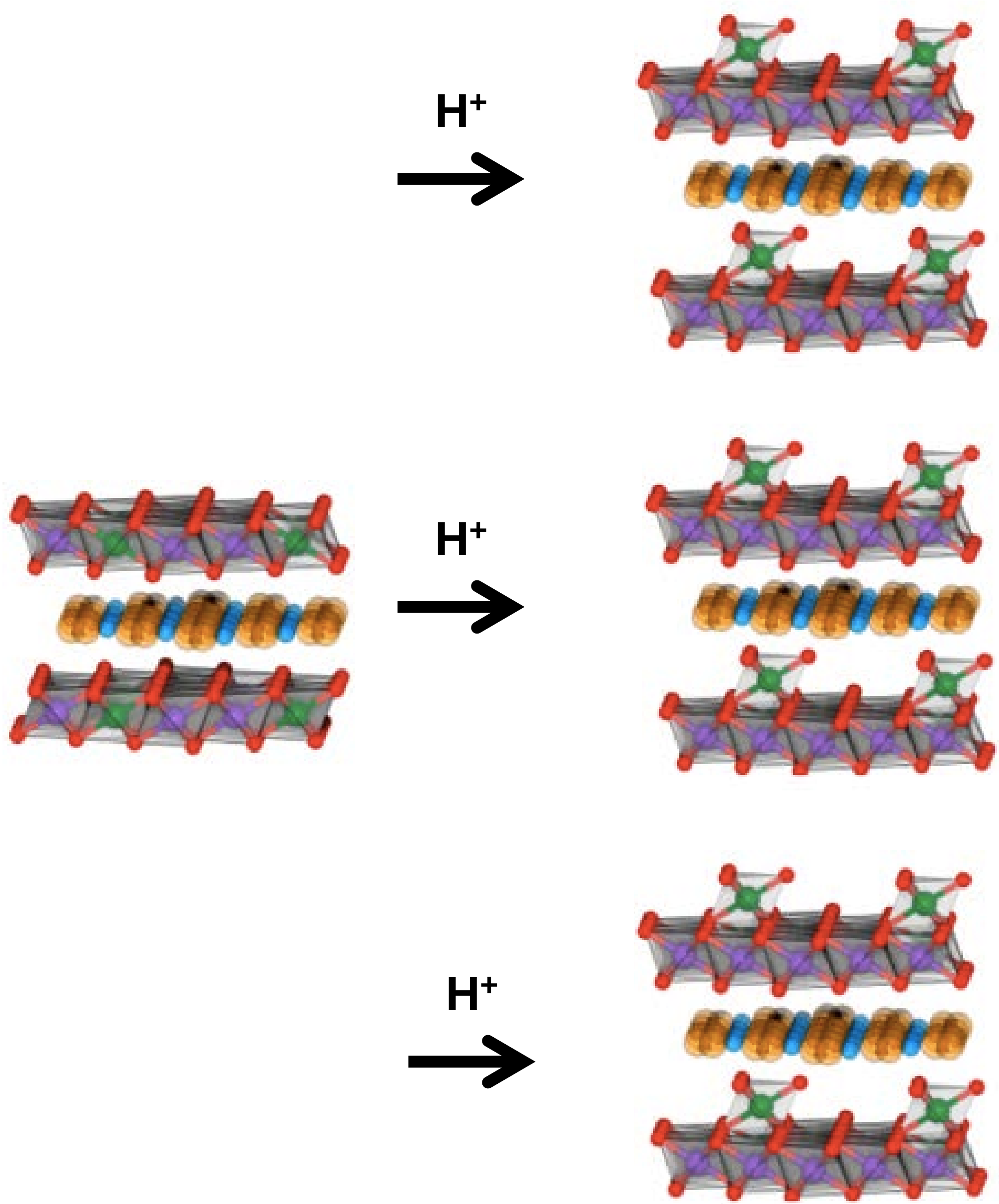

Triclinic

Hexagonal

Varying amounts of Mn^{3+} within the interlayer, but same total amount within the structure

Triclinic

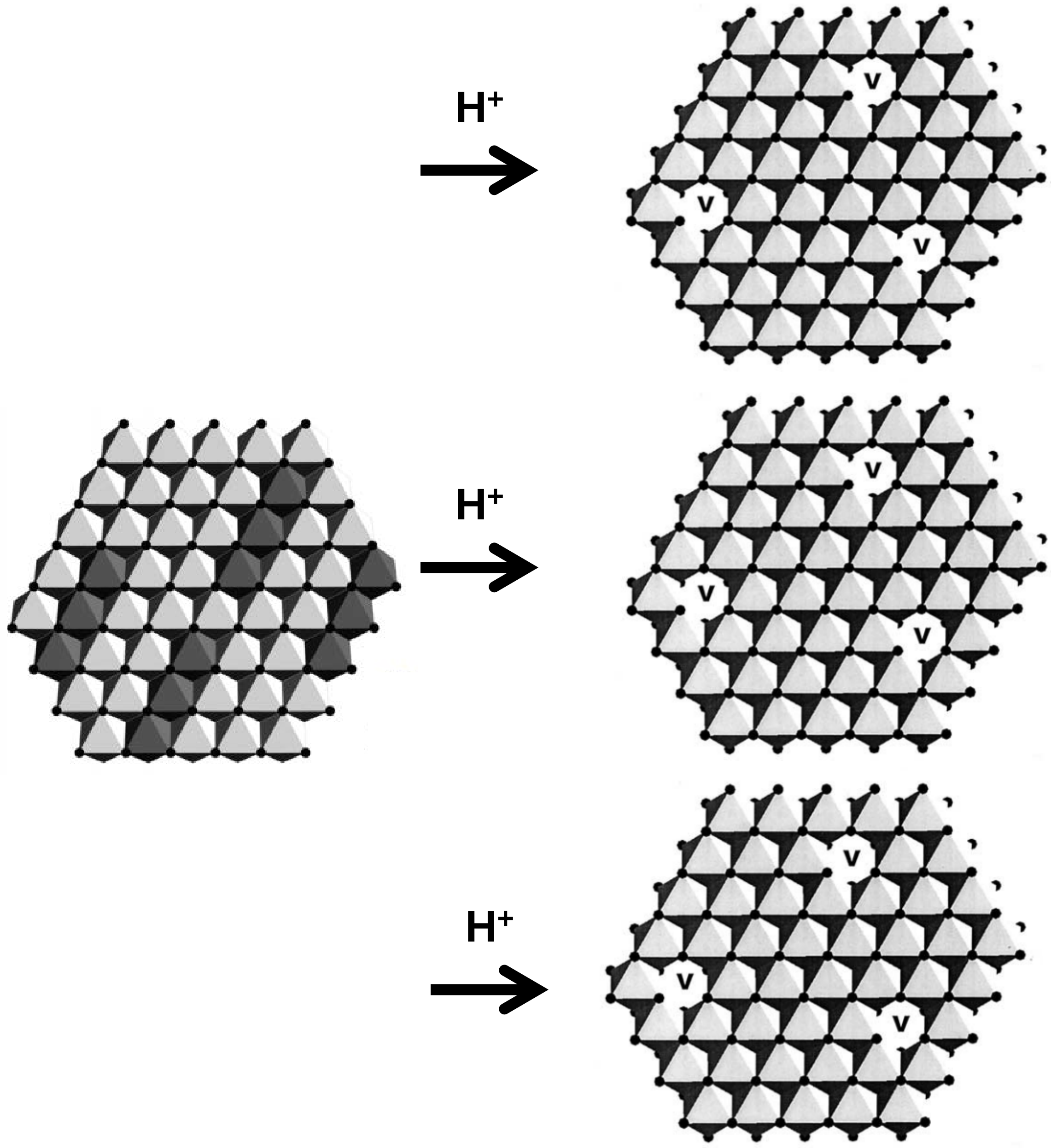

Hexagonal

Varying amounts of Mn^{3+} within the interlayer, but same total amount within the structure

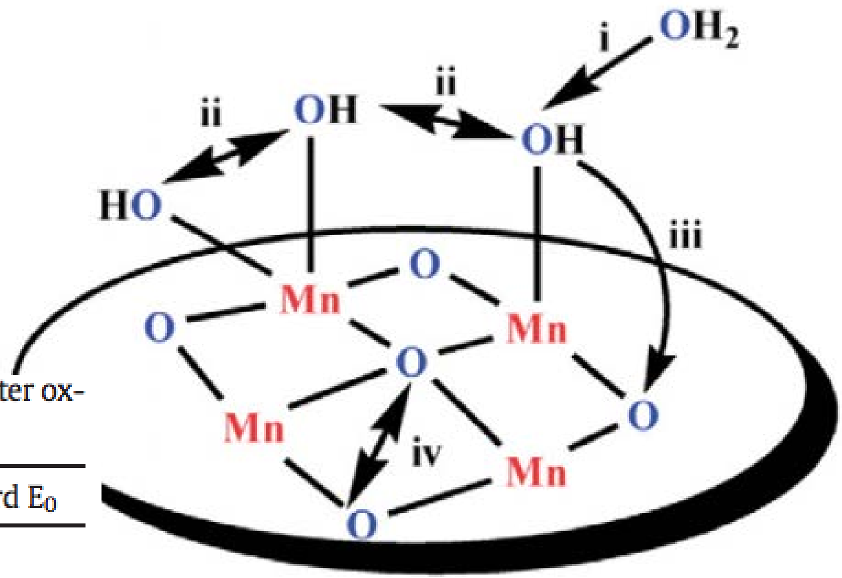

Standard Reduction Potentials measured in aqueous solution (pH = 0) for water oxidation regarding different mechanisms (E_0 vs. SHE).

Reaction	Standard E_0
Four-electron reactions	
$2H_2O \rightarrow O_2 + 4H^+ + 4e^-$	1.229
$OH^- + H_2O \rightarrow O_2 + 3H^+ + 4e^-$	1.022
$2OH^- \rightarrow O_2 + 2H^+ + 4e^-$	0.815
$4OH^- \rightarrow O_2 + H_2O + 4e^-$	0.401
Two-electron reactions	
$2H_2O \rightarrow H_2O_2 + 2H^+ + 2e^-$	1.776
$2OH^- \rightarrow H_2O_2 + 2e^-$	0.948
$H_2O_2 \rightarrow O_2 + 2H^+ + 2e^-$	0.682
$H_2O_2 + 2OH^- \rightarrow O_2 + 2H_2O + 2e^-$	−0.146
One-electron reactions	
$H_2O \rightarrow OH^- + H^+ + e^-$	2.848
$OH^- \rightarrow OH + e^-$	2.020
$H_2O_2 \rightarrow HO_2 + H^+ + e^-$	1.495
$H_2O_2 + OH^- \rightarrow HO_2 + H_2O + e^-$	0.667
$HO_2 \rightarrow O_2 + H^+ + e^-$	−0.130
$HO_2 + OH^- \rightarrow O_2 + H_2O + e^-$	−0.958

Birnessite samples (triclinic transformed to hexagonal at pH 3 and 5 as well as hexagonal sample) after electrochemistry **STATIC**

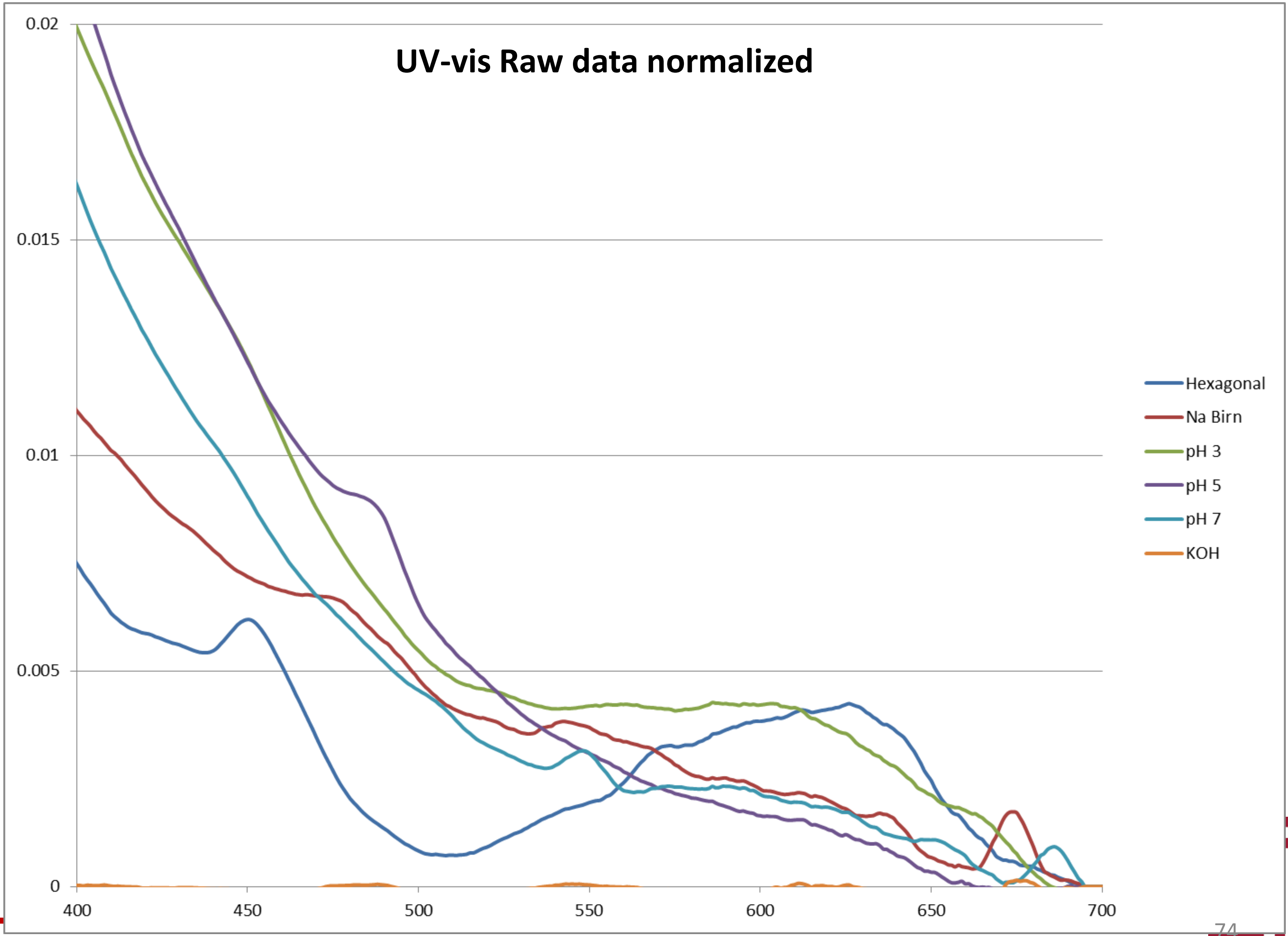

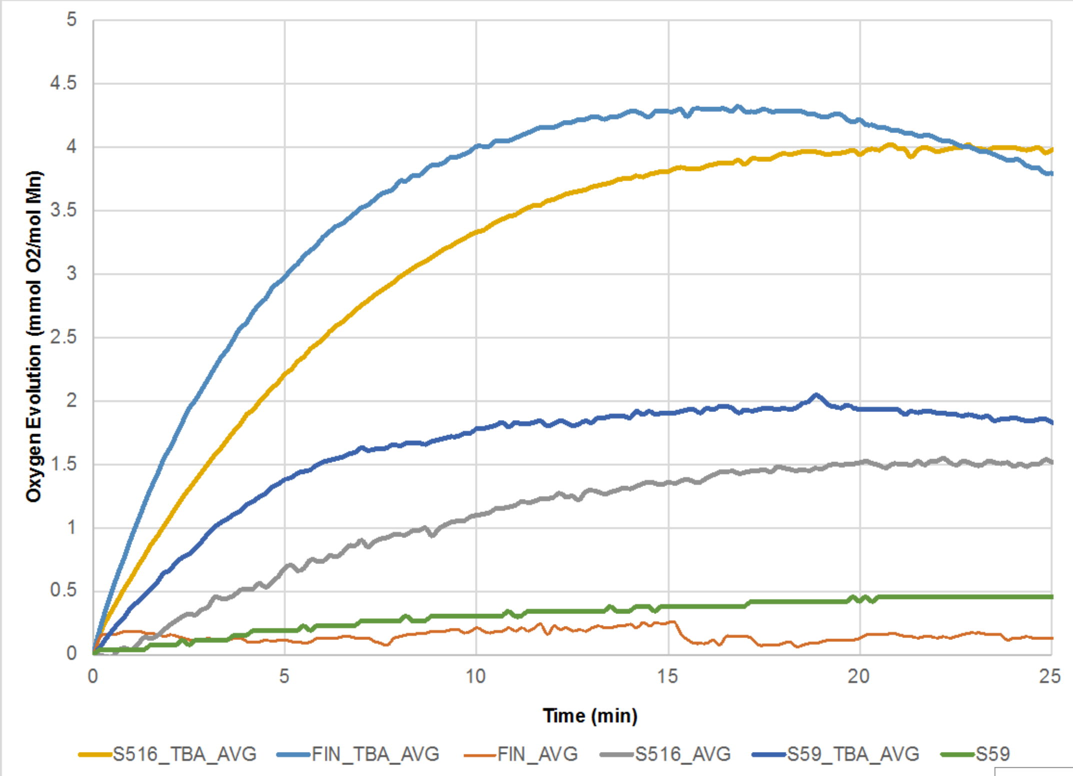
Oxygen Evolution (mmol O2/mol Mn)
Time (min)
S516_TBA_AVG
FIN_TBA_AVG
FIN_AVG
S516_AVG
S59_TBA_AVG
S59

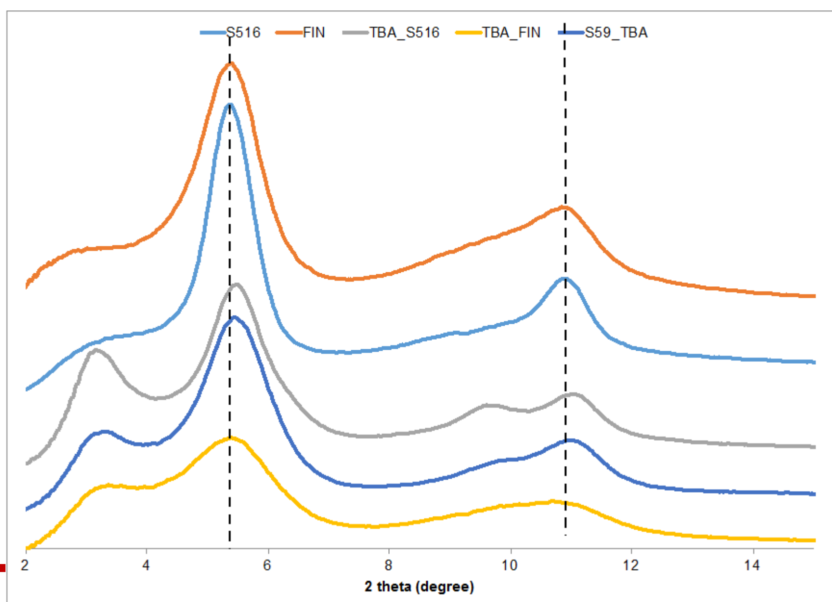
S516
FIN
TBA_S516
TBA_FIN
S59_TBA
2 theta (degree)

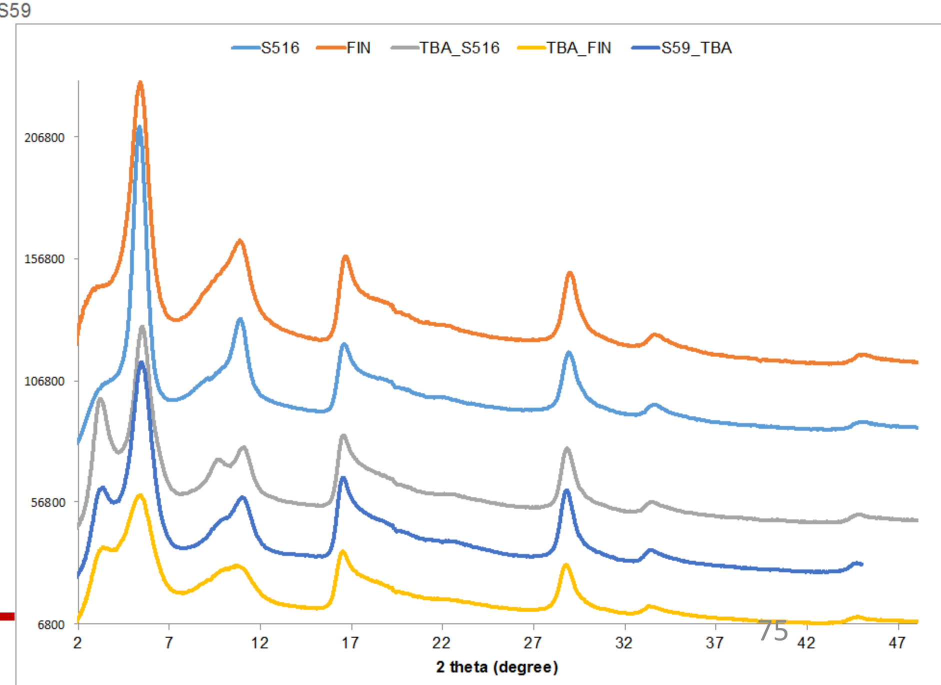
S516
FIN
TBA_S516
TBA_FIN
S59_TBA
2 theta (degree)

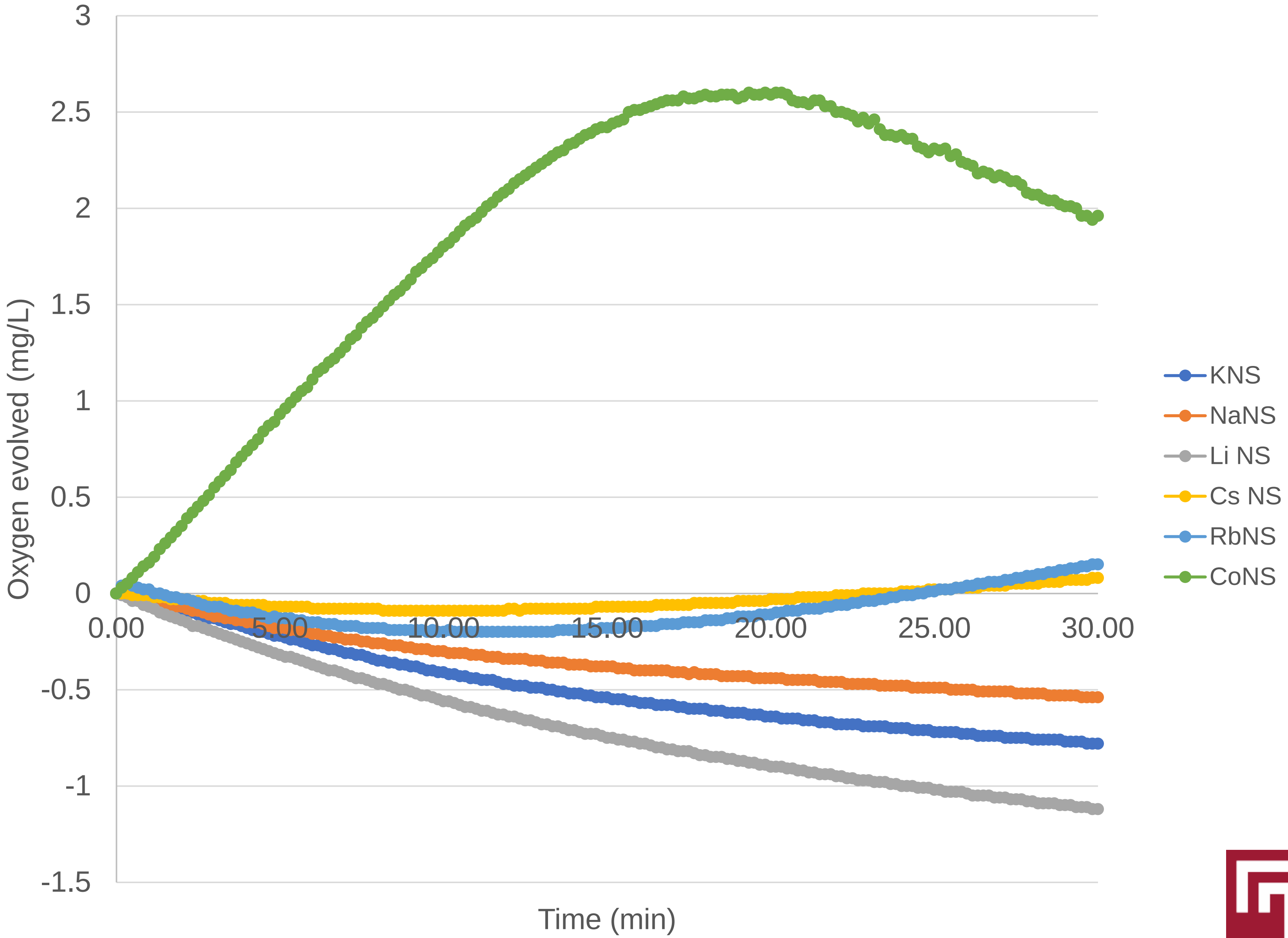
3
2.5
2
1.5
1
0.5
0
-0.5
-1
-1.5
0.00
5.00
10.00
15.00
20.00
25.00
30.00
Oxygen evolved (mg/L)
Time (min)
KNS
NaNS
Li NS
Cs NS
RbNS
CoNS

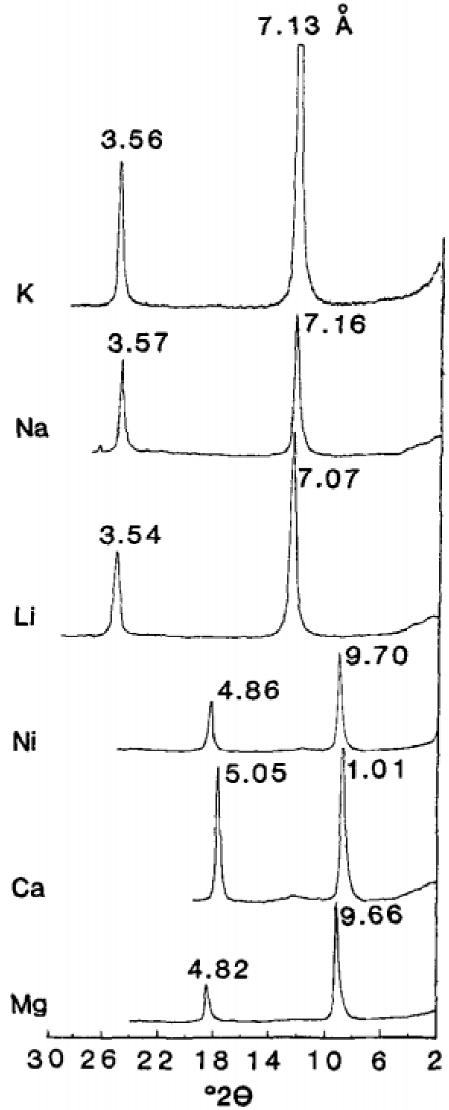

Figure 2. Basal spacings (in Å) of birnessite saturated wi
K, Na, Li, Ni, Ca, and Mg (22°C, relative humidity = 54
CuKα radiation).

Cation exchanged	Interlayer spacing *d* (001) (Å)
H pH=2	7.26
H pH=3	7.24
H pH=3.8	7.27
Li*	6.96
Na*	7.24
K	7.08
Cs	7.37
Mg†	6.96
Mg-buserite*	9.49, 7.04
Ca	9.96, 7.31
Ni	9.63
Chalcophanite (Zn)‡	6.92
Pb	7.11

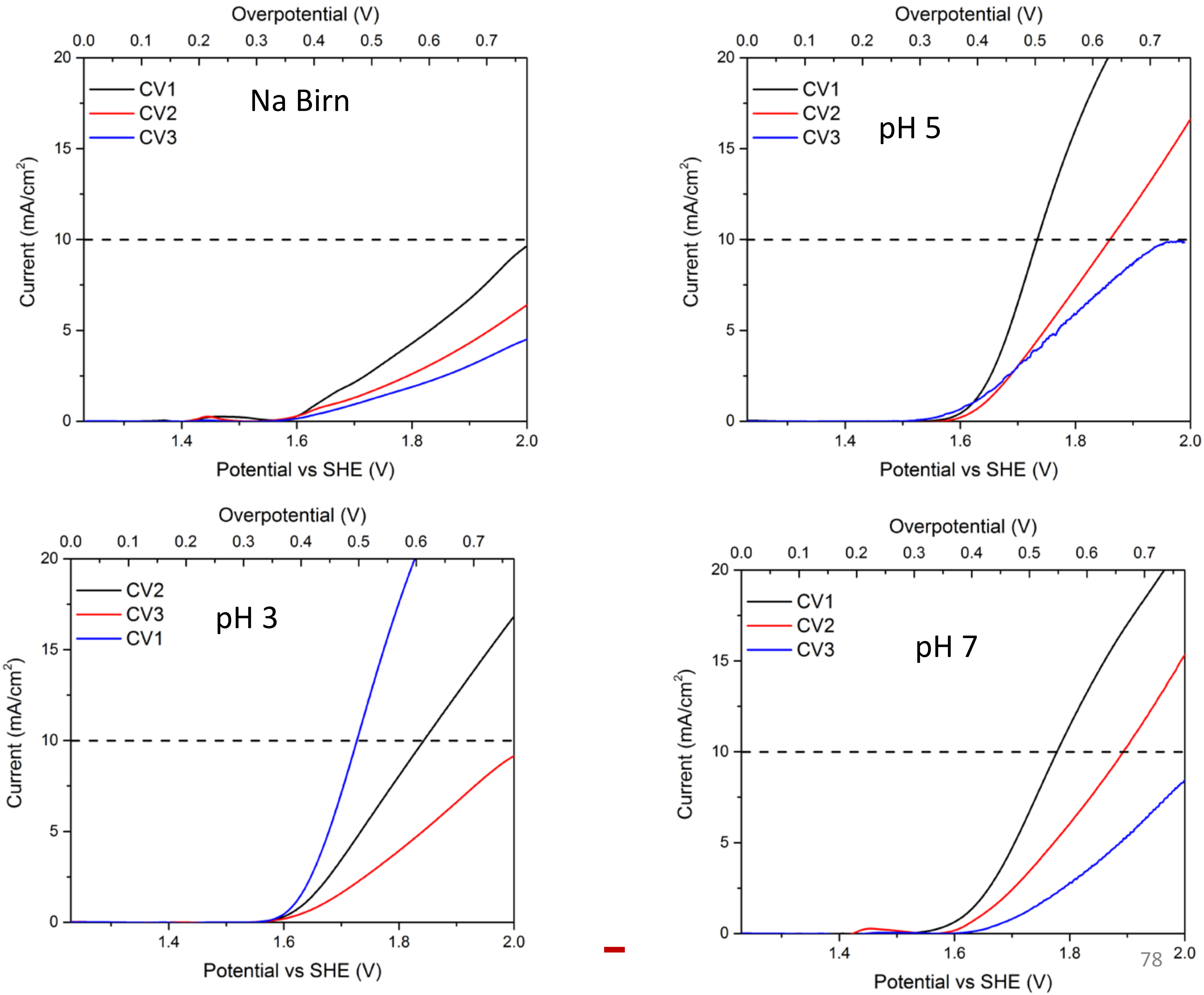
Na Birn
pH 5
pH 3
pH 7
CV1
CV2
CV3
Overpotential (V)
Current (mA/cm^2)
Potential vs SHE (V)
0.0 0.1 0.2 0.3 0.4 0.5 0.6 0.7
1.4 1.6 1.8 2.0
0 5 10 15 20

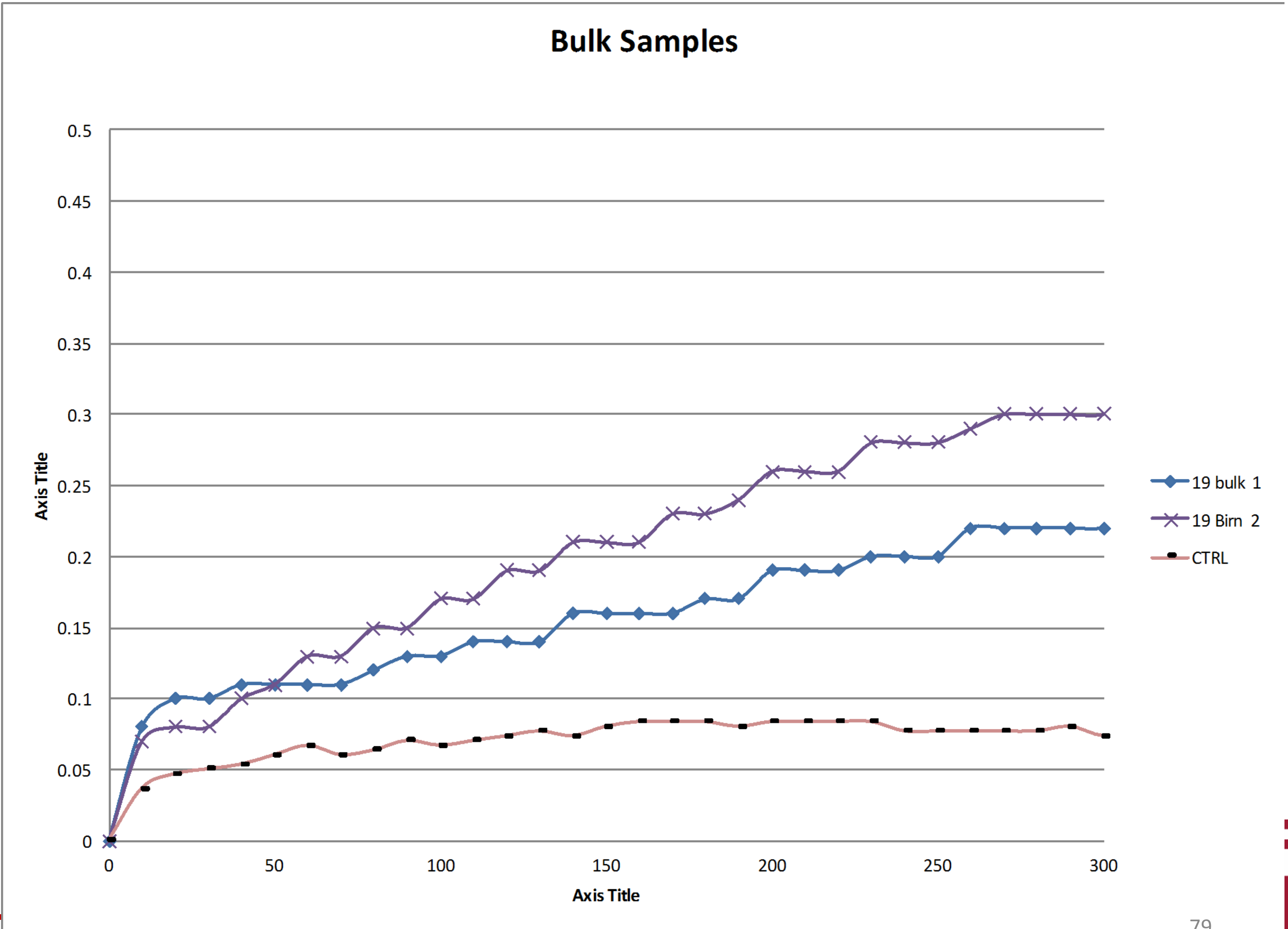
Bulk Samples
0.5
0.45
0.4
0.35
0.3
0.25
0.2
0.15
0.1
0.05
0
Axis Title
0
50
100
150
200
250
300
Axis Title
19 bulk 1
19 Birn 2
CTRL

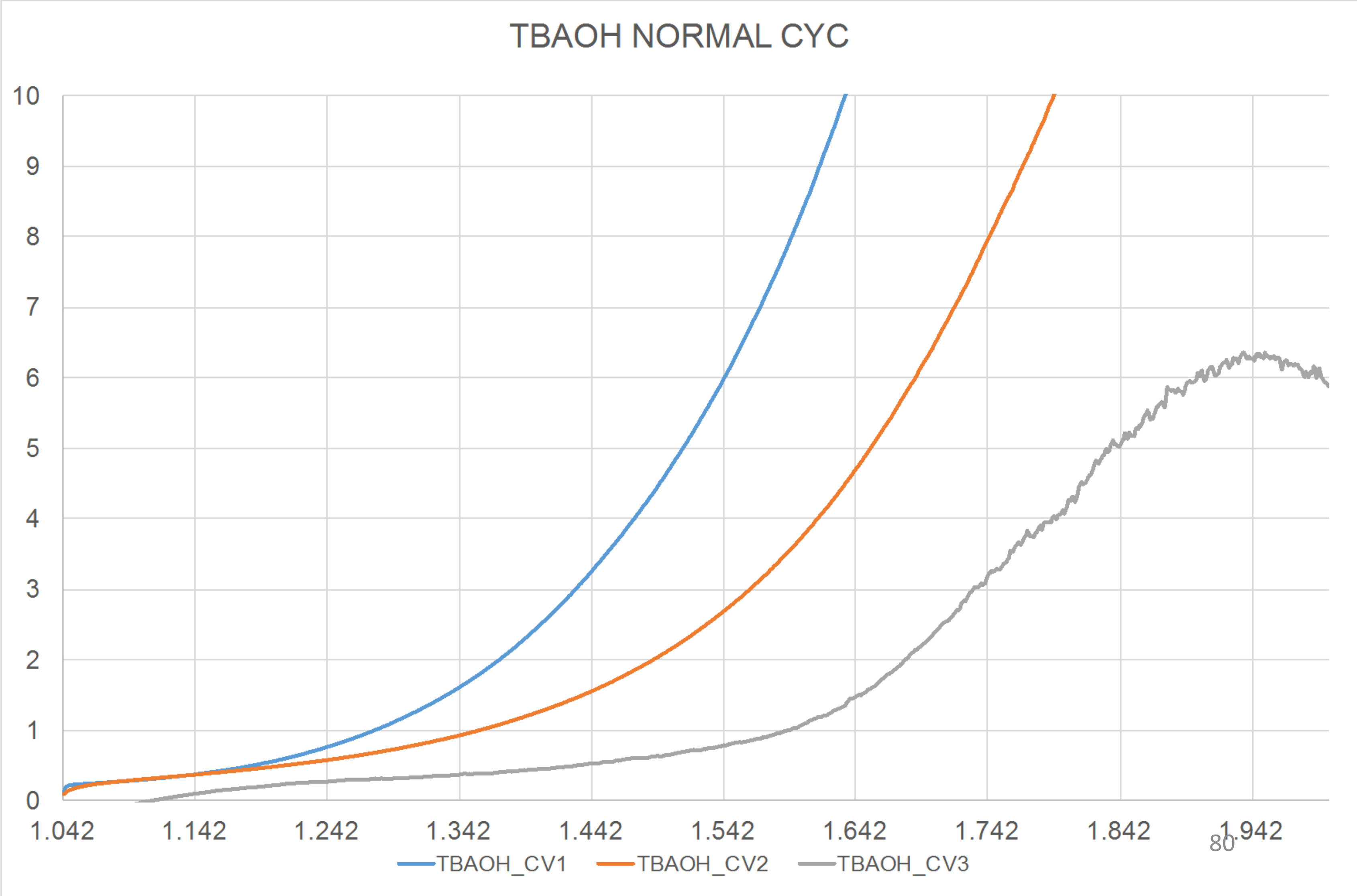

TBAOH NORMAL CYC
10
9
8
7
6
5
4
3
2
1
0
1.042
1.142
1.242
1.342
1.442
1.542
1.642
1.742
1.842
1.942
TBAOH_CV1
TBAOH_CV2
TBAOH_CV3

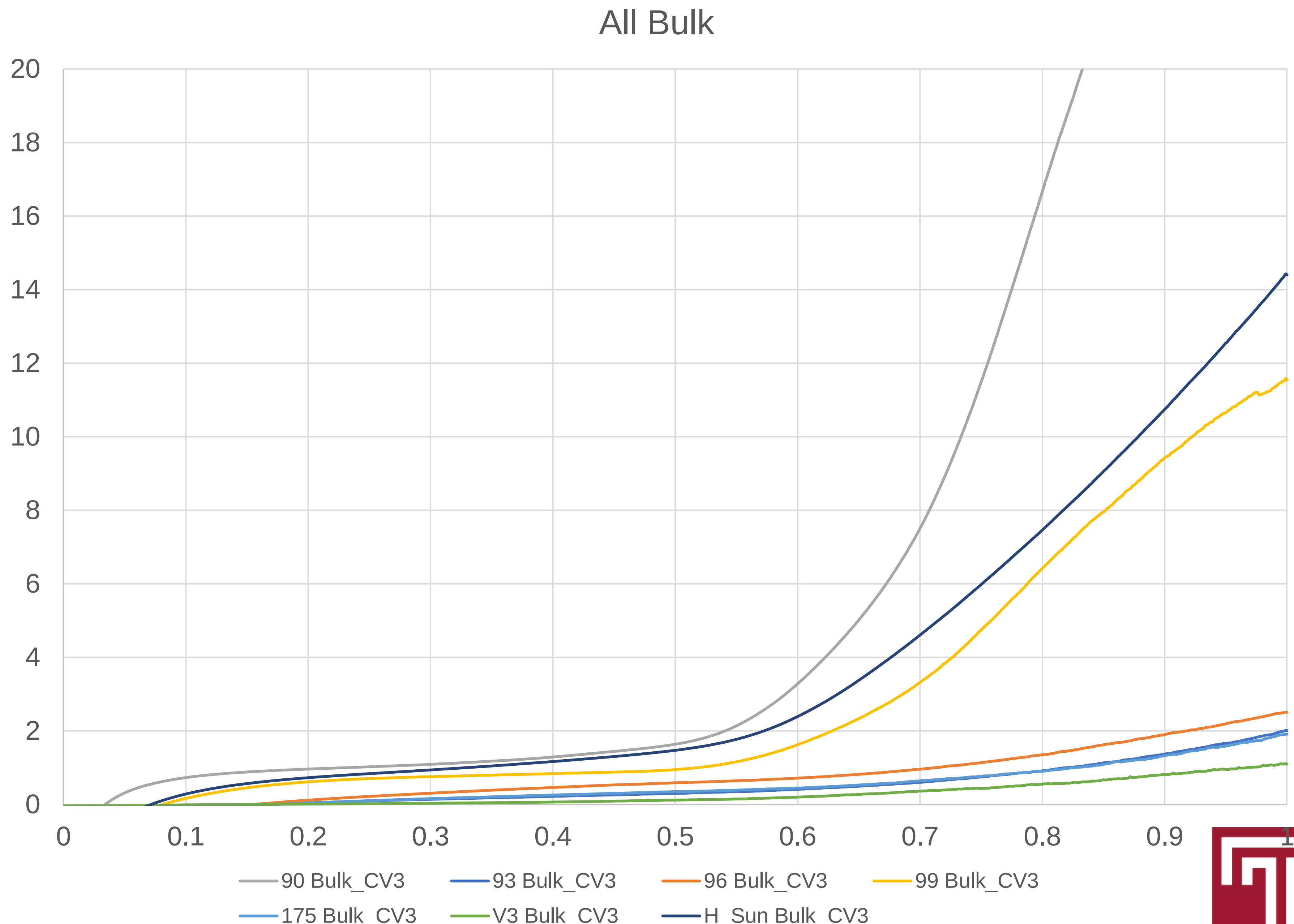
All Bulk
20
18
16
14
12
10
8
6
4
2
0
0
0.1
0.2
0.3
0.4
0.5
0.6
0.7
0.8
0.9
1
90 Bulk_CV3
93 Bulk_CV3
96 Bulk_CV3
99 Bulk_CV3
175 Bulk_CV3
V3 Bulk_CV3
H_Sun Bulk_CV3